Spring 5-7-2016

Molecular Mechanisms of Necrotic Cell Death in Ischemic Renal Injury

Yuan Ying
University of Nebraska Medical Center

MOLECULAR MECHANISMS OF NECROTIC CELL DEATH IN ISCHEMIC RENAL INJURY

by

Yuan Ying

A DISSERTATION

Presented to the Faculty of

the University of Nebraska Graduate College

in Partial Fulfillment of the Requirements

for the Degree of Doctor of Philosophy

Cellular & Integrative Physiology

Graduate Program

Under the Supervision of Professor Babu J. Padanilam

University of Nebraska Medical Center

Omaha, NE

April, 2016

Supervisory Committee:

Pamela K, Carmines, Ph.D.	Troy J, Plumb, M.D.
Steven C, Sansom, Ph. D.	Irving H, Zucker, Ph.D.

ACKNOWLEDGEMENTS

First of all, I would like to express my greatest thankfulness to Dr. Babu J. Padanilam. Dr. Padanilam is such a wonderful and easily approachable person. During the past five years, he has been very supportive and understanding. I have benefited a great deal from his scientific thoughts during my years in his lab.

I would like to thank my supervisory committee, Drs. Carmines, Plumb, Sansom, and Zucker for their valuable suggestions throughout these years. Without their support, I could never finish this project so smoothly.

I would like to thank all my lab members, Drs. Kim and Jang, and Ms. Westphal and Long for their kind support and help. I know whenever I have a question about my experiments, I can turn to them.

I would like to thank all the professors, graduate students and technicians in this department. It has been my greatest pleasure to be part of the department. I really enjoyed these five years with all these wonderful people in this great department.

Last, I would like to express my deepest thanks to my parents for their encouragement, support, and understanding. Without them, I could never achieve all these and be where I am today.

ABSTRACT

Molecular mechanisms of necrotic cell death in ischemic renal injury

Yuan Ying, M.D., Ph.D.

University of Nebraska, 2016

Supervisor: Babu J. Padanilam, Ph.D.

Acute kidney injury is a common clinical syndrome particularly in hospitalized patients. Necrotic cell death, as one type of major cell death after ischemic reperfusion injury, is partially responsible for the rapid decline in GFR. p53 is a novel apoptosis and necrosis inducer and is found to be activated after ischemic renal injury. Although previous studies suggest that p53 could be an important mediator of kidney dysfunction, no studies have examined its role in necrotic cell death and the cross talk between p53 and other necrotic cell inducers such as PARP-1 and CypD. Thus, in this study our first goal was to examine the effect of gene ablation of p53 specifically in the proximal tubules on ischemic renal injury. Our second goal was to examine the possible mechanism by which p53 may induce necrosis. Our third goal was to test if double knockout of PARP-1/CypD or PARP-1/p53 additively/synergistically protects kidney from ischemic injury. Our results suggest that knockout of p53 specifically in the proximal tubules protected the kidney form ischemic renal injury by reducing apoptotic/necrotic cell death, inflammation, and long term fibrosis. Further, we found that double knockout of PARP-1/CypD or PARP-1/p53 in the kidney had better protective effects than respective single knockout mice. In addition, kidneys from double knockout mice also have better histological findings and fewer necrotic tubules. Our data demonstrate that activation of p53 significantly increased PARP-1 expression, which could contribute to necrosis in tubular cells. Furthermore, activation of p53 significantly decreased the expression of SLC7A11, a Glu/Cys carrier in cell membrane that inhibits ferroptosis. This

result suggests that p53-mediated ferroptosis might further contribute to tubular cell death after injury. Together, our data suggest that p53 is an important necrotic cell death inducer in ischemic renal injury. p53 may induce necrosis via overexpression of PARP-1 and Bax, and promote ferroptosis by reducing the expression of SLC7A11 to induce cell death after ischemic renal injury. Our findings may have clinical implications for the pathogenesis of acute kidney injury, possibly providing potential therapeutic targets for this devastating syndrome.

TABLE OF CONTENTS

TABLE OF FIGURES

LIST OF ABBREVIATIONS

AIF …….....apoptosis-inducing factor

AKI ……acute kidney injury

ANT ……..adenine nucleotide translocator

ATN ……..acute tubular necrosis

ATP ……..adenosine triphosphate

BCL2 ……B-cell lymphoma 2

BUN ……..blood urea nitrogen

Ca^{2+}……calcium

CKD ……..chronic kidney injury

CsA ……...cyclosporine A

CTGF ……connective tissue growth factor

CypD ……cyclophilin D

cyt c……...cytochrome c

DAMPs ……damage-associated molecular pattern molecules

DKO……..double knockout

Drp1…….. dynamin-related protein 1

EMT ……..epithelial mesenchymal transition

FADD …….....Fas-associated protein with death domain

GAPDH ……glyceraldehyde 3-phosphate dehydrogenase

GFR ……..glomerular filtration rate

Gpx4 ……..glutathione peroxidase 4

GSH ……..glutathione

HAX-1 ……...HCLS1-associated protein X-1

Hsp…….heat shock protein

ICAM-1 ……..intercellular adhesion molecule 1

IL…….interleukin

IMM ……inner mitochondrial membrane

IRI ……..ischemia-reperfusion injury

KO……...knock out

LDH ……..lactate dehydrogenase

MCU ……..mitochondrial calcium uniporter

MDM2 ……mouse double minute 2 homolog

MEFs ……..mouse embryonic fibroblasts

MLKL ……....mixed lineage kinase domain-like

MOMP ……..mitochondrial outer membrane permeability

MPTP ……...mitochondrial permeability transition pore

NAD+ ……...nicotinamide adenine dinucleotide

Nec-1 ……...necrostatin-1

NFκB…….nuclear factor-κB

OMM ……outer mitochondrial membrane

PAR ……..poly(ADP-ribose)

PARP-1 ……poly (ADP-ribose) polymerase-1

PAS……...Periodic acid-Schiff

PT …….proximal tubule

RHIM ……....RIP homotypic interaction motif

RIPK1/3 ……...receptor-interacting serine/threonine-protein kinase 1/3

ROS …….reactive oxygen species

SfA …….sanglifehrin A

TGF-β1 ……transforming growth factor beta 1

TIGAR …….TP53-induced glycolysis and apoptosis regulator

TLR ……..toll like receptor

TNF ……..tumor necrosis factor

VDAC ……..voltage-dependent anion-selective channel

WT…… wild type

α-SMA …….α-smooth muscle actin

INTRODUCTION[1]

Acute kidney injury

Acute kidney injury (AKI) is a common clinical syndrome that carries a high mortality rate. It has been estimated that AKI accounts for about 2 million deaths annually worldwide. The incidence of AKI among patients admitted into intensive care units is considerably high and is frequently associated with high mortality rates (110, 141, 151). Recent studies suggest that patients who recover from AKI have increased risk of developing chronic kidney disease (CKD); CKD is also a risk factor of incident AKI (22, 119, 163).

Currently, there is no effective treatment for this syndrome. Many rational pharmacological interventions based on pathogenic factors that elicit endothelial and epithelial cell injury, vasoconstriction, vascular congestion, leukostasis and reactive oxygen species generation, have failed or were inconclusive, mainly due to lack of understanding of the pathophysiologic processes of AKI (16, 106). Identification of mechanisms involved in renal regeneration after AKI might provide new therapeutic targets to protect kidney function and prevent complications.

Pathogenesis of AKI

AKI is defined by a rapid decline in glomerular filtration rate (GFR) in hours or days. Decreased GFR will lead to the retention of metabolic wastes such as creatinine and blood urea nitrogen (BUN), and imbalance of electrolytes, fluid, and acid-base (106). AKI

[1] Some of the materials presented in this chapter were previously published: 1. Yuan Ying, Jinu Kim, Sherry N. Westphal, Kelly E. Long, and Babu J. Padanilam. Targeted deletion of p53 in the proximal tubule prevents ischemic renal injury (183). 2. Yuan Ying and Babu J. Padanilam, Regulation of necrotic cell death: p53, PARP1 and Cyclophilin D -overlapping pathways of regulated necrosis? (184)

represents a group of pathophysiological processes with different severities that result in a decline in GFR. Renal hypo-perfusion, renal parenchymal injury or obstruction of urinary flow are common causes of AKI and represent prerenal, intrarenal, and postrenal AKI respectively (16).

While prerenal AKI is considered to be a reversible process, intrarenal AKI or acute tubular necrosis (ATN) with the involvement of the renal parenchyma is usually an irreversible event even with sufficient perfusion. ATN represents a severe form of AKI with selected tubular damage. Although all segments of the nephron may be injured under a severe ischemic insult, the proximal tubules, particularly the S3 segment of the proximal tubule (PT) in the outer stripe of outer medulla, is the most commonly involved segment because of its limited glycolytic capacity, high energy requirement, and persistent near hypoxia in this area (162). S1 and S2 segments are more likely to be injured by nephrotoxins because of active endocytosis in these segments. Tubular damage not only increases tubular fluid back leak, but also activates tubuloglomerular feedback as more solute is delivered to the distal nephron. Necrotic tubules can interact with tubular proteins to form casts in the downstream segments and obstruct the nephrons to increase glomerular back pressure. All these factors inevitably lead to a reduced GFR (16, 17).

Animal models of ischemic renal injury

Ischemic renal injury, caused by compromised perfusion of renal tissues, is accepted as the leading cause of AKI. Ischemia-reperfusion injury (IRI) in the mouse is an easily employed experimental model for the investigation of the pathological mechanisms implicated in this syndrome. Extensive work has demonstrated the usefulness of this model for the study of histological, cellular, and molecular signals in ischemic renal injury,

and most of the findings can also be extended to other kidney injury disorders that result in AKI.

The warm IRI model using bilateral renal pedicle clamping is a common experimental model used in mouse and rat animals. It is different from the cold ischemia reperfusion model that mimics kidney transplantation. An ischemic period of 30 minutes duration results in moderate injury with histological changes comparable to human ATN. This model has been widely used to improve our understanding of the pathogenesis of AKI (171).

Histological changes after intrarenal AKI

Necrotic proximal tubules in the outer stripe of outer medulla represent the most dramatic findings evident by light microscopy after 30 minutes IRI in the mouse. Loss of brush borders and cell detachment from the basal membrane in the proximal tubule are also common findings. Tubular casts can be observed in downstream segments, with tubular dilation in the upstream cortical segments, although the glomeruli usually remain intact, at least under microscope. Those histological changes are directly related to the pathogenesis of AKI. As mentioned above, epithelial cell damage in the proximal tubule increases tubular fluid back leak. More fluid and solute are delivered to the distal nephron because of the inability to absorb solute in the proximal tubule, which activates tubuloglomerular feedback and reduces glomerular perfusion pressure. Cast formation in the downstream segments obstructs the nephrons and further reduces GFR. To some extent, histological damage can predict the kidney function (17, 171).

Endothelial dysfunction and hemodynamic changes after intrarenal AKI

Hemodynamic dysfunction is a major player in the pathogenesis of AKI. In many cases of AKI, a reduced renal blood flow is not sufficient to explain all of the change in

GFR (16, 17). The reduction in blood flow to outer medulla is greater than the decline in total renal blood flow. The medulla is relatively hypoxic in normal conditions due to the countercurrent exchange of oxygen between vasa recta, which is further occluded after AKI because of vulnerable anatomy of the capillaries (14, 18). Injured endothelial cells have exaggerated responses to mediators like endothelin-1 and angiotensin II but less responses to acetylcholine than normal renal vessels (17, 30). These factors together explain why this area has persistent hypoxia even when blood perfusion has restored for up to 2 days.

Inflammation after AKI

Inflammation plays an important role in the pathogenesis of AKI. Endothelial cells contribute to leukocyte migration by increasing the expression of intercellular adhesion molecule-1 (ICAM-1) and other adhesive molecules, which increases the rolling of leucocytes on the endothelial surface. Loss of endothelial cell-cell contacts also increases vascular permeability and promotes leukocyte migration. Tubular cell death might increase the release of intracellular contents such as fragmented DNA and enzymes which recruit not only innate immune responses involving neutrophils, macrophages, and NK cells, but also adaptive components such as dendritic cells and T lymphocytes. Shortly after AKI, those cells begin to accumulate in the kidney and last over several days after initial injury in mouse model. Inflammation after AKI causes further damage to the tubular cell. Reducing the inflammatory reaction after AKI can modulate the degree of injury (16, 17).

Tubular repair and fibrosis after intrinsic AKI

Tubular regeneration after AKI helps the kidney to restore normal function. It is clear that most regenerated tubular cells are derived from intrarenal cells rather than

mesenchymal stem cells or bone marrow stem cells that mainly exert paracrine effects to facilitate repair (77, 78, 103). Recent studies using lineage tracing techniques showed that damaged tubules mainly regenerate from intrinsic differentiated tubular cells. Surviving proximal tubular cells transiently dedifferentiate and adopt high regenerative capacities to repair injured tubular segments; however, the regenerated tubular cells are incomplete and often differ from normal tubules (181). This explains the long term risk of fibrosis and chronic kidney disease. Epithelial-mesenchymal transition (EMT) contributes to fibrosis because cells arrested at G2/M phase of the cell cycle generate transforming growth factor beta 1 (TGF-β1) and connective tissue growth factor (CTGF). The number of tubular cells arrested at G2/M can predicts the risk of long term fibrosis (180).

Major types of cell death

As important biologic processes, apoptotic cell death and autophagy are not only essential in normal development and homeostasis but also important in the pathogenesis of certain diseases. Autophagy is the basic catabolic mechanism that involves elimination of unnecessary or dysfunctional cellular components to preserve cellular homeostasis under baseline conditions and in response to stress. Autophagy also contributes to regulated cell death during embryonic development in *Drosophila melanogaster* and in the death of cancer cells exposed to chemotherapeutic agents, hypoxia, or specific autophagy-inducing peptides (49, 51, 52, 144).

Apoptosis is adenosine triphosphate (ATP)-dependent and is characterized by cell and organelle shrinkage, membrane blebbing, chromosome condensation, apoptotic body formation and phagocytosis. Apoptosis is generally not associated with inflammation and is considered as a less harmful type of cell death. The apoptotic mode of cell death has been comprehensively reviewed by several investigators (27, 98, 109, 132).

The third mode of cell death, necrosis, is ATP-independent and has its unique morphological characteristics such as increased cell or organelle volume (oncosis), mitochondrial swelling, rupture of the plasma membrane (cellular leakage), and consequent inflammation. Tissue detection of necrosis is usually defined in a negative fashion by excluding other types of cell death, such as apoptosis and autophagic cell death. Although the semiquantification of tissue necrosis is possible and mainly based on histology, its gross quantification remains a challenge.

Regulated necrotic cell death

As an important biologic process, cell death is not only essential in normal development and homeostasis but also important in the pathogenesis of certain diseases. In contrast to apoptosis, in which executive canonical pathway has been investigated and revealed in details, necrotic cell death was considered as a “passive” or “accidental” cell death and its molecular regulation remained largely unknown until recently. During last few years, more and more evidence suggests that necrotic cell death can be “programmed” and/or “regulated”. Multiple underlining pathways have been defined, such as necroptosis, parthanatos, ferroptosis, oxytosis, etc. Although these processes are characterized by their unique aspects of cell death processes, they also share some common features. Better understanding these different types of cell death may help us to understand the pathogenesis of certain diseases, thus provide some therapeutic targets for those diseases (50, 85, 115, 159).

Although necrosis is usually defined in a negative fashion, it has its unique morphological characteristics that are not seen in apoptosis (53, 85, 97, 159). Apoptosis is generally not associated with inflammation and it is considered as a less harmful type of cell death, while necrosis usually induces inflammation. A definite identification of necrosis in vivo may require electron microscope detection (97).

Apoptosis is initiated after the release of cytochrome c (cyt c) from mitochondria through outer mitochondrial membrane (OMM), which is formed by polymerization of Bax/Bak. Their insertion into the mitochondrial outer membrane generates a pore, leading to the leak of cyt c from the intermembranous space. In the contrast, necrosis involves the opening of inner and outer membranes of mitochondria. With increased permeability of inner mitochondrial membrane (IMM), it will no longer be able to generate ATP because of the loss of inner membrane potential. Clearly understanding the components of these transition pores across mitochondrial membrane is an important step to comprehend the mechanism of necrosis (71, 85, 115, 169).

As mentioned above, the pathophysiologic abnormalities of IRI are characterized by changes in renal hemodynamics, tubular injury and inflammation. IRI leads to many secondary effects on the renal parenchyma including dysfunction of cellular energy metabolism, production of reactive oxygen species (ROS) and DNA damage, which leads to activation of the nuclear repair enzyme poly(ADP-ribose) polymerase-1 (PARP-1) and the transcription factor p53. Activation of these molecules can induce necrotic and apoptotic tubular cell death, initiated by the opening of the mitochondrial permeability transition pore (MPTP), and outer mitochondrial membrane permeability, respectively (115, 116). Necrotic cell death in the proximal tubule after persistent ischemia translates a transient kidney dysfunction into irreversible kidney damage. Thus, focusing on the mechanism by which epithelial cells execute necrosis has the promising potentials to identify new therapeutic targets.

MPTP-mediated necrotic cell death

Although necrotic cell death has generally been considered as passive, blocking the functions of several molecules, including cyclophilin D (CypD), PARP-1 and receptor-interacting serine/threonine-protein kinase 1 (RIP1) kinase, can inhibit the classic

morphological characteristics of necrosis (50, 132). These studies provide evidence that necrosis is regulated and novel strategies to block necrosis could be developed. Necrotic cell death is associated with acute ischemic injury including myocardial ischemia, stroke, acute liver, kidney and lung injury, some of which are primarily due to MPTP formation (58). Upon MPTP formation, cytoplasmic water and solutes ≤ 1.5 kD in size move osmotically into the mitochondrial matrix, resulting in organelle swelling and eventual rupture and catastrophic energy failure, key events in necrotic cell death (10).

ROS and Calcium (Ca^{2+}) increase the probability of opening the MPTP, whereas adenine nucleotides (i.e., ADP and ATP) inhibit pore formation (13, 43). Ca^{2+}, the most noted mediator of permeability transition, enters the matrix via the mitochondrial calcium uniporter complex (MCU and MCUR1) driven by the highly negative membrane potential ($\Delta\psi$). ROS increase MPTP open probability whereas ADP and ATP inhibit pore formation (13, 43). Various molecular components of the IMM and OMM have been proposed to form the large, nonselective MPTP, including Bax/Bak (84), F1/F0 ATP synthase (3, 12, 15), voltage-dependent anion channel (VDAC), adenine nucleotide translocator (ANT), and CypD (9, 55, 63, 64, 93), although recent evidences support participation of CypD, Bax/Bak and the F1/F0 ATP synthase and is discussed below.

From the historical perspective, numerous molecular constituents of the MPTP, such as VDAC, ANT, and CypD, have been suggested as necessary for pore formation. Only the involvement of CypD has been successfully verified by genetic deletion. Until fairly recently, the model for the pore, including the ANT in the IMM with the VDAC in the OMM together forming a continuous channel across the IMS under the control of CypD, is rejected by recent evidence. Genetic deletion studies showed that ANT and VDAC are dispensable for pore formation (9, 93).

CypD is a mitochondrial matrix peptidyl-prolyl cis-trans isomerase and has an important role in controlling the opening of MPTPs (8). Convincing evidence obtained in

CypD-knockout mice suggests its relation to IRI in heart (129) and brain (140). Indeed, previous studies from our lab suggest that knockout of CypD can reduce renal IRI, mainly by reducing necrosis (34).

The identity of the OMM components of the MPTP and whether they are under the control of CypD remains largely unknown. In a recent report, Whelan et al found that mitochondria isolated from Bax/Bak double-null mouse embryonic fibroblasts (MEFs) were resistant to swelling and loss of membrane potential [Δψ] in response to Ca^{2+} challenge, suggesting that Bax/Bak is a required component of MPTP (174). Karch et al. showed that loss of Bax/Bak reduced OMM permeability (MOMP) and conductance without altering inner membrane MPTP function, but resulting in resistance to mitochondrial calcium overload and necrotic cell death (84). This result indicates that Bax/Bak regulates necrotic cell death by modifying MOMP. Collectively, these data suggest that the MPTP is an IMM-regulated process, although in the absence of Bax/Bak the OMM resists swelling and prevents organelle rupture to prevent necrotic cell death (84). The precise role of Bax/Bak in regulating the MPTP and necrosis in IRI has not been well studied.

A possible IMM component of the MPTP is the F1/F0 ATP synthase (Complex V) of the electron transport chain (15, 56). F1/F0 ATP synthases can physically interact with CypD and have the capacity to form the permeability transition pore in a Ca^{2+} dependent manner (55). This binding also decreases the catalytic activity of ATP synthase, which can be restored by cyclosporine A (CsA), an inhibitor of CypD; however, the mechanism by which the F1/F0 ATP synthase transforms from a catalytic conformation into a channel is still under intense investigation. Interestingly, the conformational change also converts the F1/F0 ATP synthase from ATP provider into ATP hydrolase, which depletes ATP and leads to necrotic cell death. Together with the action of CypD, the conformation change of F1/F0 ATP synthase ensues, leading to persistent MPTP opening and

irreversible damage to the cells (3). This hypothesis is in agreement with the role of Ca^{2+}-induced swelling, which induces release of the c-subunit from the F1, whereas CsA and ADP blocked this release.

PARP-1-mediated necrosis

The highly conserved PARP family consists of 18 members (4). PARP-1, the most studied member is an important nuclear enzyme that regulates protein functions by poly(ADP-ribosyl)ation and gene expression as a transcription cofactor (72). PARP-1 catalyzes the transfer of ADP-ribose from nicotinamide adenine dinucleotide (NAD^+) and conjugates poly(ADP-ribose) (PAR) onto various proteins as well as to PARP-1 itself, thus leading to a variety of physiologic processes including up- or down-regulation in protein function, conformational changes and promotion of protein-protein interactions (95, 96). Additionally, the role of PARP-1 as a transcriptional regulator is confirmed by genetic or pharmacological inhibition, demonstrating its influence on the expression of inflammatory genes including nuclear factor-κB (NFκB) (36, 69, 91), tumor necrosis factor-α (TNF-α) (25, 112), interleukin-1-β (IL1-β) (25), IL-6 (61, 112), ICAM-1 (61, 187), and toll like receptor 4 (TLR4) (187). Activation of PARP-1 is also required for DNA repair (68) and in the presence of DNA single- or double-strand breaks. PARP-1 transfers the ADP-ribose moiety of NAD^+ to various nuclear proteins and to PARP-1 itself. Excessive activation of PARP-1, such as in the setting of IRI, can lead to glycolytic inhibition (35), depletion of NAD^+, and consequent depletion of ATP (36). Glycolysis is dependent on NAD^+ and its depletion could lead to inhibition of ATP production through glucose metabolism. PARP-1 can also inhibit crucial enzymes in glucose metabolism, including glyceraldehyde 3-phosphate dehydrogenase (GAPDH) (62) and glucose phosphatase (hexokinase) (5) via poly(ADP-ribosyl)ation. This will further exacerbate ATP depletion and impair cellular viability, particularly in cells that are highly dependent

on glycolysis. Previous reports from our laboratory and others have demonstrated that PARP-1 inhibition or gene deletion is protective against ischemia-reperfusion (36, 124, 193), diabetes (143), and ureteral obstruction (92).

An alternative mechanism by which PARP-1-mediated cell death occurs is by parthanatos, where nuclear-to-mitochondrial translocation of PAR triggers translocation of apoptosis inducing factor (AIF) from mitochondria to nucleus. During translocation into the nucleus, AIF recruits an unidentified endonuclease, to mediate a caspase-independent cell death by inducing chromatin condensation and fragmentation into large fragments (~50 kb) (33) that are characteristic of parthanatos (45, 107). Despite the strong evidence for AIF-mediated cell death, the lack of AIF translocation in cell death models characterized by DNA damage and PARP also has been reported (44). These data demonstrate that parthanatos is dispensable in certain cell types or in response to certain cell death inducers, while it is the predominant pathway in other PARP-1-dependent models of cell death, suggesting that parthanatos is context-dependent.

Pharmacological inhibition or gene deletion of PARP-1 or knockout of PARP-1 can significantly reduce proximal tubule injury and preserve kidney function (124, 192). It is proposed that activation of PARP-1 not only depletes NAD+ and reduces ATP production to induce necrosis, but also modifies other molecules including p53 to facilitate necrosis. This notion is based on recent reports indicating that p53 can be poly(ADP-ribosyl)ated following DNA damage in neurons, which impacts p53 transcriptional regulation (121, 145). As a transcriptional factor, p53 has broad effects on gene expression. It is not clear if the expression of PARP-1 is regulated by p53 after IRI.

Expression and activation of p53 after IRI

The transcription factor p53, which was first identified as a tumor suppressor, conducts many essential cell functions like halting cell cycle, senescence, promoting

apoptosis and regulating cell metabolism (165, 166). Several studies have investigated the role of p53 after IRI. Kelly et al. first showed that the expression of p53 is increased in the medulla after IRI, and inhibition of p53 can reduce renal injury (87, 88). Molitoris et al. showed that p53–targeted siRNA attenuates ischemic acute kidney injury (126); however, Dagher et al. showed that the p53 inhibitor pifithrin-α can actually increase long-term renal fibrosis after IRI (32, 126). One study even showed protective effects of p53 on the kidney function after IRI (152). These conflicting results may reflect different experiment protocols and, probably more importantly, the global inhibition of p53 in cells including inflammatory cells. The use of p53 knockout (p53 KO) mice with the p53 gene specifically deleted in the proximal tubules is needed to focus on the role of p53 in the proximal tubular damage after IRI.

p53, glycolysis, and energy production

Like PARP-1, p53 plays a major role in ATP depletion selectively in the S_3 segments of the proximal tubule. p53 induces the expression and activation of Tp53-induced glycolysis and apoptosis regulator (TIGAR) selectively in proximal tubules after ischemia-reperfusion injury (90). The activation of TIGAR inhibits the rate-limiting, phosphofructokinase-1 activity and glucose 6-phosphate dehydrogenase activity (11, 59, 90). Therefore, it makes the proximal tubules more susceptible to ischemia and cell death in the settings of severe IRI. Thus TIGAR activation, along with PARP activation (35), could be key mechanisms involved in the cellular regulation of selective inhibition of glycolysis in the ischemic kidney proximal tubules.

p53, PARP-1 and CypD in necrotic cell death

Although it has been shown that p53 levels are significantly increased in the medulla 24 h after IRI (88), its contribution to necrotic cell death in the proximal tubule has not

been studied. Recently, it has been reported that p53 can interact with CypD and increases the opening of MPTP, thus inducing necrotic cell death (160); however, the authors found no alteration in Ca^{2+}-dependent MPTP opening, which is arguably the most fundamental regulator of permeability transition, suggesting that this may not be the only mechanism in necrotic cell death. Recent findings that p53, PARP-1, Bax/Bid and CypD participate in necrotic cell death insinuate that integration of their signaling pathways may be required to elicit necrotic cell death; however, the physical interactions and contributions of these molecules to necrotic cell death remain undefined. Given the marked interest in pharmacologically targeting necrotic pathways in IRI, delineation of these pathways may provide key insights to our understanding of the pathophysiology of IRI and to develop novel therapeutic strategies.

Necroptosis, MPTP-mediated necrosis and ferroptosis in AKI

The signaling pathway of necroptosis has been reviewed in detail recently (116, 134, 159). Briefly, necroptosis can be triggered by death receptors including TNF receptors (74, 164), stimulation of TLR (67, 81), signaling through interferon receptors (154), or recognition of intracellular viruses by DNA-dependent activator of interferon regulatory factors (157). These pathways can induce the association of RIPK1 and 3 via receptor-interacting protein–homotypic interacting motif (RHIM) RHIM-RHIM domain interactions and phosphorylation of RIPK3, which leads to aggregation of phosphorylated RIPK3 and phosphorylation of mixed lineage kinase domain-like (MLKL) by RIPK3 (108). Necroptosis generally occurs only if pro-survival transcriptional and/or apoptotic pathways are compromised. Although the terminal executive machinery of necroptosis is not completely clear, it is proposed that phosphorylation exposes the N-terminal portion of MLKL (128) to induce plasma membrane rupture and necroptosis, with release of damage-associated molecular pattern molecules (DAMPs) (20, 24, 168). Thus, MLKL

appears to be a key necroptotic effector, but exactly how it disrupts membranes is still not understood (39).

A contribution of necroptosis to ischemic injury in the kidney has been demonstrated by the protective effect of necrostatin-1 (Nec-1), which was considered as an inhibitor of RIPK1 (114). A protective role for Nec-1 in cisplatin- and hypoxia-injured tubular cells (155, 189), was also reported. Similarly, RIPK3-deficient mice were also shown to be protected against ischemic and cisplatin-induced AKI (113). A recent study questions the specificity of Nec-1 because it might have off-target effects on ferroptosis (47). Deletion of fas-associated protein with death domain (FADD) or caspase-8 or Nec-1 inhibition failed to protect isolated renal tubules from hypoxic injury (118). Similarly, the Nec-1 mediated protective effect in cyclosporin-mediated tubular damage (131) or contrast-mediated AKI (117) was not due to prevention of tubular cell death. These data suggest that the effect of genetic loss of RIPK3, or Nec-1 inhibition on reducing kidney ischemia-reperfusion injury may not be due to loss of necroptosis (118). Because these data argue against necroptosis as the primary mode of regulated cell death in renal tubules, the role of necroptosis in the pathogenesis of AKI was not pursued in this project.

Ferroptosis, a new type of cell death

Ferroptosis is a recently identified new type of cell death. It is characterized by an iron-dependent accumulation of lipid peroxides in the cell membrane. Evidence that ferroptosis plays an important role in acute renal failure was demonstrated by Angeli et al. in glutathione peroxidase 4 (Gpx4)-deficient human renal proximal tubular epithelial cells (47). Gpx4 catalyzes the reduction of hydrogen peroxide, organic hydroperoxides, and lipid peroxides utilizing reduced glutathione (GSH) and protects against oxidative stress. Gpx4 knockdown rendered cells susceptible to ferroptosis-inducing agents, indicating a Gpx4 regulated anti-ferroptotic machinery in the cells (47). In a recent study,

Linkermann et al. reported a significant role for iron-dependent ferroptosis in necrosis of renal tubules, in models of severe IRI and oxalate crystal-induced AKI (118). Pharmacological studies showed that the protective effects of the ferroptosis inhibitor ferrostatin (termed 16-86) are superior to Nec-1 and sanglifehrin A (SfA) (118). These data suggest that at least three independent pathways of regulated necrosis may be involved in IRI-mediated organ damage (118). Further studies to reveal the role in the pathogenesis of AKI are needed, since these data suggest its involvement. p53 as a transcription factor has been reported to be a regulator of ferroptosis by controlling the expression of SLC7A11, a glutamate/cysteine carrier in the membrane, which facilitates the transportation of cysteine into the cell and defends against ROS production. Activation of p53 after IRI might down regulate SLC7A11 carrier to induce ferroptosis in the epithelial cells, a hypothesis tested in this project through use of double and single knockout mice.

Therapeutic potentials targeting necrosis

Based on what we know now, a crucial step of PARP-1-and CypD-induced necrotic cell death is calcium influx and mitochondrial dysfunction (4, 43, 86). Blocking those steps might stop the positive feedback loop, and increase the chance of cell survival. Because the calcium is transported into mitochondria through the MCU transporter, this molecule was considered as a target to block calcium influx into mitochondria; however, knockout of MCU in heart did not significantly reduce infarct size after ischemia-reperfusion (120). It is possible that other mechanisms might be activated in the absence of MCU, for example ROS, which leads to the opening of MPTP.

Blocking Bax/Bak does not prevent all types of cell death, because the ATP synthase can still form the pore across the inner membrane (12, 15, 84). The presence of pore formation by ATP synthase suggests that MPTP formation is a fundamental biological

process that is important for normal biological function. It is not clear if blocking this conformational change will reduce necrosis after IRI.

CypD is another target that responds to calcium influx. It might be used to block calcium- or ROS-induced necrosis. Some evidence suggests that CsA can decrease cardiac infarction after coronary artery blockage (70). Knockout of CypD can also protect kidney tubular cells from necrotic cell death after IRI (46). If, indeed, mitochondrial dysfunction is required for PARP-1-induced necrosis, then blocking CypD should at least partially prevent PARP-1-induced necrosis.

Another possible therapeutic target is PARP-1 pathway. As mentioned above, this pathway involves multiple steps and molecules in a cascade fashion. Several PARP inhibitors have been used in laboratory studies including nicotinamide, benzamide, and newer imidazopyridine (4). The dilemma is that blocking PARP might impede DNA repair in the cell, although it can also reduce necrosis. In cancer therapy, those inhibitors are actually used to promote cell death, because of their action to block DNA repair machinery. Therefore, targeting PARP downstream molecules such as PAR, AIF, or endonuclease G might provide better results. For example, targeting the interaction between AIF and PAR or AIF and DNA might stop necrosis.

The successful application of these necrosis inhibitors in treating brain or heart ischemic diseases makes them promising candidates for treating IRI. Future studies will first need to assess the effectiveness of those drugs on the kidney function. Targeting the right segments of the nephrons that involved in the pathogenesis of IRI will be another challenge.

Cross talk between defined necrotic pathways

Attempts to integrate different types of necrotic cell death into a universal process have been made, yet it seems only some terminal changes overlapped (50, 85, 159).

Adding to this puzzle, injured cells will also manifest with a more necrotic cell death after inhibition of apoptotic pathways (50). How a cell chooses one type of cell death over the other is not well understand. One previous hypothesis is that inadequate energy production might be a reason why a cell falls into necrotic death rather than apoptosis, based on the observation that apoptosis consumes large amount of ATP, while necrosis is associated with mitochondrial dysfunction and energy depletion. If this hypothesis is true, then the status of mitochondria would be the crucial point deciding what type of cell death to develop.

PARP-1 regulates gene expression as a transcriptional cofactor and functions via poly (ADP-ribosyl)ation (4). In the presence of single- or double-strand breaks in DNA, PARP-1 transfers the ADP-ribose moiety of NAD+ to various nuclear proteins and to itself. Excessive activation of PARP-1, like in the setting of IRI, can lead to depletion of NAD+ and consequent ATP depletion. A possible mechanism relates to the sustained rise in cytosolic free calcium (Ca^{2+}) observed after ATP depletion (150). Uptake of Ca^{2+} by mitochondria as well as increased ROS levels in mitochondria during reperfusion triggers the opening of the MPTP, which requires a functional CypD.

The interaction between p53 and PARP-1 has long been established. In senescent and apoptosis cells, PARP-1 interacts with p53 and enhances the activation of p53. In the setting of necrotic cell death, the regulation of these two molecules has not been well studied, although one study showed that p53 regulates a nonapoptotic cell death through regulating the activity of PARP-1 after ROS injury (127). This suggests that PARP-1-mediated necrosis might be the downstream mechanism of p53-induced necrosis, although the translocation of p53 into mitochondria after injury could be another explanation. The use of in vivo and in vitro experiments may reveal the possible mechanisms of p53-induced necrosis and its unique role in IRI.

Can mitochondria be the downstream of necroptosis? Necroptosis was considered as an important type of cell death in IRI. Following the inhibition of caspase 8, stimulation of death receptor will lead to RIP1 will interact with RIP3, which is interfered by necrostatin-1 (117, 155, 189). The complex of RIP1/RIP3 will further activate MLKL, although the downstream mechanism is not completely understood (114). The MPTP seems to be part of the downstream machinery. First, the Bax/Bak seems to be indispensable for this type of cell death. Second, deletion of CypD can partially protect cells from necroptosis (83, 123). In contrast to these observations, in kidney IRI blocking both pathways after IRI has additive protection, which suggests that CypD dependent cell death and necroptosis are possible two separate pathways (113). Although PARP-1 was considered as the downstream target of RIP1/RIP3 complexes, recent evidences argue against this hypothesis (149). Inhibition of PARP-1 and its downstream effector molecules does not protect cells from TNF-induced necroptosis. Blocking TNF-induced necroptosis also does not prevent PARP-1-induced necrosis. All of this evidence suggests that PARP-1- or CypD-induced necrosis has an independent pathway other than necroptosis; however, the overlap between PARP-1- and CypD-induced necrosis is not well understood in the IRI setting.

Summary

Although our knowledge about necrotic cell death increased significantly during the past several years, the contribution of different types of cell death to the pathogenesis of AKI is not fully understood. First, although previous studies revealed the involvement of p53 in the pathogenesis of IRI, the role of p53 in AKI is not clearly demonstrated. Conflicting results were seen in the literature (31, 32, 88, 126, 152, 180). A properly designed experiment with reliable p53 inhibition in the kidney is needed. Secondly, the mechanism of p53-induced necrosis is not fully understood. Although there is some evidence suggesting that p53 can translocate into mitochondria and induce the opening of MPTP, it has never been tested in the renal injury model. Thirdly, it is not clear if there are any connections between different cell death pathways. If mitochondrial dysfunction and energy deficiency are crucial for PARP-1-induced necrosis, will deletion of CypD add more protection to PARP-1 knockout mice to protect kidney from AKI? Double knockout of these two genes is needed to answer those questions. Similarly, both PARP-1 and p53 are activated upon DNA damage. Although the connection between these two molecules has long been recognized, the overlapping and distinctive functions of PARP-1 and p53 in IRI are not clear. It is not known if double knockout of these two genes has stronger protective effects against IRI compared with knockout of either individual gene.

In this project, first we hypothesized that knockout of p53 in the proximal tubules protects the kidney from ischemic injury. Second, we explored the possible mechanisms for the p53-induced necrosis: 1). p53 translocates into mitochondria to induce the opening of MPTP; 2). p53 regulates the expression of PARP-1 and Bax, which induces necrosis after IRI; 3). By regulating the expression of SLC7A11, p53 induces ferroptosis

after IRI. Third, we tested if double knockout of PARP-1 and CypD or PARP-1 and p53 additively or synergistically protects kidney from ischemic injury.

Figure 1: A schema of our hypothesis.

Ischemia/reperfusion to the kidney parenchyma leads to many secondary effects including disruption of cellular energy metabolism, production of ROS, and DNA damage. These secondary effects lead to activation of the nuclear repair enzyme PARP-1 and the transcription factor p53. Further, activation of p53 can induce the expression of Bax, which facilitates the MOMP for necrosis. Activated PARP-1 rapidly depletes intracellular NAD+ and ATP, and simultaneously inhibits GAPDH, which reduces glycolytic capacity in proximal tubules. ROS and Ca^{2+} increase the probability of MPTP opening via activation of CypD. The mitochondrial translocation of p53 as a mechanism for p53-induced necrosis is also tested in this study (see the dashed line).

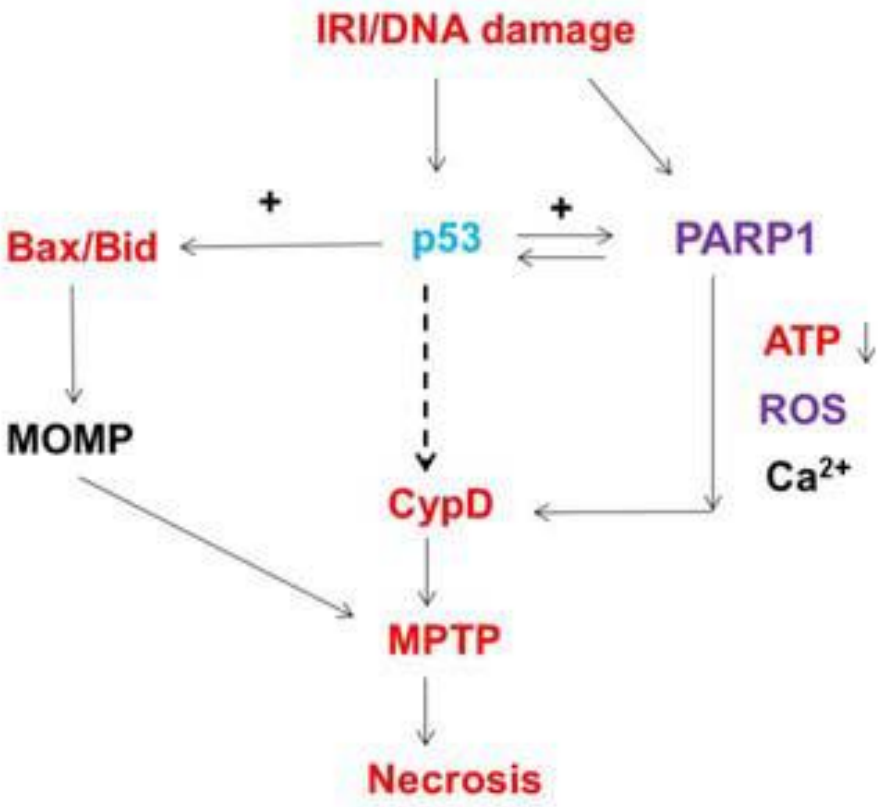

Figure 1. A schema of our hypothesis

CHAPTER 1: SPECIFIC DELETION OF p53 IN PROXIMAL TUBULE PREVENTS IRI [2]

Introduction

AKI is a clinical syndrome characterized by a rapid decline in GFR over a period of hours to days, leading to retention of metabolic waste products and disrupted fluid, electrolyte, and acid-base balance (16). IRI, which results from compromised perfusion of renal tissues, is the leading cause of AKI (110, 111). The persistent perfusion deficit in the medulla and limited anaerobic glycolytic capacity make the PT the most vulnerable tubular segment to ischemic injury (125, 162, 179). Pathologically, IRI is characterized by apoptotic/necrotic cell death and inflammation in the outer medulla, which are proportional to the severity of renal ischemia (87, 88). Pro- and anti-apoptotic signaling pathways in the proximal tubule cell are precisely regulated by essential factors such as p53, glycogen synthase kinase 3 beta and B-cell lymphoma 2 (BCL2) family proteins (26, 76, 88, 185). Therefore, it is crucial to understand the roles of these molecules in regulating tubular cell apoptosis in the pathogenesis of IRI.

The transcription factor p53, which was first identified as a tumor suppressor, performs many essential cell functions, such as halting the cell cycle, promoting senescence and apoptosis, and regulating cell metabolism (185). In response to various cell stresses and DNA damage, p53 is rapidly stabilized. Activated p53 controls the transcription of target genes that are usually key factors in cellular stress pathways (100). Classical models of p53 activation require three steps: stabilization, sequence-specific DNA binding, and transcription initiation through interaction with other transcription

[2] Some of the materials presented in this chapter were previously published: Yuan Ying, Jinu Kim, Sherry N. Westphal, Kelly E. Long, and Babu J. Padanilam. Targeted deletion of p53 in the proximal tubule prevents ischemic renal injury (183).

factors (100). Although the transcriptional activation of p53 was considered the major mechanism by which p53 responds to cell stresses, several studies suggest that transcription-independent activity of p53 can potentiate apoptosis by directly interacting with members of BCL2 family proteins (28, 185). Recently, Angelina et al. reported that p53 interacts with CypD and increases the opening of the mitochondrial permeability transition pore, thereby inducing necrotic cell death (160). These findings suggest that p53 may have additional functions in the cytoplasm separate from its transcriptional activity.

The involvement of p53 has been reported in nephrotoxic and ischemic renal injury (126, 170, 194). Although previous studies showed that p53 levels are significantly increased in the medulla 24 h after IRI (88), the contribution of p53 to tubular cell death and kidney dysfunction is still unclear. Further, global inhibition of p53 as a therapeutic strategy may not be feasible as it has a wide array of functions. Thus, considering the importance of p53 in promoting apoptotic/necrotic cell death, we hypothesized that knockout of p53 specifically in the proximal tubule significantly reduces tubular cell death and kidney dysfunction after IRI. This hypothesis was tested by using knockout mice with the p53 gene specifically deleted in the proximal tubule.

Methods

Generation of PT-specific p53 knockout (PTp53 KO) mice and global p53 KO rats. Homozygous p53–floxed mice (C57BL/6J background) were obtained from Jackson Laboratories (Bar Harbor, ME). The breeding strategy for transgenic mice that expressed Cre recombinase under the control of kidney-specific Pepck promoter (Pepck-Cre) was reported elsewhere. KO mice with the p53 gene specifically disrupted in renal proximal tubular epithelial cells (genotype p53fl/fl, Cre+/-) were developed by mating p53-floxed mice (wild type, WT) with Pepck-Cre transgenic mice. A routine PCR protocol was used for genotyping from tail DNA samples with the following primer pairs: Cre, 5'-CGGTGCTAACCAGCGTTTTC -3' and 5'- TGGGCGGCATGGTGCAAGTT -3'; and p53, 5'- GGTTAAACCCAGCTTGACCA -3' and 5'- GGAGGCAGAGACAGTTGGGA G -3'. Male littermates of genotype p53fl/fl, Cre-/- were used as controls (WT). p53 KO rats ($Tp53^{tm1(EGFP-Pac)}$ QlyRrrc) were obtained from Rat Resource & Research Center, University of MO, Columbia, MO. All animals were born at the expected Mendelian frequency and did not display any gross physical or behavioral abnormalities. Animal experiments were approved by the Institutional Animal Care and Use Committee of the University of Nebraska Medical Center.

Induction of IRI. IRI was induced in male mice as described previously (34-36). All animals were given free access to food and water. The mice were anesthetized by intraperitoneal administration of a cocktail containing ketamine (200 mg) and xylazine (16 mg) per kilogram of body weight. Ischemic injury was induced by bilateral renal pedicle clamping using microaneurysm clamps (Roboz Surgical Instrument, Gaithersburg, MD) and keeping mice core body temperature at 37℃. After 30 min of occlusion, the clamps were removed, and kidney reperfusion was verified visually. Sham-operated control animals underwent the same surgical procedure, except for the

occlusion of the renal arteries. During the surgery, all animals were placed on a heating pad to maintain body temperature at 37 ℃. Blood samples were collected at the time of sacrifice or from the orbital sinus under isoflurane anesthesia at 0, 6, 24 and 48 h post-IRI for measurement of serum creatinine and BUN. Similarly, rats were also given bilateral renal pedicle clamping for 45 minutes before repression. At the end of each time point (1 d, 5 d or 16 d), renal tissue was collected, fixed in Bouins solution or snap frozen using liquid nitrogen, and stored at -80°C for future experiments.

Measurement of plasma creatinine and BUN. Plasma creatinine and BUN were measured to evaluate renal function using a Quantichrom assay kit (BioAssay Systems, Hayward, CA) according to the manufacturer's protocol.

Morphological studies. Wild type and knockout mice that underwent IRI were sacrificed at 1 or 16 d. The kidneys then were processed at the University of Nebraska Medical Center histology core facility. Briefly, kidneys were fixed in formalin, embedded in paraffin, and cut into 5 μm sections. The tissue sections were then stained with Periodic acid-Schiff (PAS).

Immunofluorescence for neutrophils. Formalin-fixed mouse kidney sections were processed for immunostaining as described previously (192). The slides were sequentially incubated with rabbit anti-mouse neutrophil antibody (Accurate, Westbury, NY) at a 1:100 dilution overnight at 4 ℃, followed by FITC-conjugated goat anti-rabbit IgG (Vector Labs, Burlingame, CA) at a 1:200 dilution for 1 h at room temperature. Neutrophil infiltration was quantified by counting the number of stained cells per field.

Immunohistochemistry for macrophages and phospho-Histone-3 (p-H3) staining. Formalin-fixed mouse kidney sections were processed for immunostaining by sequential incubation with rabbit anti-F4/80 antibody (18705-1-AP, Proteintech, Chicago, IL) and anti-p-H3 antibody (sc-8656-R, Santa Cruz, Santa Cruz, CA) at a 1:100 dilution overnight at 4 ℃, followed by HRP-conjugated goat anti-rabbit IgG (Vector Labs,

Burlingame, CA) at a 1:200 dilution for 1 h at room temperature. The color development was induced by diaminobenzamide reagent (Vector Labs, Burlingame, CA) according to the manufacturer's instructions. Macrophage infiltration and p-H3 positive cells were quantified by counting the number of stained cells per field.

Lipid hydroperoxide assays were performed in the kidney extracts using kits (BioVision, Mountain View, CA) according to manufacturer's instructions.

Apoptosis detection by TUNEL staining. TUNEL staining of kidney tissue sections was carried out using the In Situ Cell Death Detection kit, Fluorescein (Roche, Indianapolis, Indiana) according to manufacturer's protocol.

Collagen deposition by Sirius red. The rehydrated paraffin sections were stained with Sirius red solution (0.1% Direct Red 80 and 1.3% picric acid; Sigma, St. Louis, MO) and washed twice in acidified water (0.5% acetic acid; Sigma). Then, the sections were dehydrated and cleared before being observed under the microscope (92).

α-smooth muscle actin (α-SMA) immunofluorescence staining. Formalin-fixed mouse kidney sections were processed for immunostaining as described previously (192). The slides were sequentially incubated with mouse anti-α-SMA antibody (A5228, Sigma) at a 1:500 dilution overnight at 4 ℃, followed by FITC-conjugated horse anti-mouse IgG (Vector Labs) at a 1:200 dilution for 1 h at room temperature. α-SMA deposition was quantified by measuring α-SMA positive area per field.

Western blot analysis. Briefly, whole renal tissue extracts (80 μg protein/lane) were separated on 10% SDS-PAGE gels and then transferred to Immobilon membranes (Millipore, Bedford, MA). The membranes were incubated with anti-p53 (2524, Cell Signaling, Beverly, MA), anti-p21 (sc-6246, Santa Cruz, Santa Cruz, CA), anti-activated Bax (sc-23959, Santa Cruz), anti-cleaved caspase-3 (9664, Cell Signaling), anti-Bid (611866, BD bioscience, San Jose, CA), anti-Siva (sc-48768, Santa Cruz), anti-α-SMA (A5228, Sigma), anti-p-Smad3 (ab51451, Abcam Cambridge, MA), anti-phospho-

Ser/Thr-Pro, MPM-2 antibody (05-368, Millipore) and anti-GAPDH (sc-25778, Santa Cruz) antibodies overnight at 4°C. After washing, the membranes were incubated with horseradish peroxidase-conjugated secondary antibodies against the appropriate primary antibodies (1:5,000, Vector Laboratories, Burlingame, CA), exposed to Western Lighting Plus-ECL (NEL104001EA; PerkinElmer, Waltham, MA), and then developed with X-ray film. The area of each band was analyzed using NIH image software (Image J). For quantification, band densities were measured using ImageJ. The relative densities were measured by dividing the density of target protein by the density of loading control (GAPDH) for the same lane. Then the fold changes were calculated by dividing each of the relative densities of target protein by the relative density of WT-sham. When only two lanes were used for comparison, the variability of the relative density of control group was calculated by normalizing the individual values of the controls to the mean of the control group.

Proximal tubular cell culture and in vitro experiment. Primary proximal tubule epithelial cells were isolated from PTp53 KO or WT male mice and cultured as described previously (35, 66). The porcine-derived proximal tubular cell line LLC-PK1 (ATCC, Rockville, MD) was cultured to 80 to 90% confluent monolayer cultures as described previously (136). The cells were incubated with 1, 2 or 5 mM H_2O_2 for 1 h to induce necrosis (127). These concentrations and times were chosen for trypan blue staining as previously described (35, 113). Pifithrin-α at different concentrations was administered in the culture media 30 min before injury. Lactate dehydrogenase (LDH) release was measured enzymatically using a CytoTox 96® Non-Radioactive Cytotoxicity Assay kit (Promega, Madison, WI).

Statistics. All data are expressed as means ± SE. Two-way and one-way ANOVA were used to compare the mean values of all groups, followed by Tukey's multiple comparison test to compare the mean values between two groups. An unpaired t-test

was also used to compare the means of two different groups. A *P* value < 0.05 was considered statistically significant.

Results

Deletion of p53 in the proximal tubule reduces p53 expression after IRI. We analyzed the expression of p53 and one of its target genes, p21, after injury in whole kidney tissues. Indeed, 24 h after IRI, the expression of p53 (Fig. 2A, B) and p21 (Fig. 2A, C) was significantly increased in WT male littermates to that in sham-operated mice kidneys. However, the expression level of p53 was only slightly increased and p21 expression was not altered in PTp53 KO mice after IRI compared to that in sham-operated mice kidneys. The slightly increased levels of p53 in IRI-induced PTp53 KO may be due to p53 expression in cells other than the PT. Due to the difficulty in detection of p53 in renal tissue, we carried out Western blot analysis for p53 in PT isolated from PTp53 KO mice. Our data further confirmed successful deletion of p53 in the PT (Fig. 3). These data suggest that p53 is induced and is involved in transcriptional regulation after IRI.

PT-specific knockout of p53 reduced deterioration of renal function after IRI. To test whether the absence of p53 in the PT changes the course of IRI, kidney function after IRI in PTp53 KO mice and in WT littermates was assessed. BUN levels were increased in WT mice 6 h after IRI and peaked during 24 - 48 h compared with WT sham-operated mice. The increase in BUN level was significantly less in PTp53 KO mice 6 - 48 h after IRI compared with WT mice (Fig. 4A). Plasma creatinine levels were also increased in WT mice 6 - 48 h after IRI compared with WT sham-operated mice. Similar to the BUN levels, the increase of plasma creatinine was less in PTp53 KO compared with WT at 6, 24, and 48 h after IRI (Fig. 4B). No significant difference in renal function occurred among sham-operated WT and KO mice (Fig. 4A and B). Moreover, there were no significant differences in BUN or plasma creatinine values between WT and heterozygous mice after IRI (data not shown). These data suggest that specific deletion

of the p53 gene in the proximal tubule leads to renal functional protection after IRI in mice.

PT-specific knockout of p53 decreased renal histological damage after IRI. Ischemic kidneys from WT mice showed widespread necrosis, brush border blebbing, and sloughed cells in the proximal straight tubule, whereas these features were much less apparent in ischemic kidneys from PTp53 KO mice. The histological changes after IRI were quantified by counting and scoring the percentage of tubules that displayed tubular necrosis, cast formation, and tubular dilation (Fig. 5A, B). The cumulative score of histological damage in the outer medulla at 1, 5 and 16 days as well as necrosis at 1 d (Fig 5C) was significantly lower in PTp53 KO kidneys compared with WT kidneys post-IRI, demonstrating that gene ablation of p53 reduced tubular damage and cellular necrosis.

Renal inflammation was reduced after IRI in PTp53 KO mice. The infiltration of leukocytes in the outer medulla of WT and PTp53 KO mice at 1, 5 and 16 days post-IRI was assessed by immunostaining for neutrophils and macrophages. As shown in representative photographs (Fig 6A and 7A), WT mice exhibited increased infiltration of neutrophils and macrophages in the outer medulla, which was attenuated in PTp53 KO mice. The numbers of positively stained cells were counted in a blinded manner and quantitative data indicate that the accumulation of neutrophils and macrophages was reduced in the outer medulla of PTp53 KO mice compared to that of WT mice at all-time points after IRI (Fig. 6B and 7B).

Attenuated oxidative stress after IRI in PTp53 KO mice. Oxidative stress was assessed by lipid hydroperoxide levels in the kidney. Quantification of the whole kidney lipid peroxide levels at 5h, 1 and 2 days post-IRI demonstrates that its levels were significantly decreased in PTp53 KO mice compared to that of WT mice at all time points (Fig 8A).

PT-Specific deletion of p53 decreased PARP-1 expression after IRI. PARP-1 can induce necrotic cell death after IRI. PARP-1 expression was examined by Western blot analysis. PARP-1 expression was significantly increased in WT kidneys after IRI but its expression was downregulated in PTp53 KO mice (Fig 8B). This novel finding suggests that increased PARP-1 function may be one of the mechanisms by which p53 activation regulates necrosis.

PT-specific KO of p53 decreased apoptosis after IRI. To determine whether there is a change of apoptotic levels in the outer medulla of WT mice compared with PTp53 KO mice, TUNEL assay was performed together with Western blot analysis for pro-apoptotic proteins. The outer medulla of wild type mice exhibited increased numbers of TUNEL-positive cells compared with that of PTp53 KO mice (Fig. 9). Cleaved caspase-3 expression was increased in WT kidney 24 h after IRI compared with p53 KO mice (Fig 10A, B) further confirming increased apoptosis. Similarly, Western blot analysis showed enhanced activation of Bax in the kidney of wild type mice compared with that of PTp53 KO mice 24 h after IRI, while total Bax was not changed. The expression of pro-apoptotic proteins Bid and Siva was also increased in WT mice after IRI in compared to PTp53 KO mice (Fig. 10A, C-E). These data suggest that specific deletion of p53 in the proximal tubule decreases apoptotic cell death after IRI by decreasing the levels of pro-apoptotic proteins.

Loss of p53 reduced renal fibrosis after IRI. To investigate whether deletion of p53 reduces renal fibrosis, collagen deposition in the kidneys of WT and PTp53 KO mice was measured using Sirius red staining and α-SMA immunofluorescence staining. Sixteen days after IRI, WT mice showed a dramatic increase of Sirius red-positive area in the kidneys compared with PTp53 KO mice, indicating that deletion of p53 reduces renal fibrosis in the later stage of IRI (Fig. 11A, B). No change in the Sirius red staining was seen at 5 d post-injury. α-SMA expression, on the other hand, was decreased in

PTp53 KO mice compared with WT mice at 5 after IRI, as demonstrated by immunostaining and Western blot analysis (Fig. 11C, D). p-Smad3, a downstream signaling molecule of TGFβ, was also increased in wild type mice, but significantly reduced in PTp53 KO mice at 16 d post-IRI (Fig. 12).

Loss of p53 reduced cell cycle arrest after IRI. Cell cycle arrest at G2/M phase is associated with late kidney fibrosis in ischemic renal injury. Histone H3 is phosphorylated during mitosis at Ser-10 in the G_2/M phase (142). p-H3 staining was performed to detect G2/M phase arrest. In wild type mice, the number of p-H3 positive cells was significantly higher compared with PTp53 KO mice at 1, 5 and 16 d after IRI (Fig. 13). To confirm that the cells are truly arrested at the G2 phase and not in mitotic phase, we assessed the number of mitotic cells at the above time points. Mitotic entry is accompanied by the phosphorylation of several molecules including MPM-2 (mitotic protein monoclonal 2) that may regulate the mitotic processes (101, 173). Immunostaining using anti-phospho-Ser/Thr-Pro, MPM-2 antibody (05-368, millipore) demonstrated that the number of cells at M phase was increased in WT mice 1 d after IRI compared with KO mice, but it only accounted for a small fraction of cells arrested at G2/M phase, indicating that most p-H3 positive cells were arrested at G2 phase (Fig. 14). The number of cells at M phase was negligible at 5 and 16 d in both WT and PTp53 KO mice tissues.

Loss of p53 reduced necrotic cell death of PTC. To further study the role of p53 in necrotic cell death, we used an in vitro H_2O_2-induced necrosis model. Necrosis was assayed using trypan blue staining and lactate dehydrogenase (LDH) release assay. After 1 h treatment with 1 or 2 mM H_2O_2, PTp53 KO primary PTC had less trypan blue-positive cells than WT PTC (Figure 15A). Pharmacological inhibition of p53 using pifithrin-α also reduced LDH release in LLC-PK1 cells after 5 mM H_2O_2 treatment (Figure

15B). These data indicate that deletion or inhibition of p53 reduces H_2O_2–induced necrosis.

Figure 2: p53 and p21 expression in p53 WT and PTp53 KO mice after IRI.

(A) Representative images of Western blot analysis showing expression levels of p53 and p21 at 24 h after IRI. (B, C) The expression levels of p53 and p21 in sham and IRI-induced kidneys were quantified (n = 4 in each group). * $P < 0.05$ compared with WT-IRI; † $P < 0.05$ compared with WT-Sham. GAPDH served as a loading control (183).

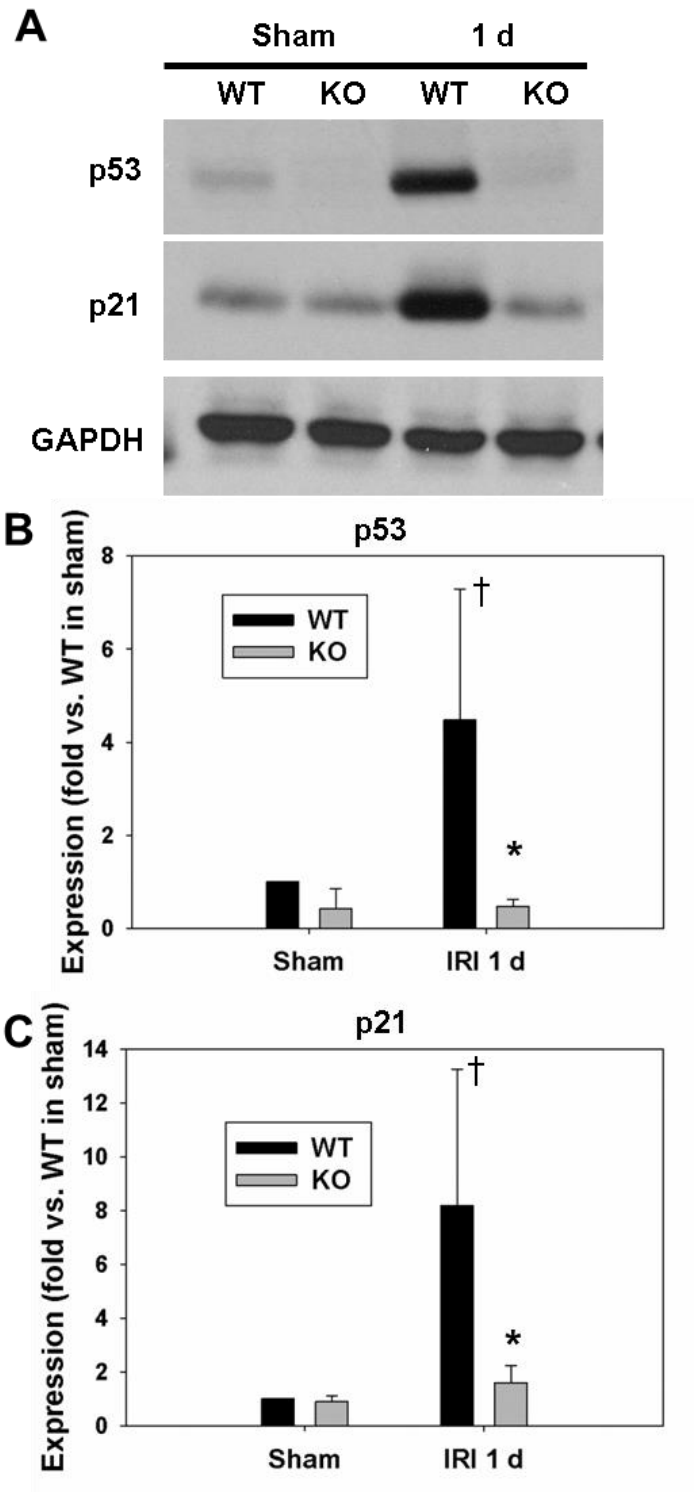
A
Sham
1 d
WT
KO
WT
KO
p53
p21
GAPDH
B
p53
Expression (fold vs. WT in sham)
WT
KO
†
*
Sham
IRI 1 d
C
p21
Expression (fold vs. WT in sham)
WT
KO
†
*
Sham
IRI 1 d

Figure 3: Western blot showing p53 levels in proximal tubules of WT and PTp53 KO mice before IRI.

* $P < 0.05$ compared with WT, $n = 4$ (183).

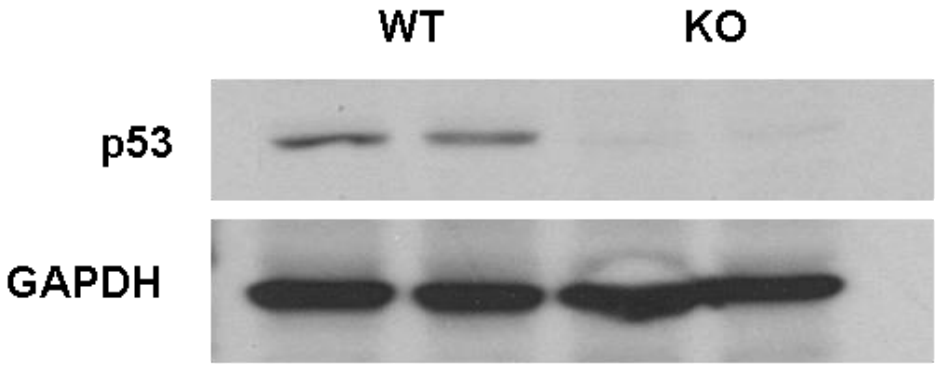
WT
KO
p53
GAPDH

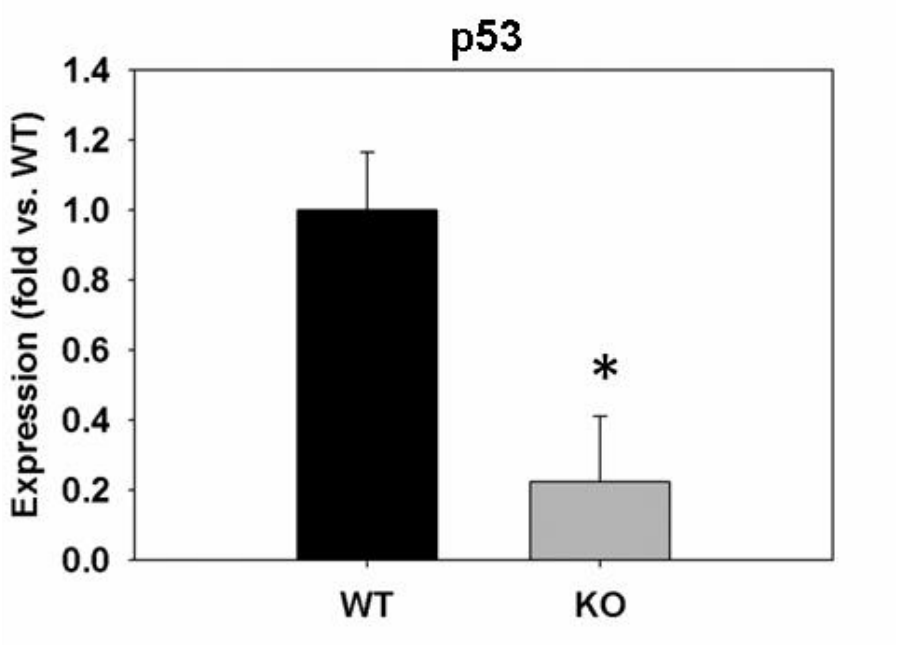
p53
Expression (fold vs. WT)
1.4
1.2
1.0
0.8
0.6
0.4
0.2
0.0
*
WT
KO

Figure 4: Kidney function in p53 WT and KO mice after IRI.

(A) Plasma creatinine and (B) BUN levels from WT and PT p53 KO mice (*n* = 6) at 6 h, 1 d, 2 d and 3 d after IRI. * *P* < 0.05 compared with WT-IRI; † *P* < 0.05 compared with WT-Sham (183).

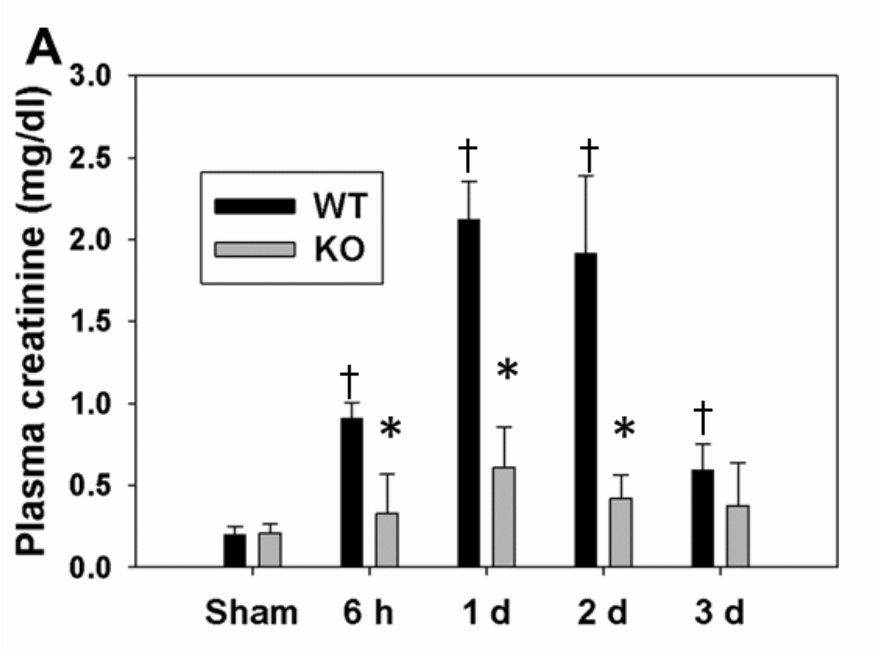
A
Plasma creatinine (mg/dl)
3.0
2.5
2.0
1.5
1.0
0.5
0.0
WT
KO
†
*
Sham
6 h
1 d
2 d
3 d

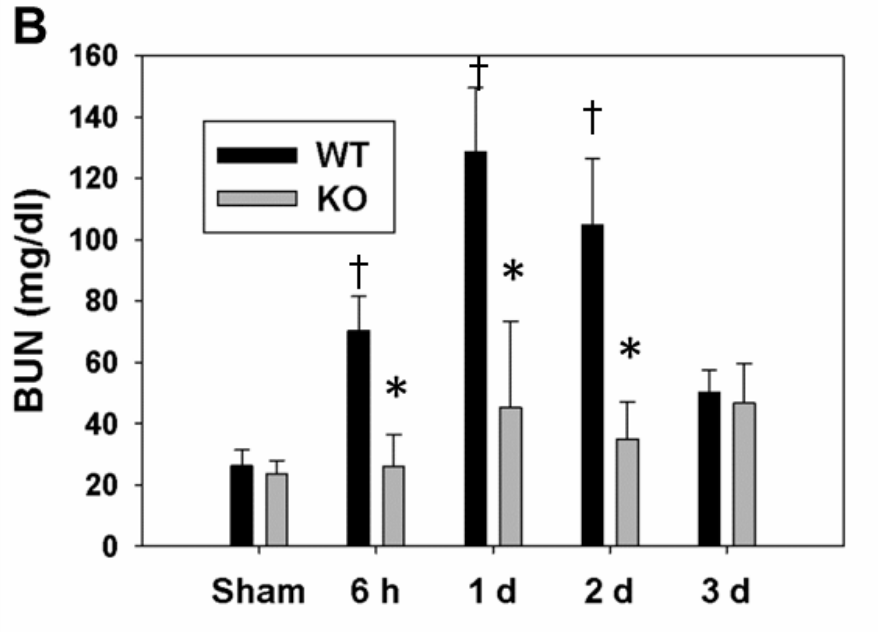
B
BUN (mg/dl)
160
140
120
100
80
60
40
20
0
WT
KO
†
*
Sham
6 h
1 d
2 d
3 d

Figure 5: Kidney histological changes in p53 WT and PTp53 KO mice after IRI.

(A) WT or PTp53 KO mice underwent sham surgery or IRI. Renal histological changes in the outer medulla after IRI were assessed by PAS staining at 1, 5 and 16 d after IRI. Magnification is 400×. (B) Histological damage in the outer medulla assessed in PAS-stained kidney sections was scored by counting the percentage of tubules that displayed tubular necrosis, cast formation, and tubular dilation as follows: 0 = normal; 1 = < 10%; 2 = 10–25%; 3 = 26–50%; 4 = 51–75%; and 5 = > 75%. Ten fields (200× magnification) per kidney were used for counting. (C) The number of necrotic tubules was counted in PAS-stained kidney sections at 1 d after IRI. *P < 0.05 compared with WT-IRI; † P < 0.05 compared with Sham (same genotype); n = 6 (183).

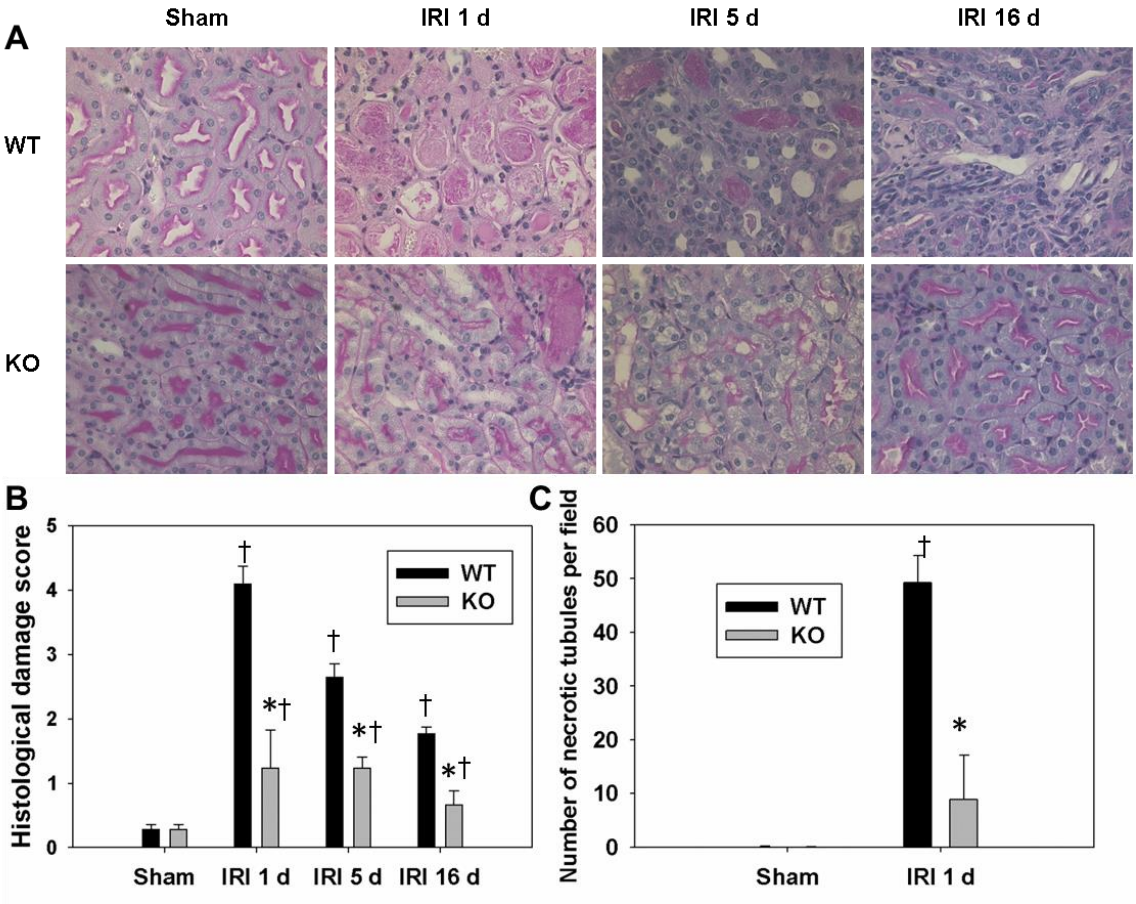
A
Sham
IRI 1 d
IRI 5 d
IRI 16 d
WT
KO
B
Histological damage score
WT
KO
Sham
IRI 1 d
IRI 5 d
IRI 16 d
C
Number of necrotic tubules per field
WT
KO
Sham
IRI 1 d

Figure 6: Neutrophils infiltration in the kidney after IRI.

(A) Typical neutrophil accumulation in the outer medulla of WT and PTp53 KO kidneys at 1, 5 and 16 d post IRI. Neutrophils (PMN) were identified by immunofluorescence using a neutrophil-specific antibody. Number of neutrophils (B) accumulation in the outer medulla of WT and p53 KO kidneys post-IRI was measured at 1, 5 and 16 d after IRI in high magnification (200×) fields. * $P < 0.05$ compared with WT-IRI; † $P < 0.05$ compared with WT-Sham; $n = 4$ (183).

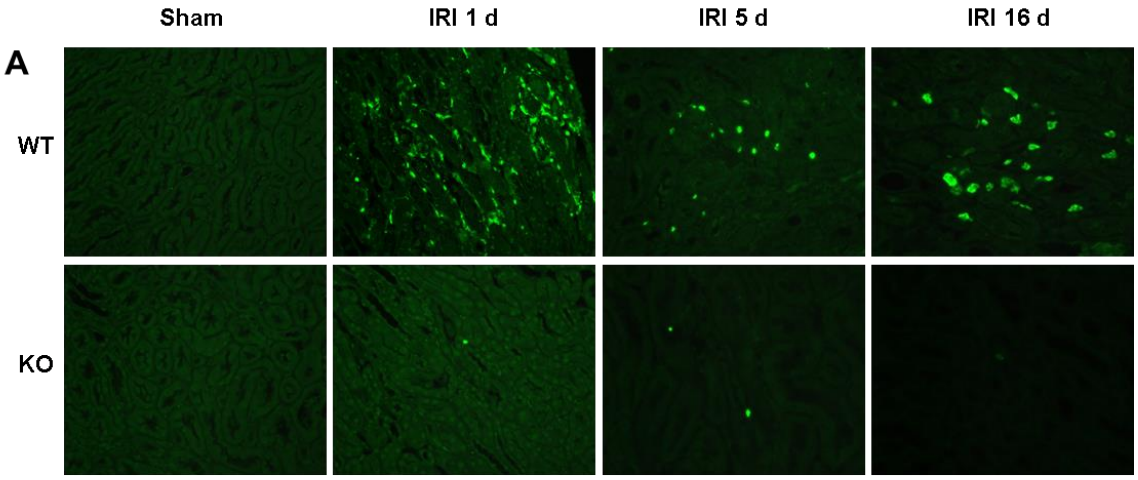
Sham
IRI 1 d
IRI 5 d
IRI 16 d
A
WT
KO

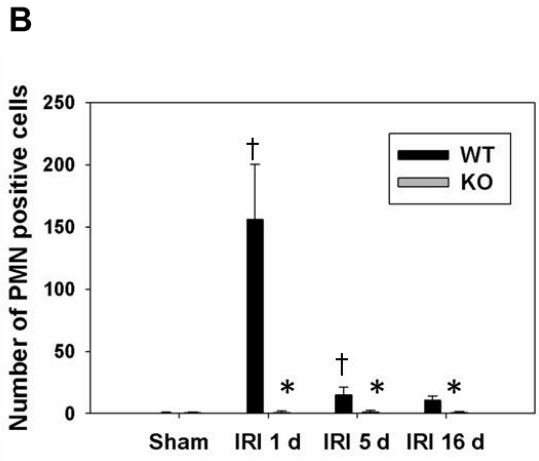
B
Number of PMN positive cells
250
200
150
100
50
0
WT
KO
†
†
*
*
*
Sham
IRI 1 d
IRI 5 d
IRI 16 d

Figure 7: Macrophages infiltration in the kidney after IRI.

(A) Typical macrophage accumulation in the outer medulla of WT and PTp53 KO kidneys at 1, 5 and 16 d post IRI. Macrophages were identified by DAB staining using anti-F4/80 antibody. Images are representative of four independent experiments. Number of macrophages (B) accumulation in the outer medulla of WT and p53 KO kidneys post-IRI was measured at 1, 5 and 16 d after IRI in high magnification (200×) fields. * $P < 0.05$ compared with WT-IRI; † $P < 0.05$ compared with Sham (same genotype); $n = 4$ (183).

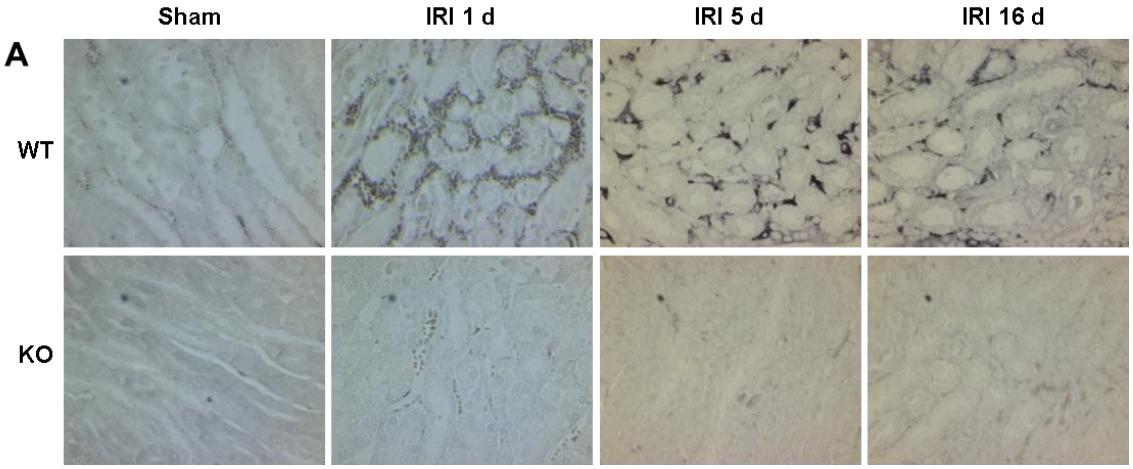
Sham
IRI 1 d
IRI 5 d
IRI 16 d
A
WT
KO

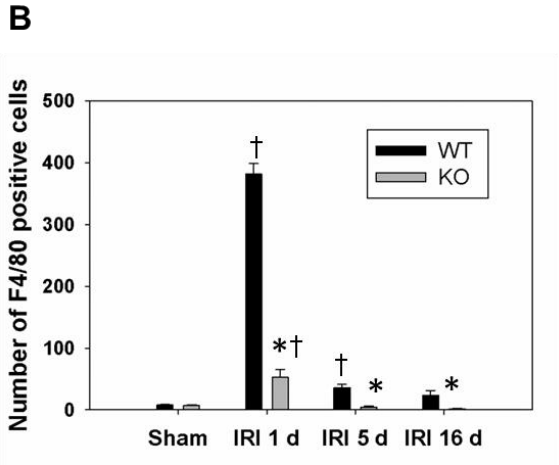
B
Number of F4/80 positive cells
500
400
300
200
100
0
WT
KO
†
*†
†
*
*
Sham
IRI 1 d
IRI 5 d
IRI 16 d

Figure 8: Lipid hydroperoxide levels and PARP-1 expresion in the WT and PTp53 KO mice after IRI.

(A) Lipid hydroperoxide levels in the WT and PTp53 KO mice after IRI. *P < .05 compared with WT-IRI; n = 6. (B) Western blots showing increased expression of PARP-1 24 h after IRI in WT kidneys. * P < 0.05 compared with WT-IRI; † P < 0.05 compared with WT-Sham; n = 3 (183).

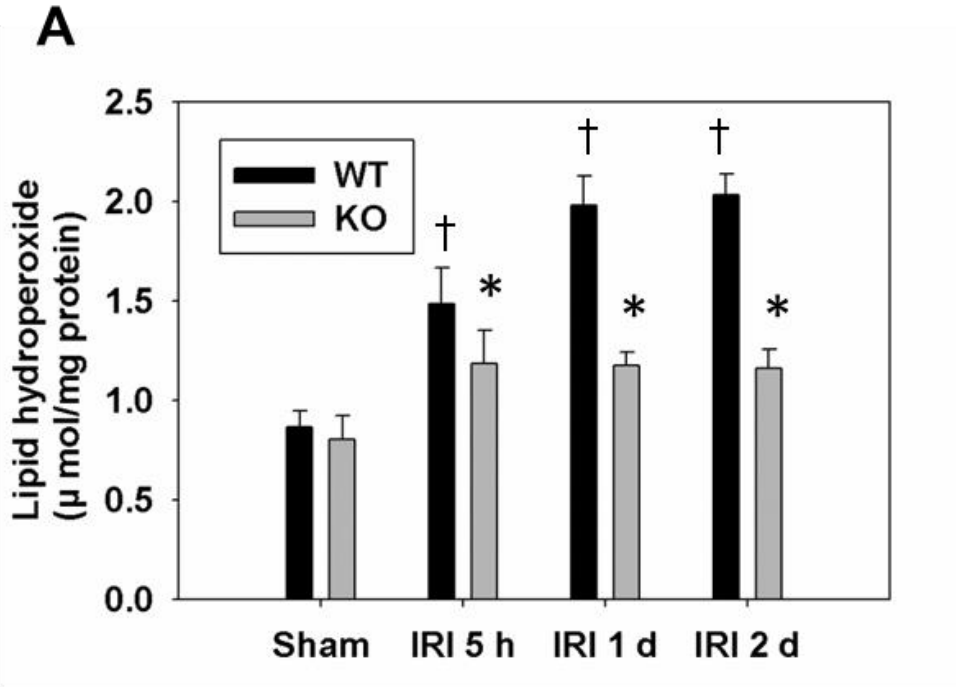
A
Lipid hydroperoxide (μ mol/mg protein)
2.5
2.0
1.5
1.0
0.5
0.0
WT
KO
†
*
Sham
IRI 5 h
IRI 1 d
IRI 2 d

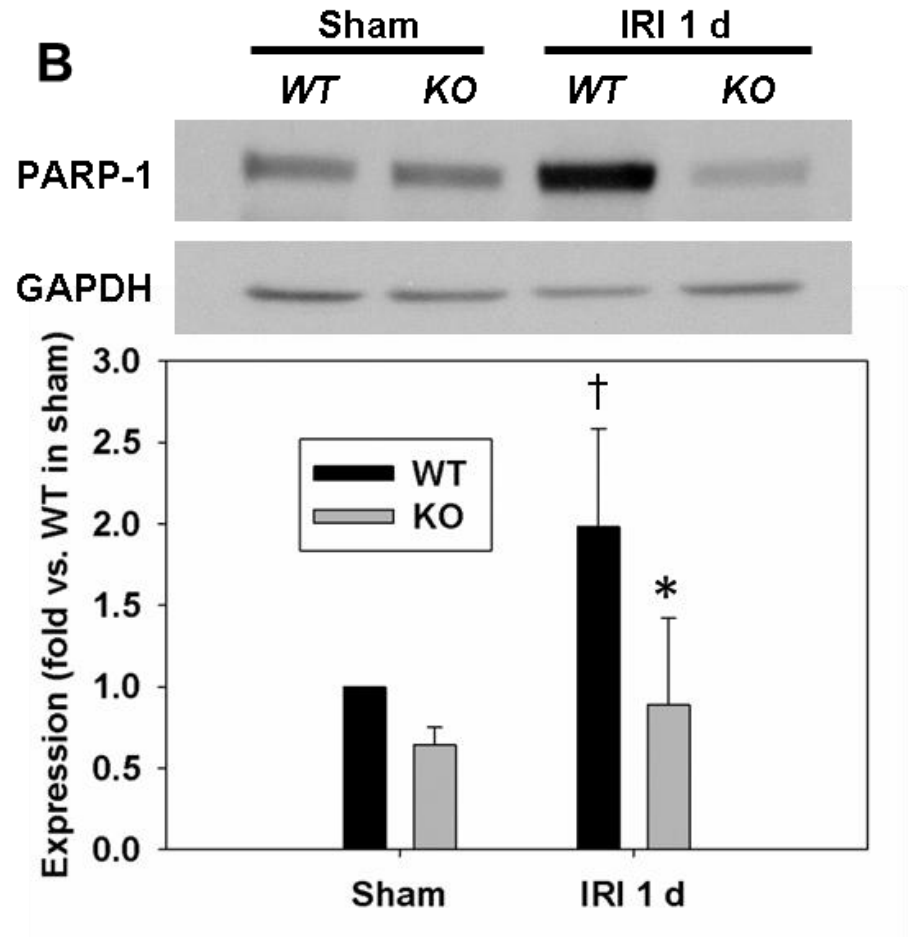
B
Sham
IRI 1 d
WT
KO
WT
KO
PARP-1
GAPDH
Expression (fold vs. WT in sham)
3.0
2.5
2.0
1.5
1.0
0.5
0.0
WT
KO
†
*
Sham
IRI 1 d

Figure 9: TUNEL staining for apoptosis after IRI.

(A) Apoptosis detection by TUNEL staining in WT and PTp53 KO kidneys at 1, 5 and 16 d post IRI. Images are representative of four independent experiments. (B) TUNEL assay to detect apoptotic cells was done using the In Situ Cell death detection kit in kidneys derived from WT or PTp53 KO at 1, 5 and 16 d after IRI. Number of TUNEL positive cells was measured in 10 randomly chosen high magnification (200×) fields per kidney. * $P < 0.05$ compared with WT-IRI; † $P < 0.05$ compared with WT-Sham; $n = 5$ (183).

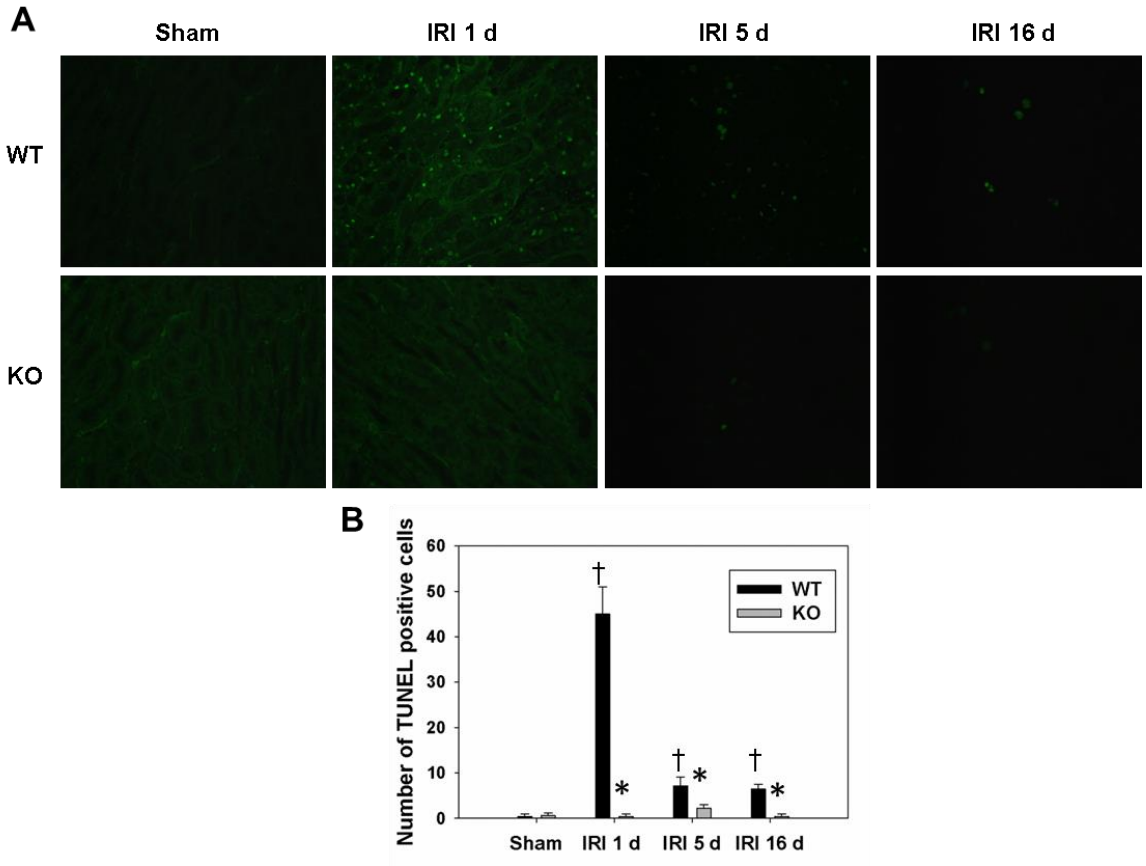
A
Sham
IRI 1 d
IRI 5 d
IRI 16 d
WT
KO
B
Number of TUNEL positive cells
60
50
40
30
20
10
0
WT
KO
†
*
Sham
IRI 1 d
IRI 5 d
IRI 16 d

Figure 10: The expression of apoptotic molecules after IRI.

(A-E) Representative Western blots images showing increased expression of cleaved Caspase-3, Bax, Bid, and Siva in WT and PTp53 KO mice after 24 h IRI. * $P < 0.05$ compared with WT-IRI; † $P < 0.05$ compared with WT-Sham; $n = 3$-5 (183).

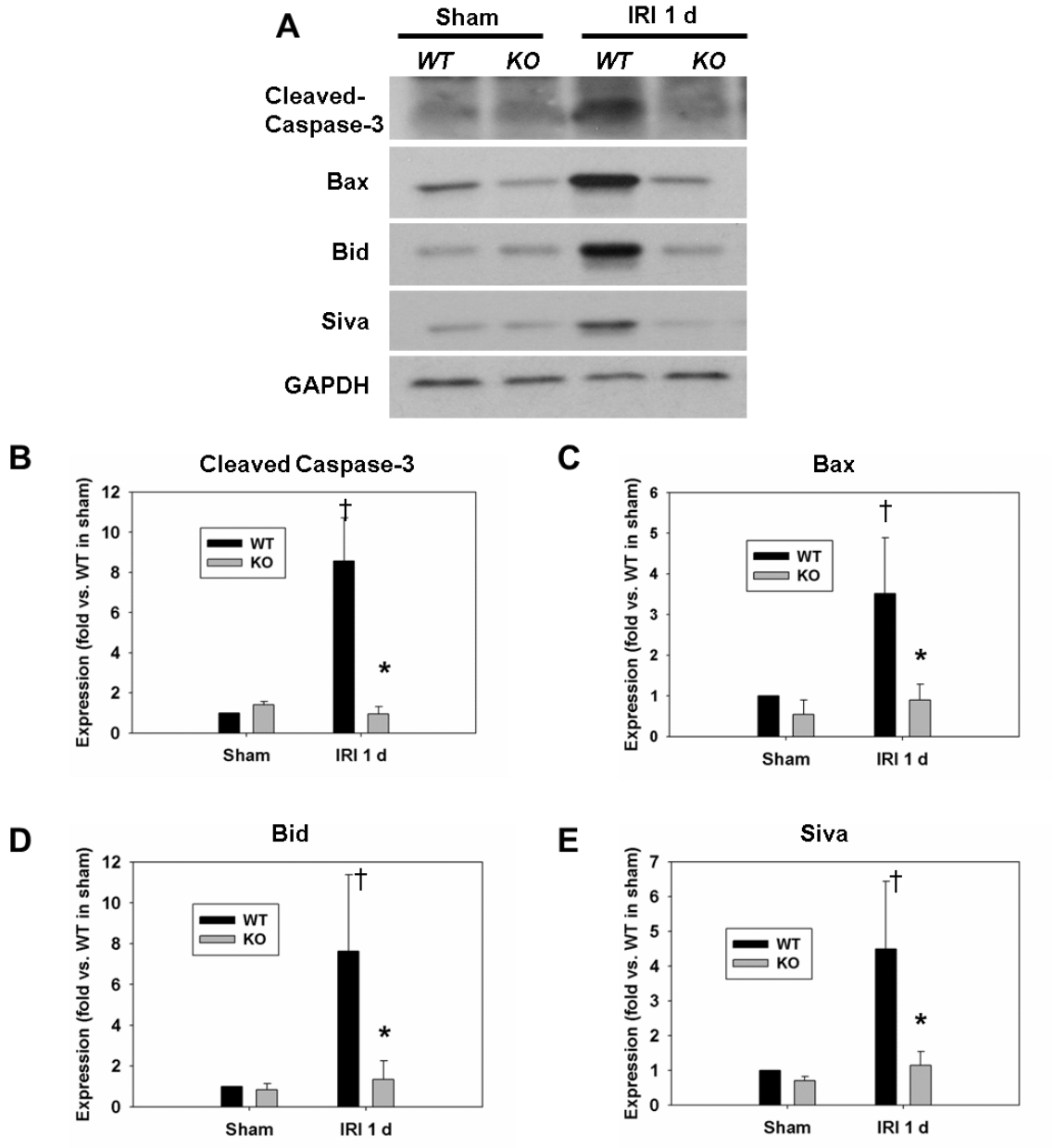
A
Sham
IRI 1 d
WT
KO
WT
KO
Cleaved-Caspase-3
Bax
Bid
Siva
GAPDH
B
Cleaved Caspase-3
C
Bax
D
Bid
E
Siva
Expression (fold vs. WT in sham)
WT
KO
Sham
IRI 1 d
†
*

Figure 11: Kidney fibrosis in WT and PTp53 KO kidneys after IRI.

(A) Collagen deposition detected by Sirius red staining in WT and PTp53 KO kidneys at 5 and 16 d after IRI; (B) The Sirius red-positive area was measured in four randomly chosen high power (200×) fields per kidney using the NIH Image J software. (C, D) Immunofluorescence staining of α-SMA in outer medulla. The α-SMA -positive area was measured in four randomly chosen high power (200×) fields per kidney. * $P < 0.05$ compared with WT-IRI; † $P < 0.05$ compared with Sham (same genotype); $n = 4$ (183).

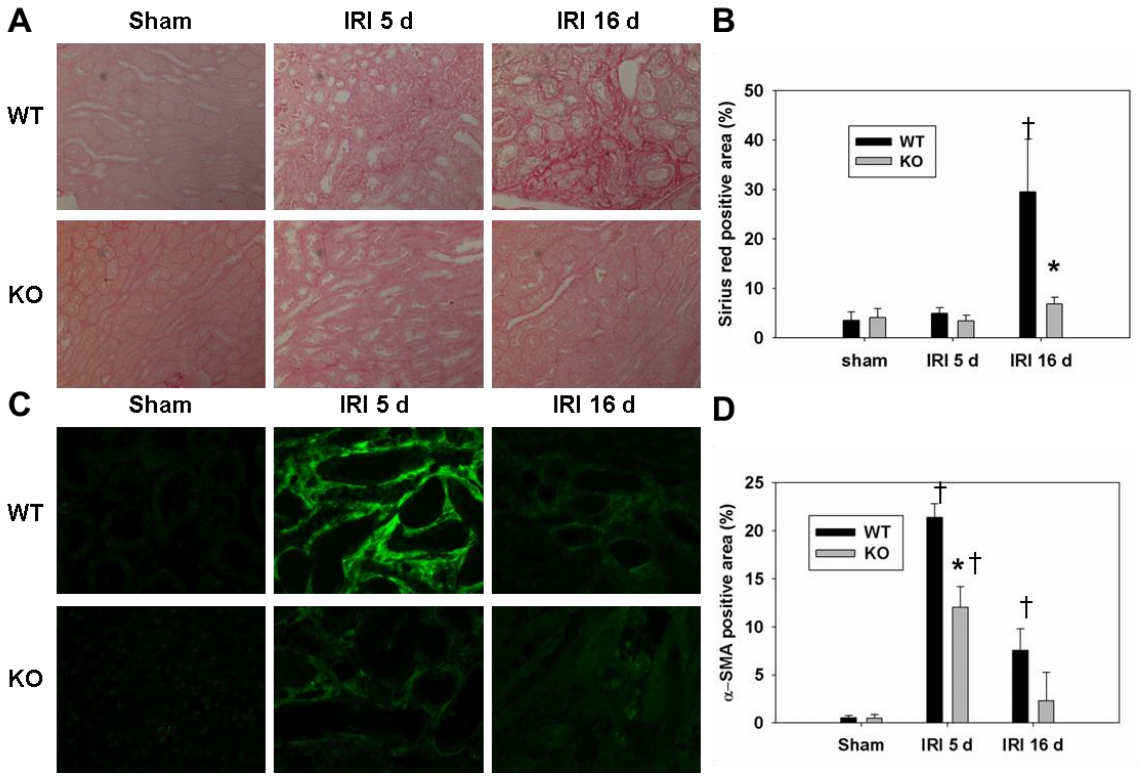
A
Sham
IRI 5 d
IRI 16 d
WT
KO
B
Sirius red positive area (%)
50
40
30
20
10
0
WT
KO
†
*
sham
IRI 5 d
IRI 16 d
C
Sham
IRI 5 d
IRI 16 d
WT
KO
D
α–SMA positive area (%)
25
20
15
10
5
0
WT
KO
†
*†
†
Sham
IRI 5 d
IRI 16 d

Figure 12: The expression of α-SMA and p-Smad3 in WT and PTp53 KO kidneys after IRI.

(A, B) Representative Western blot images and quantified data for expression of α-SMA in WT and PTp53 KO kidneys at 1, 5, and 16 d after IRI. (A, C) Representative Western blots films and quantified data for expression of p-Smad3 in WT and PTp53 KO kidneys at 1, 5, and 16 d after IRI. * $P < 0.05$ compared with WT-IRI; † $P < 0.05$ compared with Sham (same genotype); $n = 3$. GAPDH served as a loading control (183).

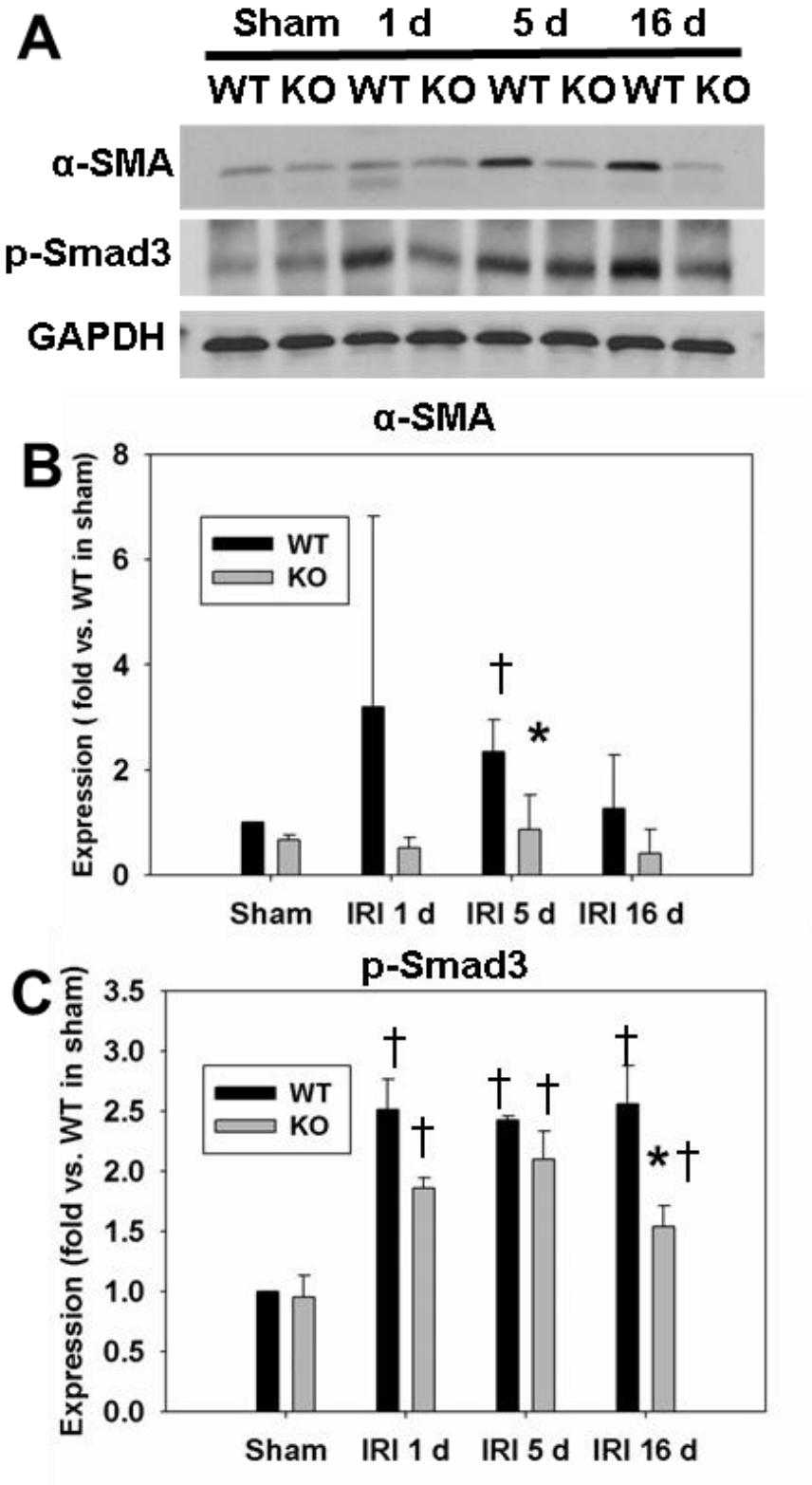
A
Sham
1 d
5 d
16 d
WT KO WT KO WT KO WT KO
α-SMA
p-Smad3
GAPDH
α-SMA
B
Expression (fold vs. WT in sham)
WT
KO
Sham
IRI 1 d
IRI 5 d
IRI 16 d
p-Smad3
C
Expression (fold vs. WT in sham)
WT
KO
Sham
IRI 1 d
IRI 5 d
IRI 16 d

Figure 13: Cell cycle arrest at G2/M phase after IRI.

(A) Cell cycle arrest at G2/M phase was analyzed by p-H3 staining. Representative images of p-H3 staining in WT and PTp53 KO kidneys at 1, 5 and 16 d after IRI. Images are representative of five independent experiments. (B) Number of p-H3 positive cells in WT and PTp53 KO kidneys at 1, 5, and 16 d after IRI was counted in 10 randomly selected high power (200×) fields per kidney. * $P < 0.05$ compared with WT-IRI; † $P < 0.05$ compared with WT-Sham; $n = 4$ (183).

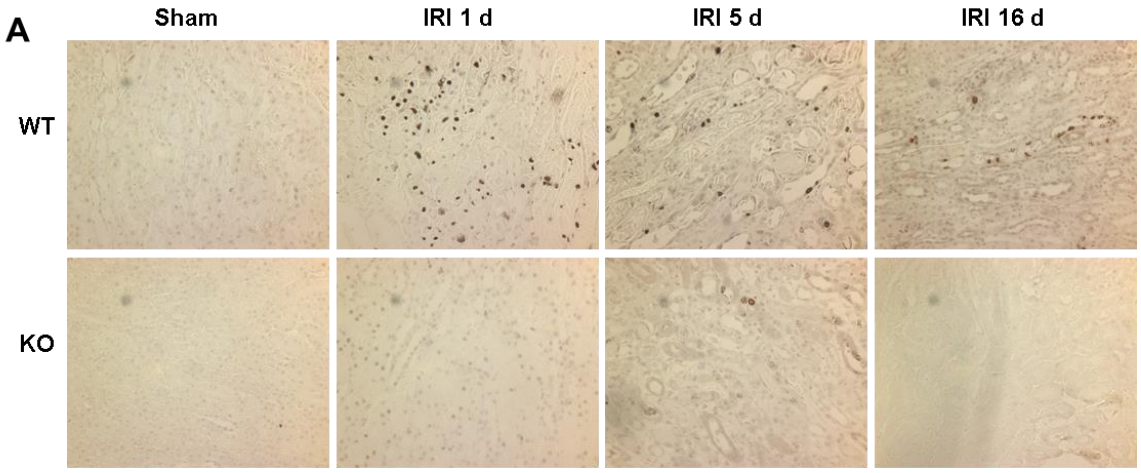
A
Sham
IRI 1 d
IRI 5 d
IRI 16 d
WT
KO

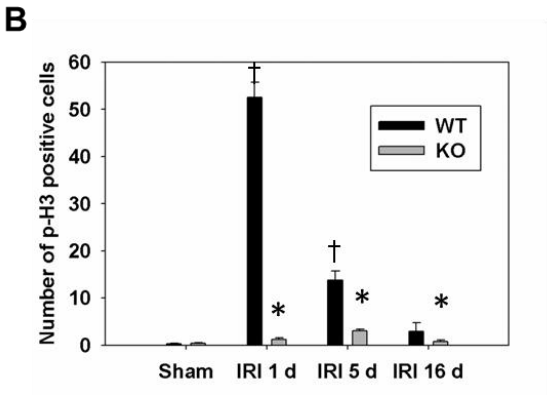
B
Number of p-H3 positive cells
60
50
40
30
20
10
0
WT
KO
†
*
Sham
IRI 1 d
IRI 5 d
IRI 16 d

Figure 14: Cells arrested at M phase after IRI in WT and PTp53 KO kidneys.

(A, B) Cells at M phase were marked by anti-phospho-Ser/Thr-Pro MPM-2 antibodies. * $P < 0.05$ compared with WT-IRI 1 d; † $P < 0.05$ compared with WT-Sham; $n = 4$ (183).

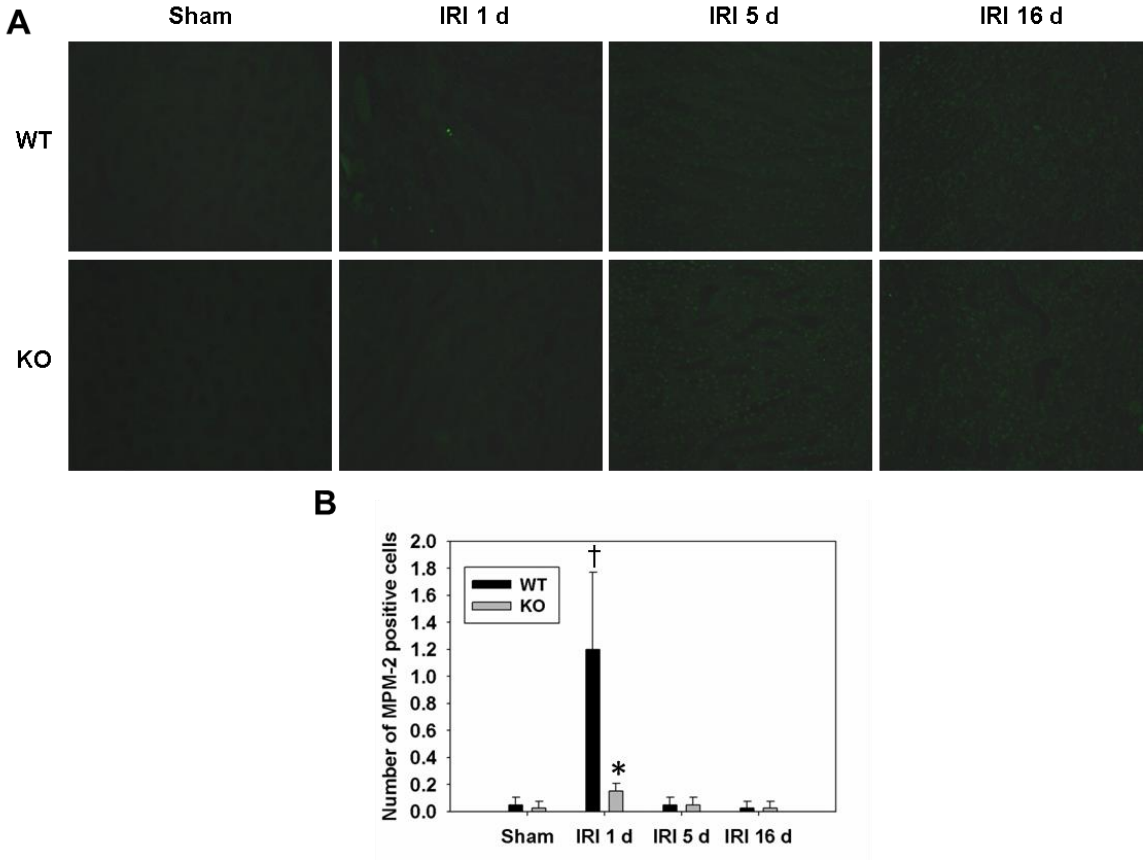
A
Sham
IRI 1 d
IRI 5 d
IRI 16 d
WT
KO
B
Number of MPM-2 positive cells
2.0
1.8
1.6
1.4
1.2
1.0
0.8
0.6
0.4
0.2
0.0
WT
KO
†
*
Sham
IRI 1 d
IRI 5 d
IRI 16 d

Figure 15: The protective effects of p53 deletion or inhibition on necrosis in vitro.

(A) Percentage of trypan blue positive cells after H_2O_2 treatment in primary PTC derived from PTp53 KO compared with WT mice cells. * $P < 0.05$ compared with WT-H_2O_2 treatment; † $P < 0.05$ compared with WT-control; $n = 4$. (B) Percentage of LDH activity after 5 mM H_2O_2 treatment in LLC-PK1 cells with or without different concentrations of the p53 inhibitor pifithrin-α. * $P < 0.05$ compared with H_2O_2 treatment alone; † $P < 0.05$ compared with control; $n = 4$ (183).

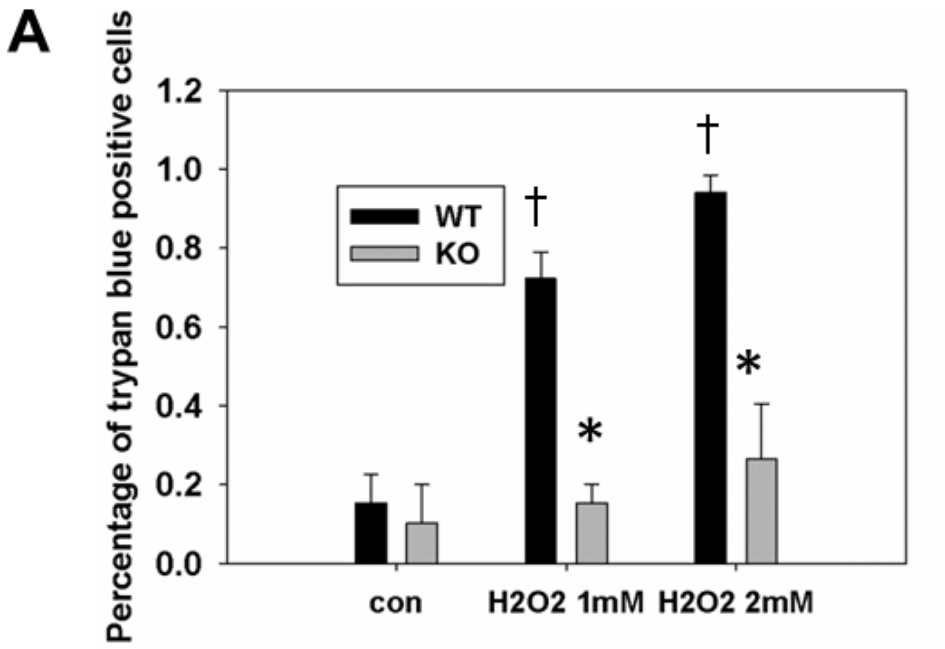
A
Percentage of trypan blue positive cells
1.2
1.0
0.8
0.6
0.4
0.2
0.0
WT
KO
†
†
*
*
con
H2O2 1mM
H2O2 2mM

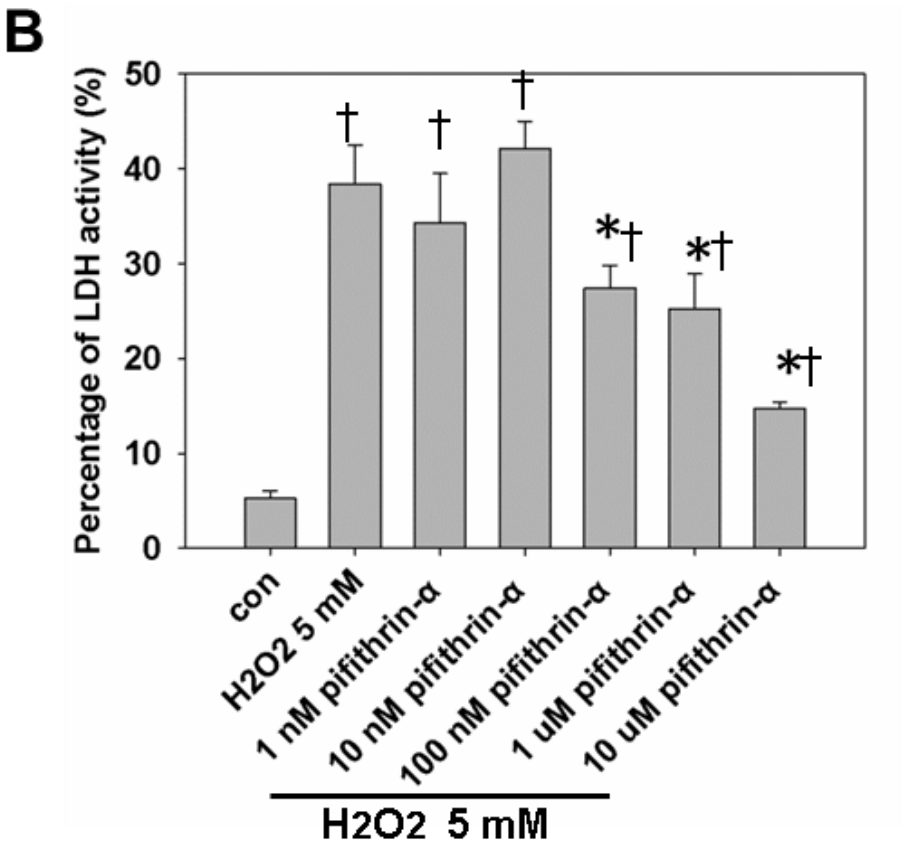
B
Percentage of LDH activity (%)
50
40
30
20
10
0
†
†
†
*†
*†
*†
con
H2O2 5 mM
1 nM pifithrin-α
10 nM pifithrin-α
100 nM pifithrin-α
1 uM pifithrin-α
10 uM pifithrin-α
H2O2 5 mM

Global knockout of p53 in rats did not protect renal function after IRI. To test whether the absence of p53 in the whole kidney protects kidney function after IRI in p53 KO rats and in WT littermates, BUN levels were increased in WT rats 24 h after IRI compared with WT sham-operated rats. p53 KO and heterozygous rats had similar levels of BUN 24 h after IRI compared with WT rats (Fig. 16). Plasma creatinine levels were also increased in WT rats 24 h after IRI compared with WT sham-operated rats. Similar to the BUN levels, p53 KO and heterozygous rats had comparable levels of creatinine 24 h after IRI compared with WT rats (Fig. 16). These data suggest that global deletion of the p53 gene does not lead to renal functional protection after IRI in rats.

Global knockout of p53 in rats did not decrease renal histological damage after IRI. Ischemic kidneys from WT rats showed widespread necrosis, brush border blebbing, and sloughed cells in the proximal straight tubule. Similar features were observed in ischemic kidneys from p53 KO rats. The histological changes after IRI were quantified by counting and scoring the percentage of tubules that displayed tubular necrosis, cast formation, and tubular dilation (Fig. 17). The cumulative score of histological damage in the outer medulla at 1 d was similar between p53 KO kidneys and WT kidneys post-IRI, demonstrating that global gene ablation of p53 in kidney does not reduce tubular damage.

Global knockout of p53 in rats had decreased apoptosis after IRI. To determine whether there is a change of apoptotic levels in the outer medulla of WT rats compared with p53 KO rats, TUNEL assay was performed. The outer medulla of wild type rats exhibited increased numbers of TUNEL-positive cells compared with that of p53 KO rats (Fig. 18). These data suggest that global deletion of p53 in the kidney decreases apoptotic cell death after IRI.

Loss of p53 did not reduce renal fibrosis after IRI. To investigate whether global deletion of p53 reduces renal fibrosis, collagen deposition in the kidneys of WT and p53

KO rats was measured using Sirius red staining and α-SMA immunofluorescence staining. Sixteen days after IRI, p53 KO rats showed a dramatic increase of Sirius red-positive area in the kidneys similar to WT rats, indicating that global deletion of p53 does not reduce renal fibrosis in the later stage of IRI in rats (Fig. 19). α-SMA expression was not decreased in p53 KO rats compared with WT rats at 16 days after IRI, as demonstrated by immunostaining and Western blot analysis (Fig. 20).

Figure 16: Kidney function in p53 WT or global KO rats after IRI.

Plasma creatinine (A) and BUN (B) levels from WT, p53 heterozygous (HZ) and global p53 KO rats (n = 5) at 1 d after IRI. † $P < 0.05$ compared with Sham.

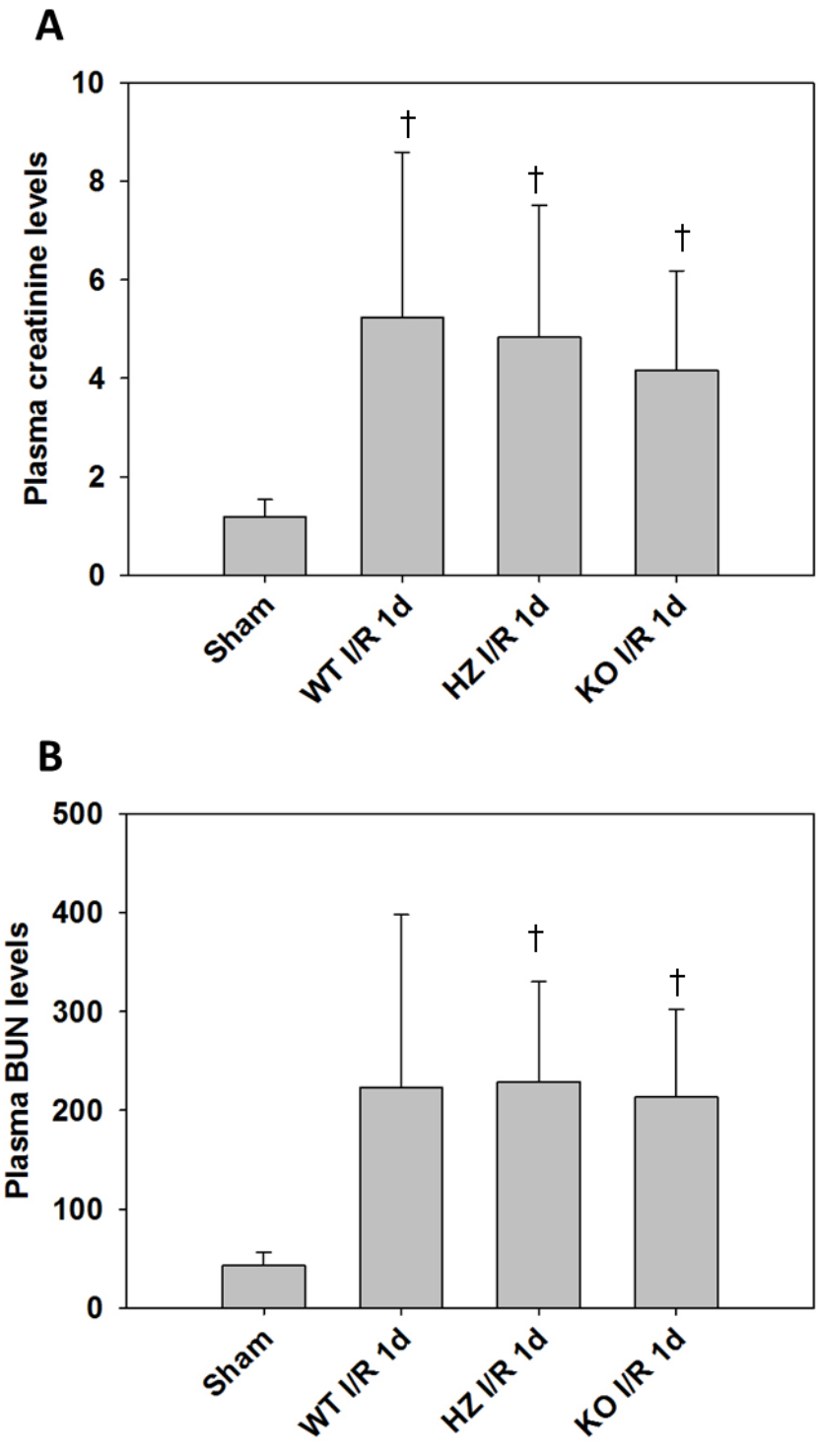
A
Plasma creatinine levels
10
8
6
4
2
0
†
†
†
Sham
WT I/R 1d
HZ I/R 1d
KO I/R 1d
B
Plasma BUN levels
500
400
300
200
100
0
†
†
Sham
WT I/R 1d
HZ I/R 1d
KO I/R 1d

Figure 17: The kidney histological changes in p53 WT and global p53 KO rats after IRI. Renal histological changes in the outer medulla after IRI were assessed by PAS staining at 1 d after IRI. Magnification is 400×. Histological damage in the outer medulla assessed in PAS-stained kidney sections was scored by counting the percentage of tubules that displayed tubular necrosis, cast formation, and tubular dilation as follows: 0 = normal; 1 = < 10%; 2 = 10–25%; 3 = 26–50%; 4 = 51–75%; and 5 = > 75%. Ten fields (200× magnification) per kidney were used for counting, † $P < 0.05$ compared with Sham, $n = 6$.

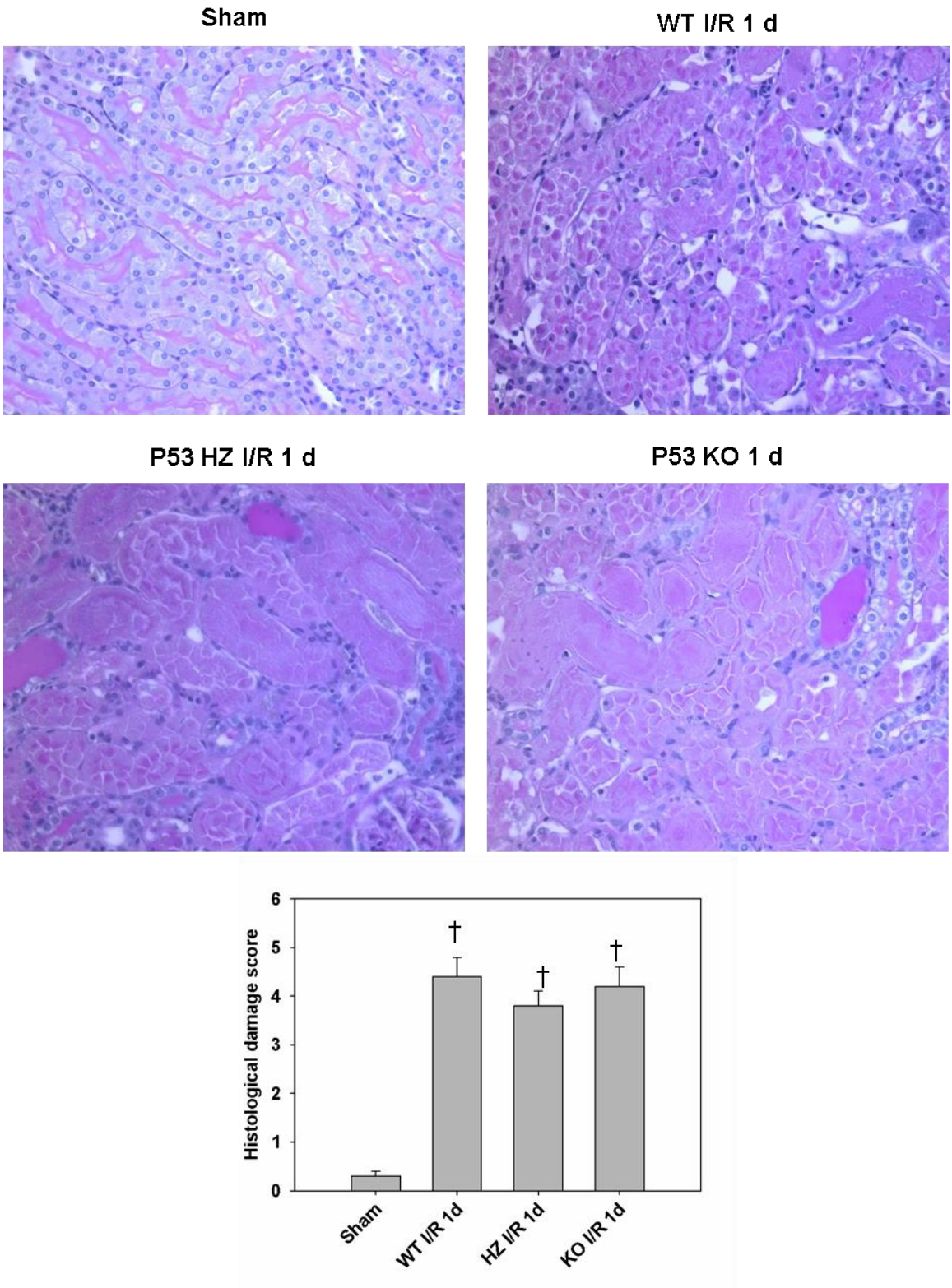
Sham
WT I/R 1 d
P53 HZ I/R 1 d
P53 KO 1 d
Histological damage score
0
1
2
3
4
5
6
†
†
†
Sham
WT I/R 1d
HZ I/R 1d
KO I/R 1d

Figure 18: TUNEL staining in p53 WT and global p53 KO kidneys after IRI.

Apoptosis detection by TUNEL staining in WT and p53 KO kidneys at 24 hours post IRI. Images are representative of four independent experiments. Number of TUNEL positive cells was measured in 10 randomly chosen high magnification (200×) fields per kidney. * $P < 0.05$ compared with WT-IRI; † $P < 0.05$ compared with Sham; $n = 6$.

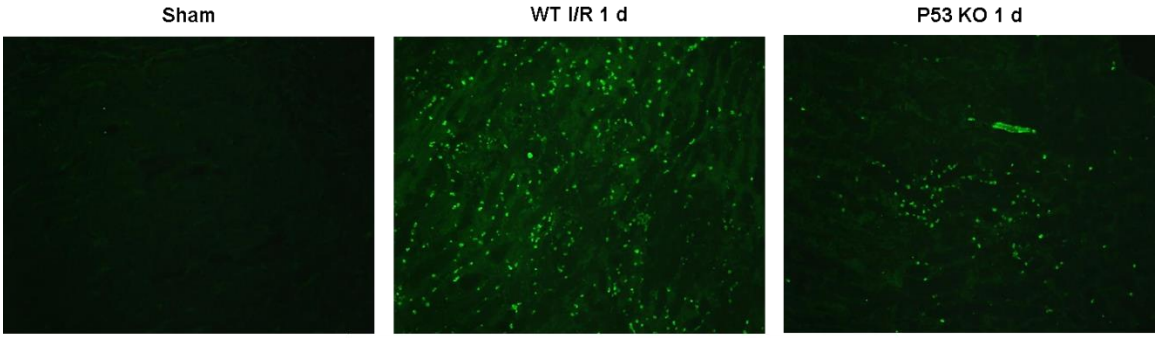
Sham
WT I/R 1 d
P53 KO 1 d

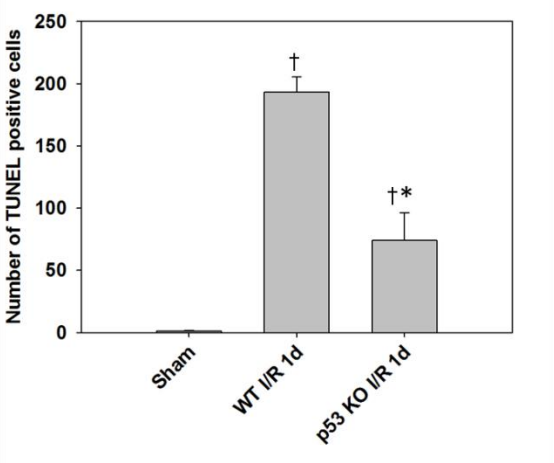
Number of TUNEL positive cells
250
200
150
100
50
0
†
†*
Sham
WT I/R 1d
p53 KO I/R 1d

Figure 19: Collagen deposition after IRI in p53 WT and global p53 KO rats.

Collagen deposition detected by Sirius red staining in WT and p53 KO kidneys at 16 d after IRI; (B) The Sirius red-positive area was measured in four randomly chosen high power (200×) fields per kidney using the NIH Image J software. † $P < 0.05$ compared with Sham.

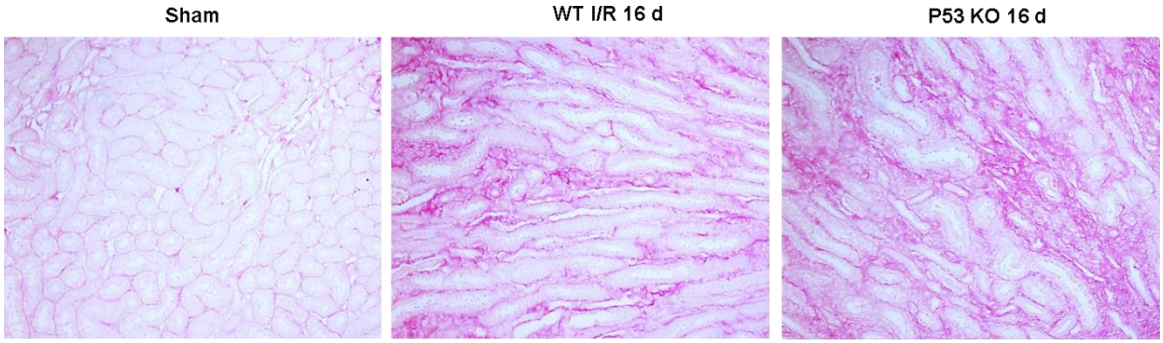
Sham
WT I/R 16 d
P53 KO 16 d

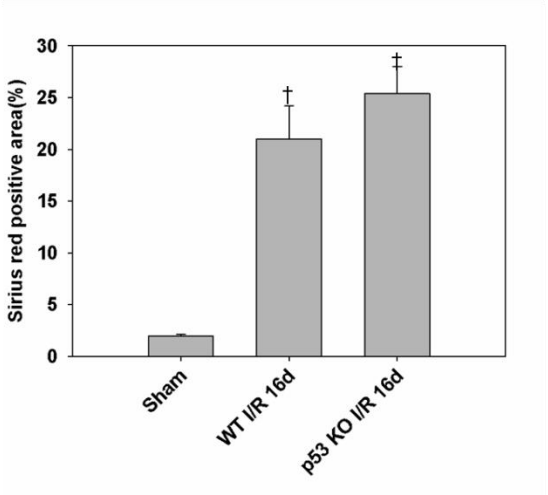
Sirius red positive area(%)
30
25
20
15
10
5
0
†
‡
Sham
WT I/R 16d
p53 KO I/R 16d

Figure 20: α-SMA staining in WT and global p53 KO rats after IRI.

Immunofluorescence staining and western blot of α-SMA in outer medulla. The α-SMA-positive area was measured in four randomly chosen high power (200×) fields per kidney. † $P < 0.05$ compared with Sham.

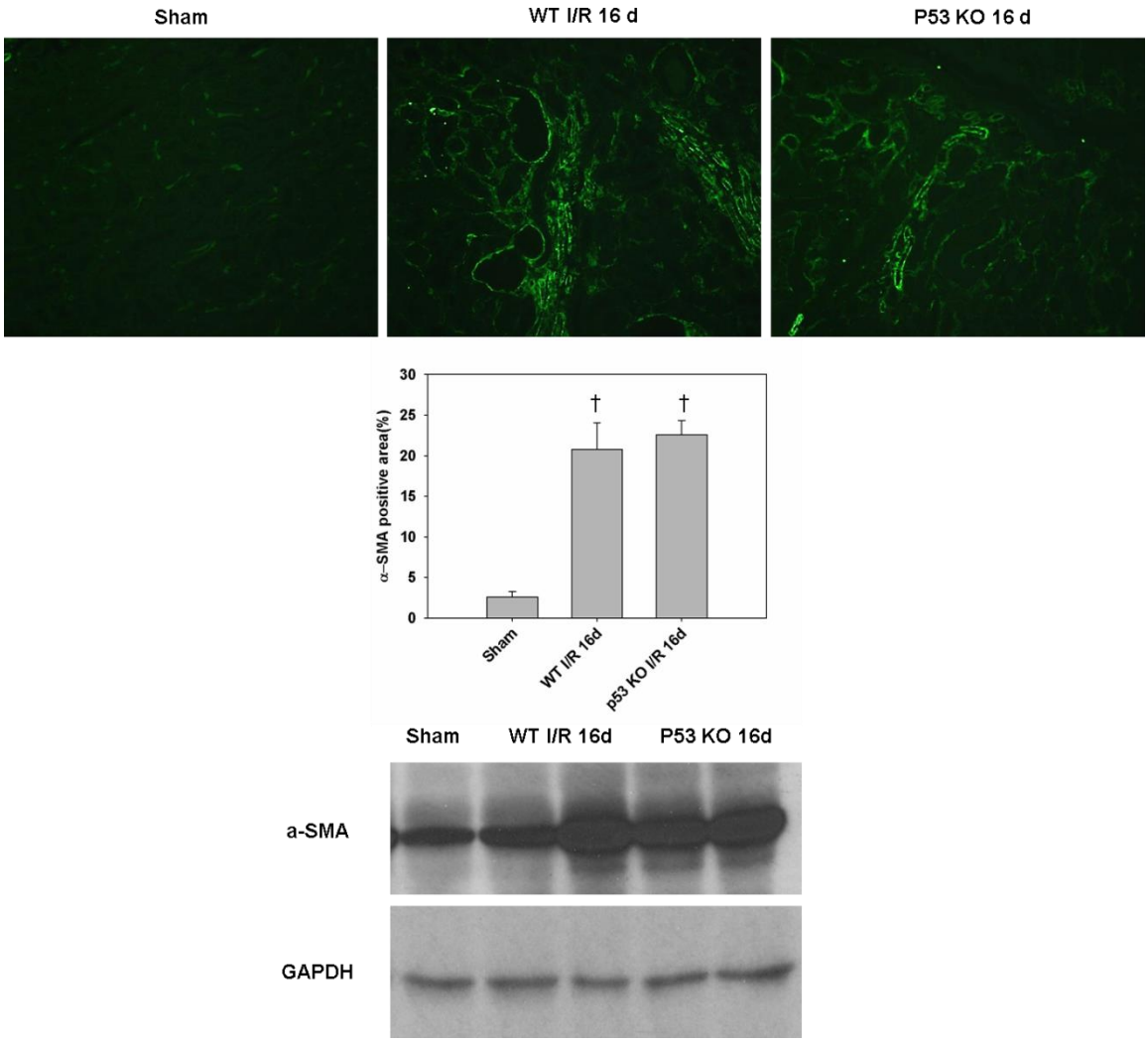
Sham
WT I/R 16 d
P53 KO 16 d
α-SMA positive area(%)
30
25
20
15
10
5
0
†
†
Sham
WT I/R 16d
p53 KO I/R 16d
Sham
WT I/R 16d
P53 KO 16d
a-SMA
GAPDH

Discussion

Ischemic renal injury is strongly associated with proximal tubular cell necrosis and apoptosis (71). It has been shown that interference with many cell death mediators provides protective effects on renal function (76, 87, 88). Among these molecules, p53 has gained particular attention because of its key role in senescence, apoptosis and even necrosis (166). Indeed, our studies show that specific knock out of p53 gene in the proximal tubule significantly improves kidney function and reduces apoptosis after IRI, along with attenuated inflammatory response and long-term fibrosis. These findings support the concept that p53 is a critical mediator of apoptosis after IRI.

Several studies have investigated the role of p53 in IRI. Kelly et al. first showed that p53 expression is increased in the renal medulla after IRI (88), and inhibition of p53 can reduce renal injury in rats. Molitoris et al. showed that systemic administration of p53-targeted siRNA into mice attenuates ischemic acute kidney injury (126). However, Dagher et al. showed that the p53 inhibitor pifithrin-α can actually increase long-term renal fibrosis after IRI (32), and Sutton et al. showed that global p53 deficiency exacerbates injury (152). These conflicting results may reflect different experimental protocols and, probably more importantly, differing effects of global inhibition of p53 in cells within the kidney. This controversy suggests that the role of p53 in the pathophysiology of IRI is much more complicated and incompletely understood.

In this study, we used knockout mice with p53 gene specifically deleted in the proximal tubule to study its effect on the kidney damage after IRI. This strategy not only specifically targets the proximal tubule, the major injury site of IRI (162), but also excludes the normal function of p53 in other cells within the kidney, like inflammatory cells recruited after IRI, in which absence of p53 may prolong inflammatory responses and increase renal injury. The deletion of p53 in the proximal tubule not only significantly

reduces apoptotic cell death in the outer medulla, but also preserves tubular architecture. Although the exact mechanisms by which reduced tubular cell damage preserves renal function are not fully understood, a possible explanation is that the maintenance of structural integrity reduces tubular cell shedding and cast formation in the later segments of nephrons, and thus mitigates tubular obstruction and preserves kidney function. Our studies in knockout mice also show reduced inflammatory responses and fibrosis, which may be the consequences of decreased cell death within the kidney.

It is well established that p53 is known as “the guardian of the genome”, and mutated p53 frequently exists in many forms of tumors (166). This indicates that p53 is important for the regulation of cell proliferation and cell death. The regulation of p53 involves interactions with mouse double minute 2 homolog (MDM2), resulting in alterations in p53 protein levels (100). Protein modifications like phosphorylation and acetylation are also important for the activation of p53 (100). Hypoxia-induced DNA damage by reactive oxygen species may contribute to activation of p53 and lead to p53-induced apoptosis (65). Thus, the p53 pathways have been broadly investigated in the emergence and progression of ischemic injuries. The role of p53 in mediating cell death in ischemic neuronal injury is well established, but is not well understood in ischemic renal injury (75).

The effects of p53 activation after IRI involve changes in transcriptional activity and transcription independent functions (100, 166). First, the downregulation of p21, one of the major transcriptional products of p53 (41, 42), in knockout mice is expected, indicating increased selected transcription induced by p53. Although p21 is considered more as a cell cycle regulator than an apoptotic modulator (19, 42), activation of p21 by p53 may contribute to reduced cell proliferation after injury, thus restoring tubular structure. Second, an increased level of activated Bax without an increase in total Bax suggests that p53 induces Bax activation independent of transcription (28).

The MOMP is required for the execution of necrotic cell death as it forms part of MPTP. Although Bax and Bak were considered as proapoptotic molecules, emerging evidence clearly demonstrate that Bax and Bak are integral components of the MOMP of the MPTP (185). p53 can control the MOMP by (1) regulating the expression and function of Bax and Bid at the transcriptional level (28); (2) direct interaction with pro-apoptotic Bax/Bak and anti-apoptotic Bcl2 to modulate the pore activity (185) and (3) suppressing Bcl2 expression via activation of microRNAs (21, 153). However, the role of p53 in regulating Bcl2 family members to elicit necrosis remains undefined.

As discussed earlier, Bax/Bak in their non-oligomerized form induced a low level of permeability of the outer mitochondrial membrane that is distinct from its mode of releasing cytochrome c in apoptosis, and permits necrosis through the MPTP (84). A recent study also showed that p53 can translocate to mitochondria to interact with CypD and induce the opening of MPTP regardless of Bax/Bak activated MOMP (1). However, our data demonstrated that the significant decrease in necrosis in PTp53 KO ischemic kidneys is possibly through diminished expression of PARP-1, Bax and Bid.

Recently, Vaseva et al. showed that p53 may also be implicated in necrotic cell death through its interaction with CypD in the inner membrane of mitochondria, and subsequent opening of mitochondrial permeability transition pores (160). However, it is still unknown how this in vitro finding can be translated into in vivo IRI models. Indeed, our data showed significantly reduced tubular cell necrosis in the outer medulla of PTp53 KO mice in contrast to WT mice after IRI (Fig. 2). It is possible that mitochondrial translocation of p53 after IRI contributes to necrotic cell death rather than apoptotic cell death. Further studies may be needed to clarify this point.

Studies from other groups verified the importance of having p53 deleted only in the proximal tubules (152, 188). Sutton *et al*. first showed that global p53 deficiency or pharmacological inhibition of p53 increases and prolongs leukocyte infiltration into the

renal parenchyma, which exacerbates renal injury after IRI. Another study from Zhang *et al*. showed that PTp53 knockout mice were protected from IRI, while mice with p53 gene knockout in other segments were sensitive to IRI (188). Indeed, our data from p53 global knockout rats showed that those rats had similar sensitivity to IRI and developed long term fibrosis similar to wild type rats, although p53 KO rats had reduced level of TUNEL positive cells. Those data suggest that the p53 gene in non-PT cells is also crucial for preserving the kidney function after IRI, possibly through a reduced inflammatory reaction when p53 function is intact in non-PT cells (152).

In summary, this study shows p53 has strong effects on tubular cell death after IRI that can determine the final outcome of injury. Absence of p53 in the proximal tubule significantly preserves renal function and markedly reduces kidney damage, inflammation, and long-term fibrosis. Targeting proximal tubular cell death may provide a more efficient therapeutic strategy that may change the outcomes of IRI.

CHAPTER 2: THE MECHANISM OF p53-INDUCED CELL DEATH[3]

Introduction

The tumor suppressor protein p53 is a stress-responsive transcription factor because of its ability to activate multiple target genes in response to diverse stress conditions, including oxidative stress, genotoxic damage, oncogene activation, and hypoxia. These p53 targets have prominent biological functions including cell cycle arrest, apoptosis, senescence, metabolism, and autophagy modulation (57). Moreover, recent evidence suggests that p53 also exists in cytoplasm, directly interacts with multiple cytoplasmic proteins, and modifies their activity (166). In addition, recent studies revealed a role for p53 in regulating necrotic cell death by inducing the opening of MPTP, and altering mitochondrial dynamics (28, 160). Our in vivo and in vitro data from chapter 1 also support that idea that p53 plays a role in mediating necrotic cell death in PT. Further understanding the mechanism of p53-induced necrosis is needed.

The MOMP is required for the execution of necrotic cell death as it is part of MPTP. Although Bax and Bak are widely considered to be proapoptotic molecules, emerging evidence clearly demonstrate that Bax and Bak are integral components of the MOMP of the MPTP. Recent studies, however, showed that p53 can translocate to mitochondria to interact with CypD and induce the opening of MPTP regardless of Bax/Bak activated MOMP (84, 86). This study emphasized the importance of p53-CypD interaction in the necrosis, which seems to be independent of MOMP. This is a possible explanation for the decreased necrotic tubules in the kidney after p53 deletion. So we first hypothesized

[3] Some of the materials presented in this chapter were previously published: 1. Yuan Ying, Jinu Kim, Sherry N. Westphal, Kelly E. Long, and Babu J. Padanilam. Targeted deletion of p53 in the proximal tubule prevents ischemic renal injury (183). 2. Yuan Ying and Babu J. Padanilam, Regulation of necrotic cell death: p53, PARP1 and Cyclophilin D -overlapping pathways of regulated necrosis? (184)

that p53 translocates into mitochondria to induce the opening of MPTP, which leads to necrosis after IRI.

A reciprocal regulation of PARP-1 by p53 was described by Montero et al. in ROS-induced cell death (127). Genetic deletion of p53 in MEFs, human breast or colorectal cancer cells conferred increased resistance to ROS and PARP-mediated necrotic cell death (127). PARP activity at baseline and after ROS stimulation was reduced in the absence of p53. The mechanism by which p53 regulates PARP-1 activation and necrosis, in the setting of ROS-induced DNA damage, remains to be defined. Interestingly, inhibition of PARP-1-mediated necrosis led to p53-mediated caspase activation and apoptosis, indicating that PARP-1-mediated necrosis might be a downstream pathway of p53 signaling. Our data in chapter 1 demonstrated significant decreases in necrosis in p53 KO ischemic kidneys accompanied by decreased expression of PARP-1, Bax and Bid. Based on these data, we tested the second hypothesis that p53 regulates the expression of PARP-1, which induces necrosis after IRI.

Methods

Immunostaining: Briefly, the mouse kidney sections or cell samples were rehydrated, incubated in PBS containing 0.1% sodium dodecyl sulfate (SDS; Sigma) for 5 min and incubated with antibodies, including anti-p53 (Cell Signaling, 1 in 1000) overnight at 4°C. The slides then were treated with FITC -labeled secondary antibodies (Jackson Immuno Research). Samples were viewed using a Leica fluorescent microscope or confocal microscope and the images were captured using a computerized microscope recording system.

Immunofluorescence detection for GFP. Cell sample sections were processed for immunostaining as described previously (192). Samples were viewed using a Leica fluorescent microscope or confocal microscope and the images were captured using a computerized microscope recording system.

Cell culture and in vitro hypoxia. Primary proximal tubule epithelial cells were isolated from PT-specific p53 KO or WT male mice and cultured as described previously (35, 66). Renal proximal tubule cell lines (pig LLC-PK cell line and human HK-2 cell line) were cultured to 80-90% confluency in normal media, and exposed to hypoxic conditions. Cells were placed into GasPak plastic pouches (BBL GasPak Pouch Systems, Becton Dickinson), tightly sealed and placed back into the incubator for the indicated times. These pouches can generate a CO_2-enriched hypoxic microenvironment with an oxygen concentration < 2% and a CO_2 concentration > 4% within 2 h of incubation (modified from manufacturer's instruction).

Gene delivery**.** For the *in vitro* experiments, tubular cell lines were transfected with expression constructs for 1 d. For the experiments in which the cells were treated with GFP-p53 (Addgene, Cambridge, MA), cells were transfected with GFP-p53 plasmid for

24 to 48 h. The GFP-PARP-1 was obtained from Dr. Heinrich Leonhardt (Ludwig Maximilians University Munich).

Western blot analysis. Briefly, cell samples (50 μg protein/lane) were separated on 10% SDS-PAGE gels and then transferred to immobilon membranes (Millipore, Bedford, MA). The membranes were incubated with anti-p53 and anti-PARP-1 (Cell Signaling, Beverly, MA antibodies overnight at 4°C. After washing, the membranes were incubated with horseradish peroxidase-conjugated secondary antibodies against the appropriate primary antibodies (1:5,000, Vector Laboratories, Burlingame, CA), exposed to Western Lighting Plus-ECL (NEL104001EA; PerkinElmer, Waltham, MA), and then developed with X-ray film. The area of each band was analyzed using NIH image software (Image J). The relative densities were measured by dividing the density of target protein by the density of loading control (GAPDH) for the same lane. Then the fold changes were calculated by dividing each of the relative densities of target protein by the relative density of WT-sham. The variability of the relative density of control group was calculated by normalizing the individual values of the controls to the mean of the control group.

Statistics. All data are expressed as means ± SE. An unpaired t-test was used to compare the means of two different groups. A P value < 0.05 was considered statistically significant.

Results

Successful transfection of PARP-1-GFP and p53-GFP plasmids in the kidney. First, we analyzed the expression of PARP-1-GFP and p53-GFP with the plasmid vector, p53-GFP, in LLC-PK1 cell line. Indeed, immunoblotting demonstrated that the expression of PARP-1 and p53 were induced (Fig. 21) after transfection. Their molecular weight was also as predicted.

To test if p53 or PARP-1 translocate from nucleus into mitochondria, we analyzed the localization of PARP-1 and p53 after H_2O_2 or hypoxia-reoxygenation treatment. PARP-1- and p53-GFP did not translocate into mitochondria after hypoxia-reoxygenation or H_2O_2 treatment. As expected, the signals of PARP-1 and p53-GFP were mainly detected in the nucleus (Fig. 22, 23). After 4 hours of H_2O_2 treatment, the signals from PARP-1- and p53-GFP were still mainly in the nucleus without significant increase in the mitochondria (Fig. 22, 23). We repeated those experiments at different time points and with different H_2O_2 dosage; however, no significant mitochondrial translocation was observed. We concluded that mitochondrial translocation of PARP-1 or p53 was not the main mechanism for PARP-1- or p53-induced necrosis.

Knockout of p53 reduces PARP-1 expression in primary tubular cells. Since we observed a decreased expression of PARP-1 in PTp53 knockout mice, we postulated that p53 induces necrosis by increasing PARP-1 expression. To test this hypothesis, we used primary proximal tubular cells isolated from WT and PTp53 KO mice. Indeed, with hypoxia-reoxygenation treatment, p53 KO primary PT cells had decreased expression of PARP-1 after injury. Similarly, the expression of PARP-1 was heightened after over expressing p53 in LLC-PK1 cells (Fig. 24). These data suggest that p53 can regulate PARP-1 expression after activation.

Figure 21: Western blot showing the successful transfection of p53 and PARP-1 plasmids with LLC-PK1 cells.

GFP-p53 and GFP-PARP-1 both were located above their original molecular bands, indicating bigger molecule weight.

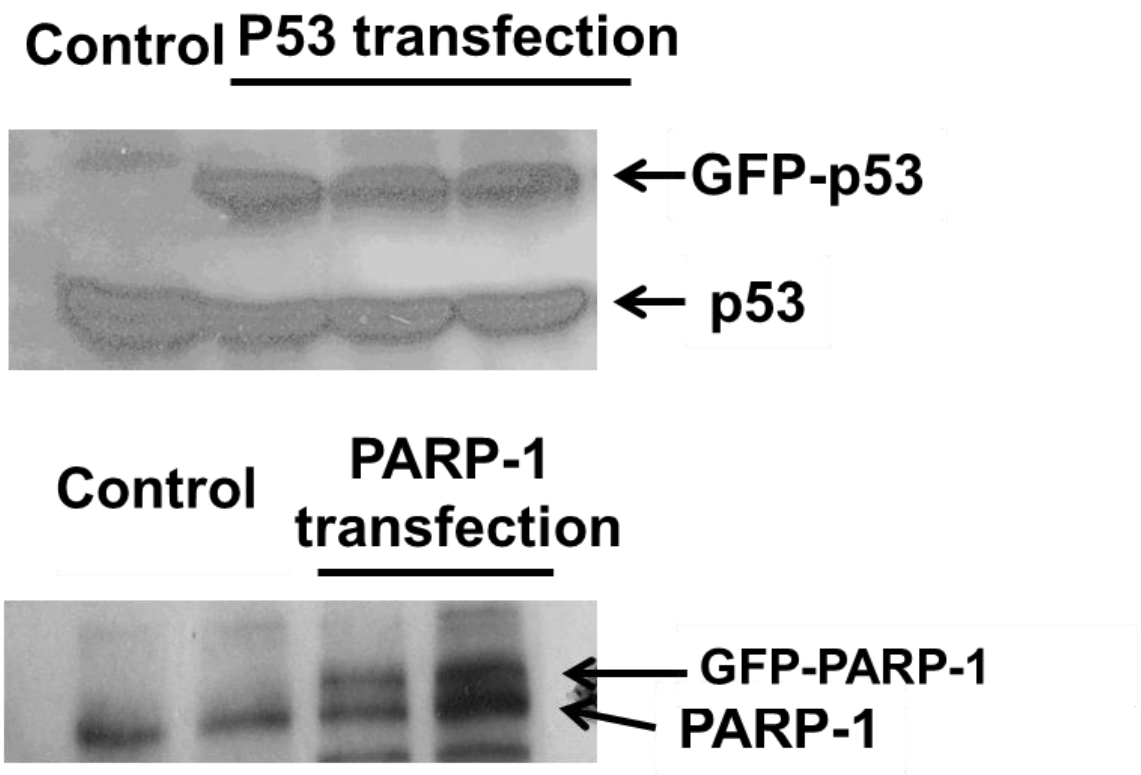
Control
P53 transfection
GFP-p53
p53
Control
PARP-1
transfection
GFP-PARP-1
PARP-1

Figure 22: Localization of GFP-p53 in transfected LLC-PK1 cells with or without H_2O_2 treatment.

Most of the GFP signals (green) were detected in nucleus (DAPI, Blue) before or after H_2O_2 treatment. No apparent mitochondrial translocation was detected.

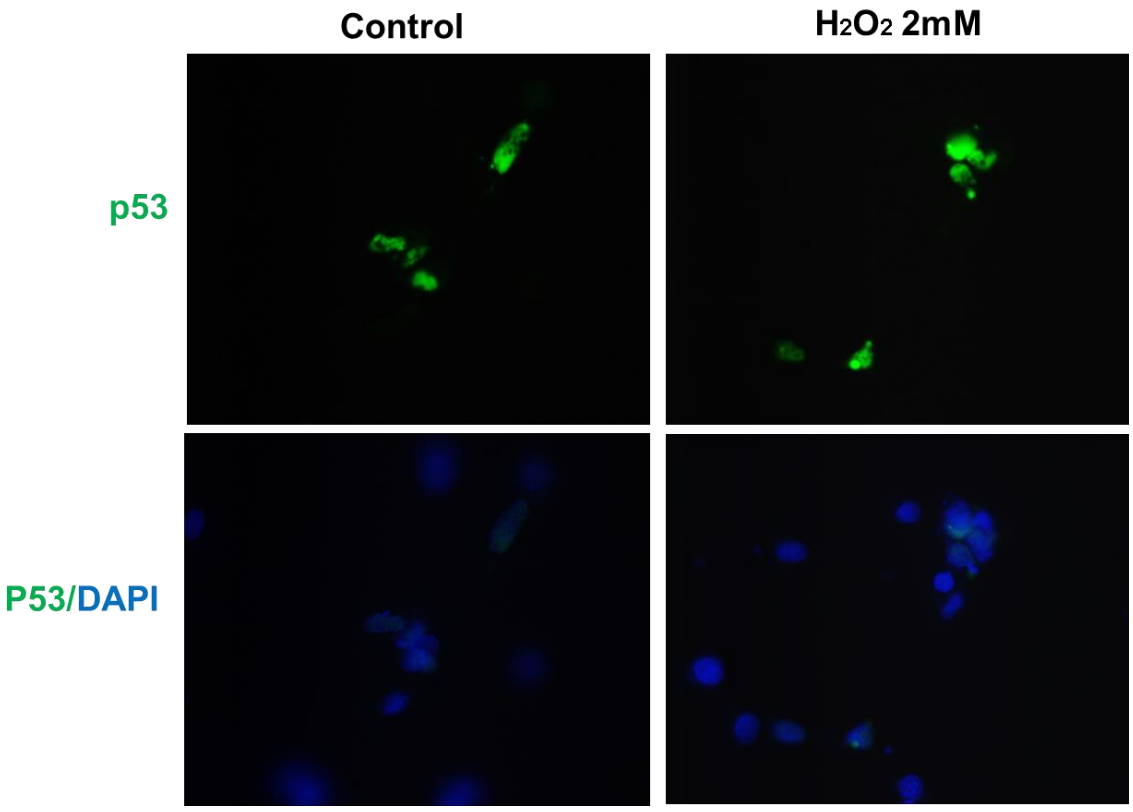
Control
H2O2 2mM
p53
P53/DAPI

Figure 23: Localization of GFP-PARP-1 in transfected LLC-PK1 cells with or without H_2O_2 treatment.

Most of the GFP signals were detected in nucleus before or after H_2O_2 treatment. No apparent cytoplasm signal was detected.

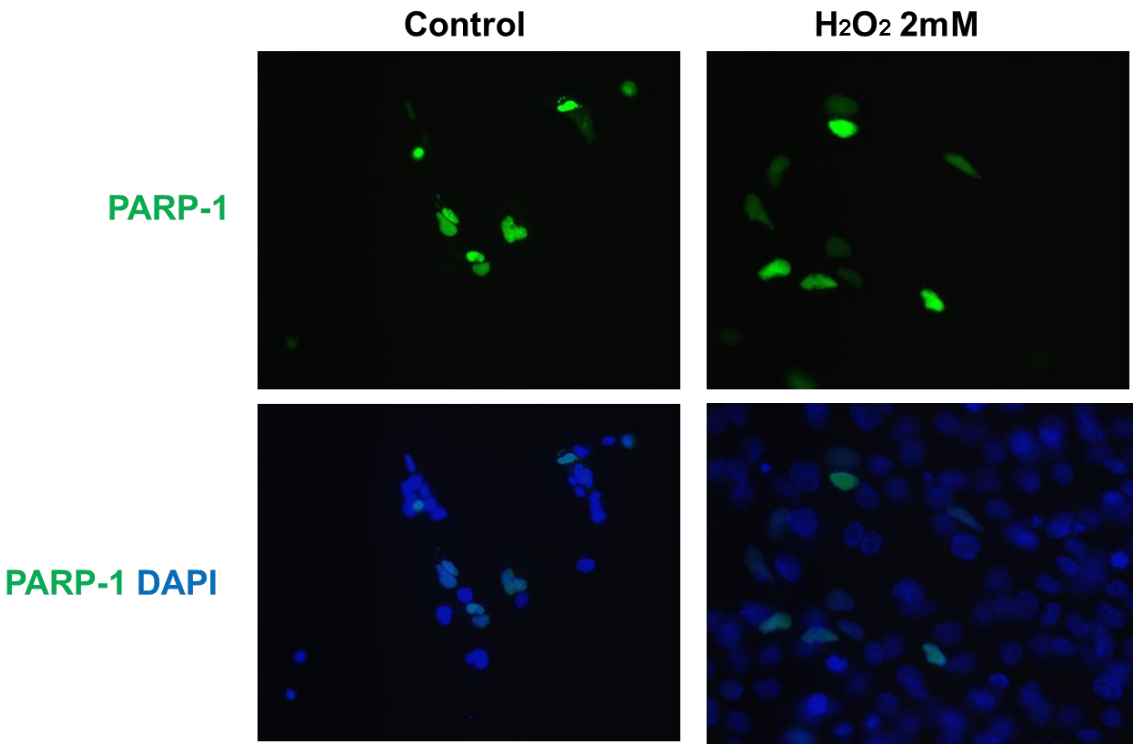
Control
H2O2 2mM
PARP-1
PARP-1 DAPI

Figure 24: p53 regulates PARP-1 expression.

(A). PARP-1 expression in primary cell culture from WT and PTp53 KO mice with hypoxia-reoxygenation treatment. (B, C). Western blot showing the expression of PARP-1 in LLC-PK1 after transfecting with GFP-p53 plasmid. * $P < 0.05$ compared with WT; $n = 3$.

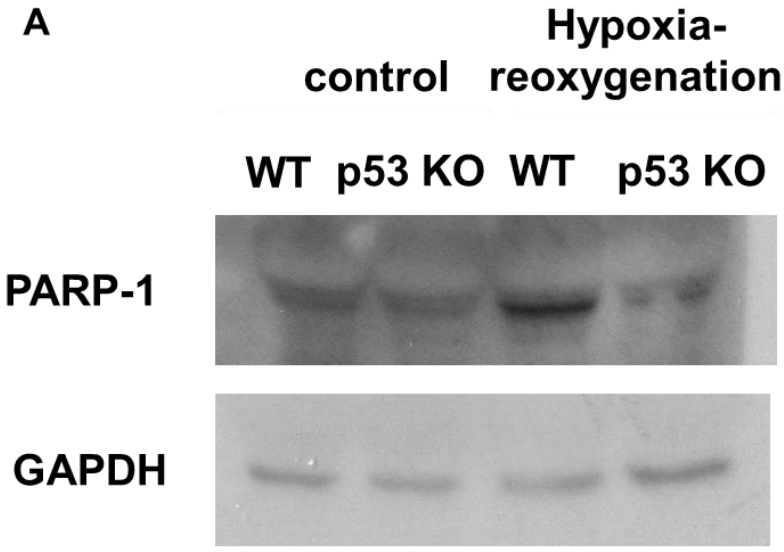
A
control
Hypoxia-reoxygenation
WT
p53 KO
WT
p53 KO
PARP-1
GAPDH

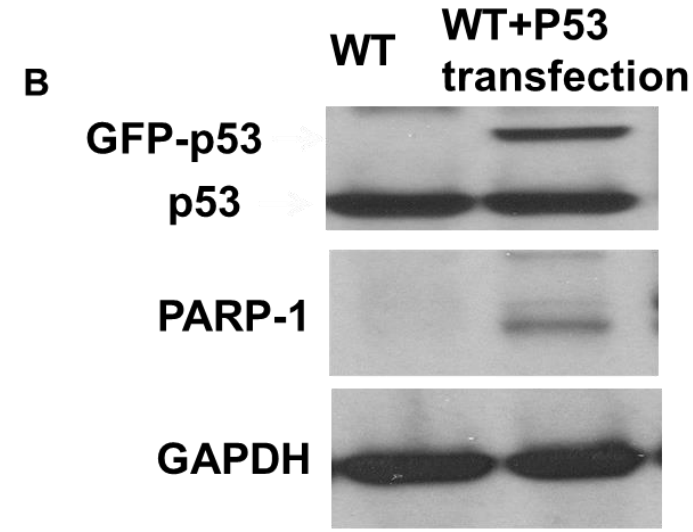
B
WT
WT+P53 transfection
GFP-p53
p53
PARP-1
GAPDH

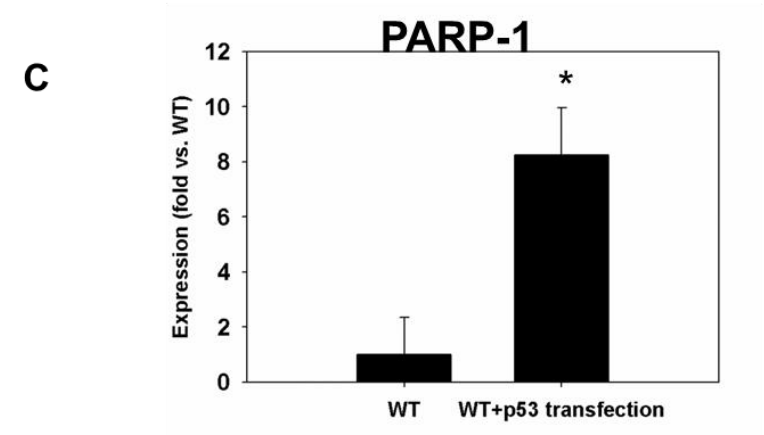
C
PARP-1
Expression (fold vs. WT)
12
10
8
6
4
2
0
*
WT
WT+p53 transfection

Discussion

Our study used p53-GFP expression system to track p53 movement within the cell after H_2O_2 and hypoxia treatment. This system allowed us to locate p53 without the limitation of antibody specificity. We did not observe an increased signal of p53 in the mitochondria at various time points and with different H_2O_2 treatment dosages. It suggests that p53-induced necrosis probably employs a mitochondria translocation-independent mechanism. Our further analyses, along with in vivo studies, suggest that the regulatory effect of p53 on the expression of PARP-1 might be partially responsible for necrotic cell death induced by p53.

The p53 tumor suppressor is activated and stabilized in response to cellular stress such as DNA damage or hypoxia (99, 166). The final outcome of p53 activation depends largely on the initial injury, the level of p53 activation, and the cell type, ranging from mild injury such as senescence to severe damage like apoptosis or necrosis (165, 167). Multiple activators that stimulate the activation of p53 also play a role in activating PARP-1 (68). PARP-1 activation depletes NAD+ and releases AIF, which lead to necrotic cell death. The initial response to DNA damage by both p53 and PARP-1 is to repair the damaged DNA and thus maintain genomic integrity (73, 80). Can p53 and PARP-1 act independently or synergistically to carry out their functions and possibly regulate necrosis?

The interaction between p53 and PARP-1 has long been recognized. In senescent cells with telomere shortening (161), PARP-1 binding was shown to be critical for p53 activation and function. p53 and PARP-1 interaction was also demonstrated in cells undergoing apoptosis in response to DNA damage, independent of poly(ADP-ribosyl)ation of p53 (102). Interestingly, in DNA damaged neurons, PARP-1 regulated p53 transcription activity by poly(ADP-ribosyl)ation (122), which was further supported

by studies in irradiation-induced DNA damaged cell lines, where pharmacological or genetic deletion of PARP-1 modulated p53 activation (158, 175).

While these reports established a role for PARP-1 in regulation of p53 activity, a reciprocal regulation of PARP-1 by p53 was described by Montero et al. in ROS-induced cell death (127). Genetic deletion of p53 conferred increased resistance to ROS and PARP-mediated necrotic cell death (127). PARP activity at baseline and after ROS stimulation was reduced in the absence of p53. These evidences suggest that the functions of p53 and PARP-1 are sometimes dependent on each other.

A regulatory effect between these two molecules is supported by our study here. In our kidney injury model, we showed that deletion of p53 in the proximal tubule not only significantly reduces p53 activation, but also leads to decreased expression levels of PARP-1 (see chapter 1). This observation suggests that p53 might have a role in regulating the expression of PARP-1. In this chapter, we went further to test this possible mechanism for p53-induced necrosis: we showed that the expression of PARP-1 in primary tubular cells from PTp53 knockout kidney was decreased after hypoxia-reoxygenation treatment compared with WT tubular cells; the expression of PARP-1 in LLC-PK1 after transfecting with GFP-p53 plasmid was also increased without injury. These data suggest that p53 regulates the expression of PARP-1, which induces necrosis. Our data suggest that p53 regulated-PARP-1 expression might play an important role in necrosis after IRI. This mechanism might be able to explain part of the protective effect we saw in PTp53 knockout mice. However, p53 and PARP-1 both have multiple functions other than inducing necrosis. A comparison of renal function, histopathology, necrosis and apoptosis demonstrated that p53 deletion had a superior protective effect compared to PARP-1 deletion. In order to determine if PARP-1 can independently regulate necrosis, we generated PARP-1/PTp53 double knockout mice

and determined the effect of double deletion of p53 and PARP-1 and these results are presented in the next chapter.

In mitochondria isolated from Bax/Bak double knockout mice, oxidative stress triggers the p53 translocation to the mitochondria and induces the formation of a CypD-p53 complex that promotes MPTP opening and necrosis (179). These results were supported by other studies demonstrating p53-CypD interaction in MPTP-dependent necrosis in different cell models, including neuronal (215), pancreatic (26), and osteoblast cells (216). Although these results provide a novel mechanism by which CypD is activated to trigger MPTP, a few questions about the universal nature of this interaction in MPTP remain to be answered. For example, the formation of MPTP in mitochondria lacking p53 and the absence of p53 involvement in calcium-induced MPTP opening are intriguing (95). Our in vitro studies using H_2O_2 and hypoxia-reoxygenation injury did not show an increased translocation of p53 into mitochondria. Most of the p53 signals were detected in the nucleus, indicating a nucleus-involved mechanism rather than a mitochondrial translocation-dependent mechanism for necrosis in renal epithelial cells. We acknowledge that GFP tagged p53 or PARP-1 have a bigger molecular weight and possibly affect their translocation; however, this is not very likely, because the GFP tag is in the C-terminal and will not alter the nuclear locating sequence, which is located in the N-terminal of p53. Further, non-GFP-tagged p53 or PARP-1 transfection did not result in increased expression of either molecule in the mitochondria as demonstrated by immunostaining (data not shown).

In summary, our data suggest that there is a regulatory effect of p53 on the expression of PARP-1 in our injury model. p53-induced PARP-1 expression might be an important mechanism by which the activation of p53 after IRI triggers tubular necrosis and renal dysfunction. Although the mitochondrial translocation of p53 is an intriguing mechanism as shown in other studies, we did not observe a significant increase in p53

translocation in our model. Other mechanisms of p53-induced necrotic cell death, such as activation of Bax/Bid to induce MOMP and induction of ferroptosis, are discussed in chapter 1 and chapter 3 respectively.

CHAPTER 3: THE EFFECT OF DOUBLE KNOCKOUT OF PARP-1/PTp53 ON IRI[4]

Introduction

Ischemic renal injury is characterized by extensive cell death in proximal tubule S3 segment (16, 17). Ischemia/reperfusion to the kidney parenchyma leads to many secondary effects including dysfunction of cellular energy metabolism, production of ROS, and DNA damage, which leads to activation of the nuclear repair enzyme PARP-1 and the transcription factor p53 (180). Activation of these molecules induces necrotic and apoptotic tubular cell death. Better understanding the role of these two molecules in necrotic cell death is crucial for creating therapeutic drugs that target necrotic pathway.

The tumor suppressor protein p53 is an anti-oncogene known for its ability to activate multiple target genes in response to diverse stress conditions. Increased expression/activity of these p53 targets could stimulate prominent biological functions including cell cycle arrest, apoptosis, senescence, metabolism, and autophagy (99, 166). Recent studies revealed roles for p53 in regulating necrotic cell death by activating independent signaling pathways that include induction of MPTP, altered mitochondrial function and dynamics. On the other hand, p53 also regulates the expression of SLC7A11 and thus plays a role in ferroptosis, which is a novel type of cell death that depends on the over production of ROS and iron overload (37, 79, 104). SLC7A11 is a glutamate/cysteine carrier in the cell membrane that facilitates the transport of cysteine into the cell and defends against ROS production and ferroptosis. Although recent

[4] Some of the materials presented in this chapter were previously published: 1. Yuan Ying, Jinu Kim, Sherry N. Westphal, Kelly E. Long, and Babu J. Padanilam. Targeted deletion of p53 in the proximal tubule prevents ischemic renal injury (183). 2. Yuan Ying and Babu J. Padanilam, Regulation of necrotic cell death: p53, PARP1 and Cyclophilin D -overlapping pathways of regulated necrosis? (184)

studies suggest that ferroptosis might be implicated in IRI (47, 115, 118), the role of p53 in regulating ferroptosis after ischemic injury has never been investigated. This chapter investigates the contribution of p53-induced ferroptosis in renal injury.

In chapter 1, we showed that PTp53 knockout mice have lower levels of PARP-1 after IRI, suggesting that p53 might play a role in regulating PARP-1 expression. This might, in part, explain why the kidney has reduced necrosis in the absence of p53. However, PARP-1 has other functions such as modifying other transcriptional factors and enzymes after its activation, while p53 also induces apoptosis, ferroptosis, and regulates energy production.

Given the marked interest to pharmacologically target necrotic pathways in IRI, delineation of these pathways may provide key insights to our understanding of the pathophysiology of IRI and to develop novel therapeutic strategies. In chapters 1 and 2 we demonstrated that p53 can regulate the expression of PARP-1 in vivo and in vitro. It is important to test if double knockout of PARP-1/PTp53 in the kidney further protects the kidney from IRI. We hypothesized that double knockout of PARP-1/PTp53 in the kidney will additively or synergistically protect the kidney from IRI, because both molecules have other functions besides inducing necrosis.

Methods (183)

Generating PARP-1/PTp53 DKO mice. Homozygous p53–floxed mice (C57BL/6J background) and PARP-1 knockout mice (PARP-1 -/-, 129S1/svImJ background) were obtained from Jackson Laboratories (Bar Harbor, ME). The breeding strategy for transgenic mice that expressed Cre recombinase under the control of kidney-specific Pepck promoter (Pepck-Cre) was reported elsewhere (13). Knockout mice with the p53 gene specifically disrupted in renal proximal tubular epithelial cells (genotype p53fl/fl, Cre+/-) were created by mating p53-floxed mice with pepck-Cre transgenic mice. Then heterozygote mice (genotype PARP-1 +/- p53fl/-, Cre+/-) were generated by breeding PARP-1 -/- mice and p53fl/fl, Pepck-Cre+/-. Breeding those heterozygote mice we got double knockout mice (PARP-1 -/- p53fl/fl, Cre+/-), single knockout mice (PARP-1 -/- or p53fl/fl, Cre+/-), and wild type mice with mixed background (PARP-1 +/+ p53fl/fl, Cre-). A routine PCR protocol was used for genotyping from tail DNA samples with the following primer pairs: Cre, 5'-CGGTGCTAACCAGCGTTTTC-3' and 5'-TGGGCGGCATGGTGCAAGTT-3'; PARP-1, 5'-CCAGCGCAGCTCAGAGAAGCCA-3', 5'-CATGTTCGATGGGAAAGTCCC-3' and 5'-AGGTGAGATGACAGGAGATC-3'; and p53, 5'-GGTTAAACCCAGCTTGACCA -3' and 5'-GGAGGCAGAGACAGTTGGGAG-3'. All animals were born at the expected Mendelian frequency. They were of normal size and did not display any gross physical or behavioral abnormalities. Animal experiments were approved by the Institutional Animal Care and Use Committee of the University of Nebraska Medical Center.

Induction of ischemic renal injury in mice. Two 2 cm dorsal flank incisions were made in the skin and muscle layer on the abdominal cavity. The kidney was exposed to visualize and isolate the renal pedicle. A microvascular clamp was placed on each renal pedicle to achieve complete cessation of arterial blood flow for 30 min to induce renal

ischemic injury. The animal was placed on a heating board during this time period to maintain body temperature at 37 ℃. The clamps were then removed and the abdomen was closed using 1-2 skin staples. Animals were sacrificed at 24 hours post-surgery. Blood was collected at 24 h following the injury.

Sham operation in mice. Mice were anesthetized with ketamine and xylazine as described for ischemic renal injury procedure. A dorsal flank incision was performed as in IRI. The kidneys were visualized but not touched. The abdomen was closed with skin staples. Skin sutures/staples were removed when animals were sacrificed post-surgery.

Ferrostatin-1 administration: Mice were injected intraperitoneally with 10 mg/Kg ferrostatin-1 30 min before IRI. Then the same protocol was used as described in mouse surgery section.

Measurement of plasma creatinine and BUN. Plasma creatinine and BUN were measured to evaluate renal function using a Quantichrom assay kit (BioAssay Systems, Hayward, CA) according to the manufacturer's protocol.

Morphological studies. Wild type and knockout mice that underwent IRI were sacrificed at 1 d. The kidneys then were processed at the University of Nebraska Medical Center histology core facility. Briefly, kidneys were fixed in formalin, embedded in paraffin, and cut into 5 μm sections. The tissue sections were then stained with PAS.

Immunofluorescence for neutrophils. Formalin-fixed mouse kidney sections were processed for immunostaining as described previously (192). The slides were sequentially incubated with rabbit anti-mouse neutrophil antibody (Accurate, Westbury, NY) at a 1:100 dilution overnight at 4 ℃, followed by FITC-conjugated goat anti-rabbit IgG (Vector Labs, Burlingame, CA) at a 1:200 dilution for 1 h at room temperature. Neutrophil infiltration was quantified by counting the number of stained cells per field.

Apoptosis detection by TUNEL staining. TUNEL staining of kidney tissue sections was carried out using the In Situ Cell Death Detection kit, Fluorescein (Roche, Mannheim, Germany) according to manufacturer's protocol.

Western blot analysis. Briefly, whole renal tissue extracts (80 μg protein/lane) were separated on 10% SDS-PAGE gels and then transferred to immobilon membranes (Millipore, Bedford, MA). The membranes were incubated with anti-p53 (Cell Signaling, Beverly, MA), anti-PARP-1 (Cell Signaling), anti-p21 (Santa Cruz, Santa Cruz, CA), anti-activated Bax (Santa Cruz), anti-SLC7A11 (Abcam, Cambridge, MA), and anti-GAPDH (Santa Cruz) antibodies overnight at 4°C. After washing, the membranes were incubated with horseradish peroxidase-conjugated secondary antibodies against the appropriate primary antibodies (1:5,000, Vector Laboratories, Burlingame, CA), exposed to Western Lighting Plus-ECL (NEL104001EA; PerkinElmer, Waltham, MA), and then developed with X-ray film. The area of each band was analyzed using NIH image software (Image J).

Statistics. All data are expressed as means ± SE. One way ANOVA was used to compare the mean values of all groups, followed by Tukey's multiple comparison tests to compare the mean values between two groups. A P value < 0.05 was considered statistically significant.

Results

Successful deletion of PARP-1 and PT-specific p53 in the kidney. First, we used whole kidney samples to analyze the expression of PARP-1 and p53 before and after injury. The expression of PARP-1 (Fig. 25) was absent in PARP-1 single knockout mice and PARP-1/PTp53 DKO mice, which were consistent with our genotyping results. Similarly, the expression of p53 and one of its target genes, p21 (Fig. 25) was decreased in p53 knockout mice and PARP-1/PTp53 double knockout mice after IRI. Western blot analysis showed the levels of activated Bax were enhanced in the kidney of wild type mice compared with that of PARP-1/PTp53 DKO mice 24 h after IRI. Collectively, these data confirmed the successful deletion of PARP-1 and PTp53 in the kidney.

Western blot showed decreased activation of Bax in PARP-1 KO, PTp53 KO and PARP-1/PTp53 DKO mice compared with that of WT mice 24 h after IRI (Fig. 25). The expression of p21, a transcriptional target of p53, was also reduced in PARP-1 KO, PTp53 KO and PARP-1/PTp53 DKO mice after IRI in contrast with WT mice. These data suggest that double deletion of PARP-1 and p53 in the proximal tubule decreases apoptotic cell death after IRI.

Double knockout of PARP-1 and PTp53 reduced deterioration of renal function after IRI. To test whether double knockout of PARP-1 and PTp53 in the kidney protects kidneys from IRI, the levels of BUN and creatinine after IRI in KO mice and in WT mice were assessed. BUN levels were significantly increased in WT mice 24 h after IRI compared with WT sham-operated mice. The increase in BUN level was significantly less in PTp53, PARP-1 single KO mice, and PARP-1/PTp53 DKO mice after IRI compared with WT mice (Fig. 26A). Elevated plasma creatinine levels were also seen in WT mice 24 h after IRI compared with sham-operated mice. Similar to the BUN levels, the increase of plasma creatinine was less in PTp53 KO and PARP-1/PTp53 DKO but

not in PARP-1 single KO mice compared with WT 24 h after IRI (Fig. 26B). The most significant decreases in BUN and creatinine were observed in PARP-1/PTp53 DKO mice. These data suggest that double knockout of the PARP-1 and p53 gene in the kidney further protects renal functional from ischemic injury. Double knockout of PARP-1/PTp53 has stronger effects on kidney function than single knockout mice, which suggests an additive protective effect.

Double knockout of PARP-1 and PTp53 decreased renal histological damage and necrosis after IRI. As expected, kidneys from WT mice after 24 h IRI showed widespread necrosis, brush border blebbing, sloughed cells, and cast formation in the proximal straight tubule, whereas these features were much less apparent in kidneys from PTp53 KO mice and PARP-1/PTp53 DKO mice. The histological changes after IRI were quantified by counting and scoring the percentage of tubules that displayed tubular necrosis, cast formation, and tubular dilation (Fig. 27). The cumulative score of histological damage in the outer medulla at 1 day was significantly lower in PARP-1/PTp53 DKO kidneys compared with WT and single KO kidneys post-IRI. These data demonstrated that gene ablation of PARP-1/PTp53 reduced tubular damage even compared with single KO mice.

Renal inflammation was reduced after IRI in PTp53 KO and PARP-1/PTp53 DKO mice. The infiltration of leukocytes in the outer medulla of WT and KO mice at 24 hours post-IRI was assessed for neutrophils using immunostaining. As shown in representative photographs (Fig 28), WT mice exhibited increased infiltration of neutrophils in the outer medulla, which was attenuated in PTp53 KO and PARP-1/PTp53 DKO mice. The numbers of positively stained cells were counted in a blinded manner and quantitative data indicated that the accumulation of neutrophils was reduced in the outer medulla of PTp53 KO mice, and PARP-1/PTp53 DKO mice, compared to that of WT and PARP-1 KO mice after IRI (Fig. 28).

Double knockout of PARP-1 and PTp53 decreased apoptosis after IRI. To determine whether there is a change of apoptotic levels in the outer medulla of WT mice compared with KO mice, TUNEL assay was performed to assess apoptotic tubular cells. The outer medulla of wild type mice exhibited increased numbers of TUNEL-positive cells compared with that of PTp53 KO and PARP-1/PTp53 DKO mice but not PARP-1 KO mice (Fig. 29). These data suggest that double deletion of PARP-1/PTp53 or PTp53 alone in the kidney decreases apoptotic cell death after IRI, while PARP-1 KO mice do not have these protective effects.

Loss of p53 increased SLC7A11 after IRI. To investigate whether knockout of p53 regulates ferroptosis in the kidney knockout mice, SLC7A11, a glutamate/cysteine carrier, was measured using western blot (Fig. 30). The expression of SLC7A11 is inhibited by p53 as shown in other studies. As described earlier, the expression of p53 (Fig. 25) was decreased in PARP-1, PTp53 knockout mice and PARP-1/PTp53 double knockout mice after IRI. On the opposite, the expression of SLC7A11 was significantly higher in single knockout and PARP-1/PTp53 double knockout mice. These data suggest that increased SLC7A11 channel in the cell might inhibit ferroptosis by increasing intracellular cysteine and glutathione synthesis.

Ferrostatin-1 protected kidney function in PARP-1 KO mice. Previously other groups reported the involvement of ferroptosis in IRI. We next asked if inhibition of ferroptosis could further protect PARP-1 KO mice from IRI. Indeed, our data showed that administration of ferrostatin-1 30 minutes before surgery significantly decreased plasma levels of BUN and creatinine compared with PARP-1 KO mice treated with vehicle (Fig. 31). It indicates that ferroptosis inhibited by ferrostatin-1 is probably mediated by p53.

Figure 25: The expression of p53, PARP-1, p21, and Bax after IRI.

Western blot showing the expression levels of p53, PARP-1, p21 and Bax in WT, PTp53 KO, PARP-1 KO, and PARP-1/PTp53 DKO mice 1 d after IRI. GAPDH level was used as a loading control.

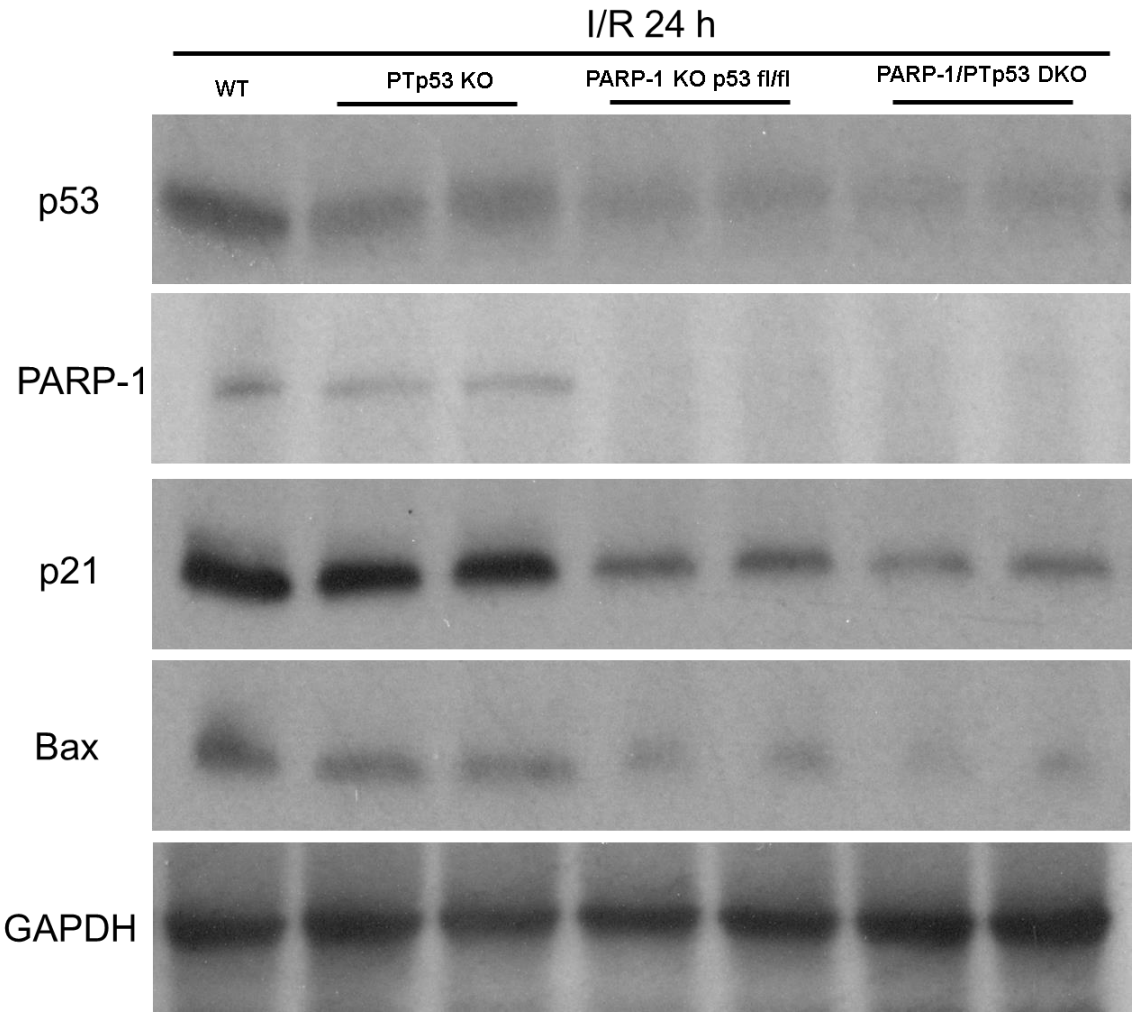
I/R 24 h
WT
PTp53 KO
PARP-1 KO p53 fl/fl
PARP-1/PTp53 DKO
p53
PARP-1
p21
Bax
GAPDH

Figure 26: Kidney function after IRI in single knockout and double knockout mice.

(A) Plasma BUN and (B) Creatinine levels from WT, PTp53 KO, PARP-1 KO, and PARP-1/PTp53 DKO mice (n = 4) at 1d after IRI. * $P < 0.05$ compared with WT-IRI; # $P < 0.05$ compared with both PTp53 KO and PARP-1 KO-IRI; & $P < 0.05$ compared with PARP-1 KO-IRI; † $P < 0.05$ compared with Sham by Tukey's multiple comparison test.

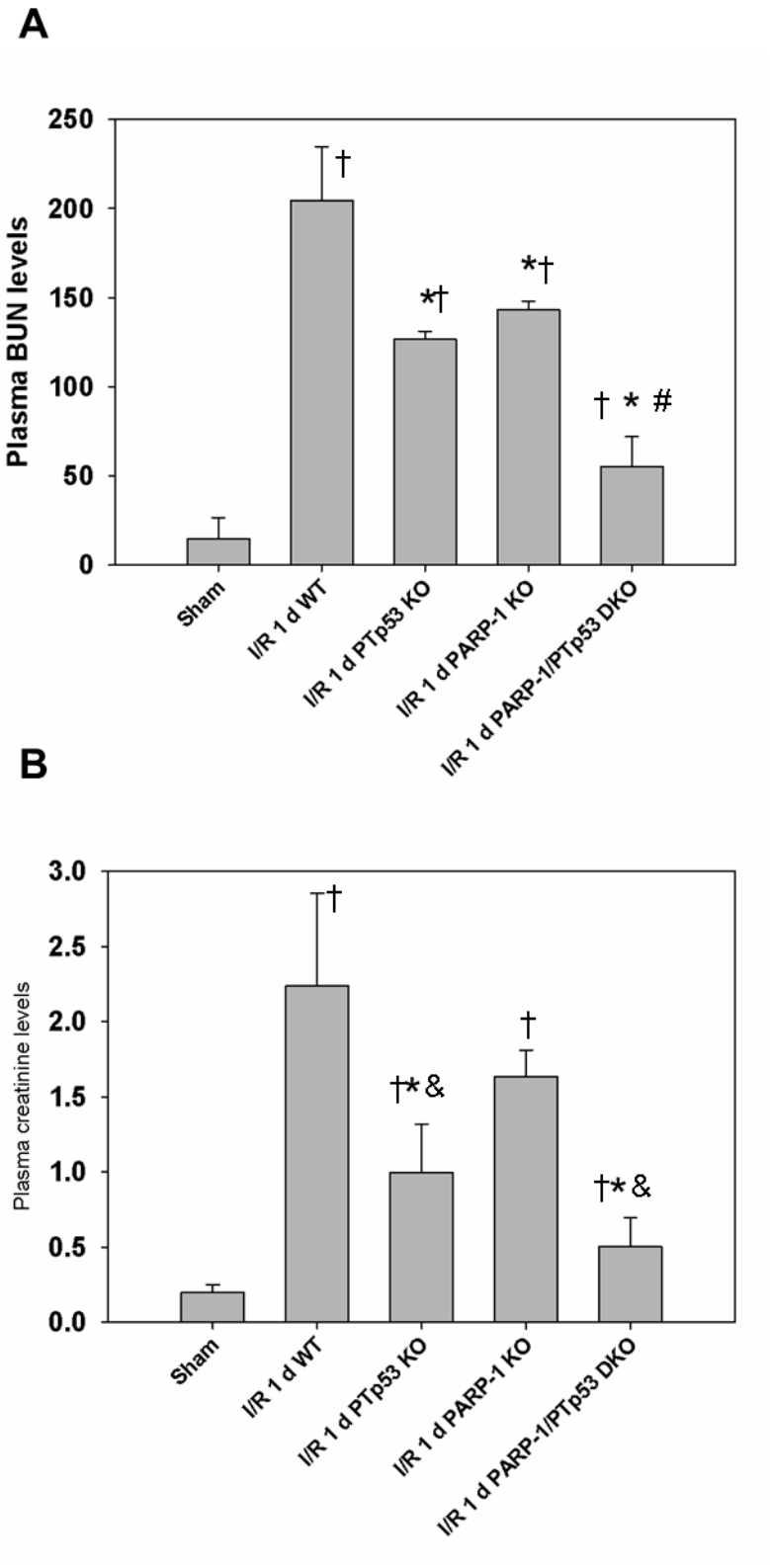
A
Plasma BUN levels
250
200
150
100
50
0
†
*†
*†
† * #
Sham
I/R 1 d WT
I/R 1 d PTp53 KO
I/R 1 d PARP-1 KO
I/R 1 d PARP-1/PTp53 DKO
B
Plasma creatinine levels
3.0
2.5
2.0
1.5
1.0
0.5
0.0
†
†* &
†
†* &
Sham
I/R 1 d WT
I/R 1 d PTp53 KO
I/R 1 d PARP-1 KO
I/R 1 d PARP-1/PTp53 DKO

Figure 27: Kidney histological damage in single and double knockout mice after IRI.

(A). Histological damage in the outer medulla assessed in PAS-stained kidney sections was scored by counting the percentage of tubules that displayed tubular necrosis, cast formation, and tubular dilation as follows: 0 = normal; 1 = < 10%; 2 = 10–25%; 3 = 26–50%; 4 = 51–75%; and 5 = > 75%. Ten fields (200× magnification) per kidney were used for counting. (B). The number of necrotic tubules in the outer medulla per field was counted in WT, PTp53 KO, PARP-1 KO, and PARP-1/PTp53 DKO mice. * $P < 0.05$ compared with WT-IRI and PARP-1 KO-IRI; # $P < 0.05$ compared with WT-IRI, PTp53 KO-IRI and PARP-1 KO-IRI; † $P < 0.05$ compared with Sham by Tukey's multiple comparison test, $n = 6$.

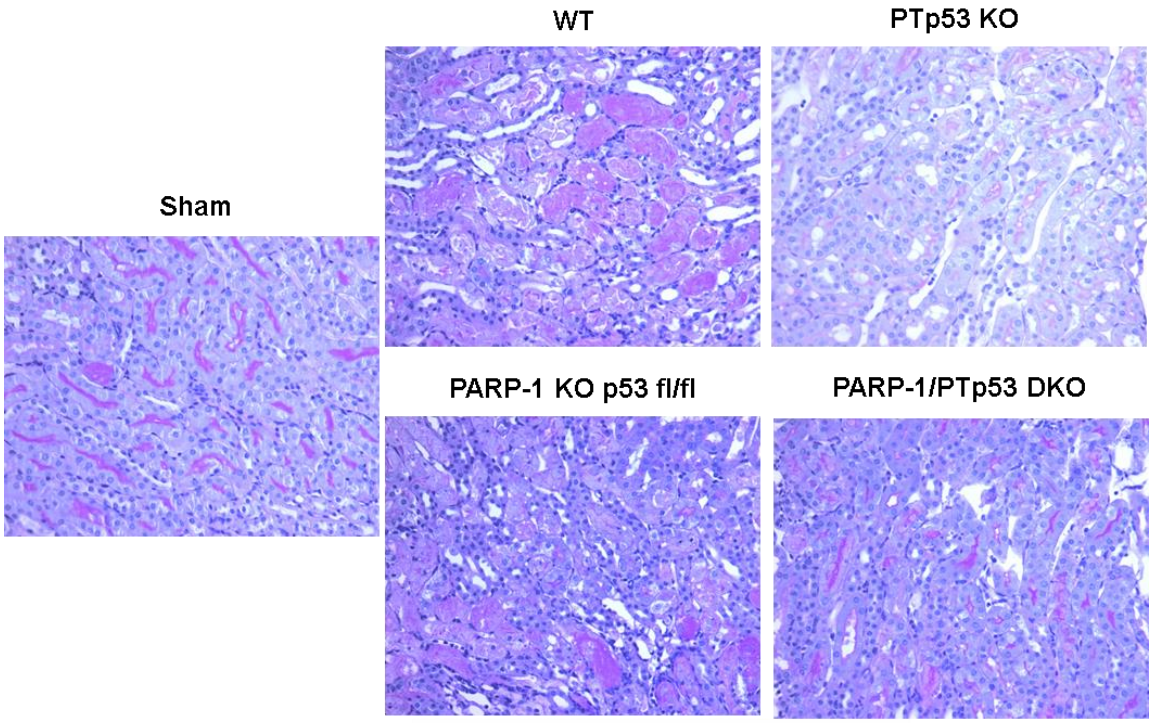
Sham
WT
PTp53 KO
PARP-1 KO p53 fl/fl
PARP-1/PTp53 DKO

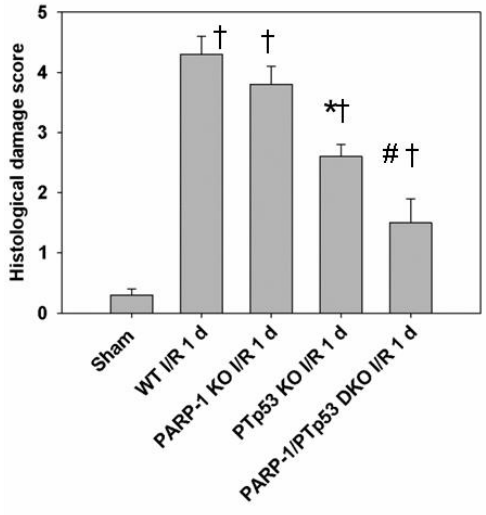
Histological damage score
0
1
2
3
4
5
†
†
*†
†
Sham
WT I/R 1 d
PARP-1 KO I/R 1 d
PTp53 KO I/R 1 d
PARP-1/PTp53 DKO I/R 1 d

Figure 28: Typical neutrophil accumulation in the outer medulla of WT, PARP-1 KO, PTp53 KO, and PARP-1/PTp53 DKO mice at 1 d post IRI.

Number of neutrophils was measured in 10 randomly chosen high magnification (200×) fields per kidney. * $P < 0.05$ compared with WT-IRI and PARP-1 KO-IRI; † $P < 0.05$ compared with Sham by Tukey's multiple comparison test; $n = 4$.

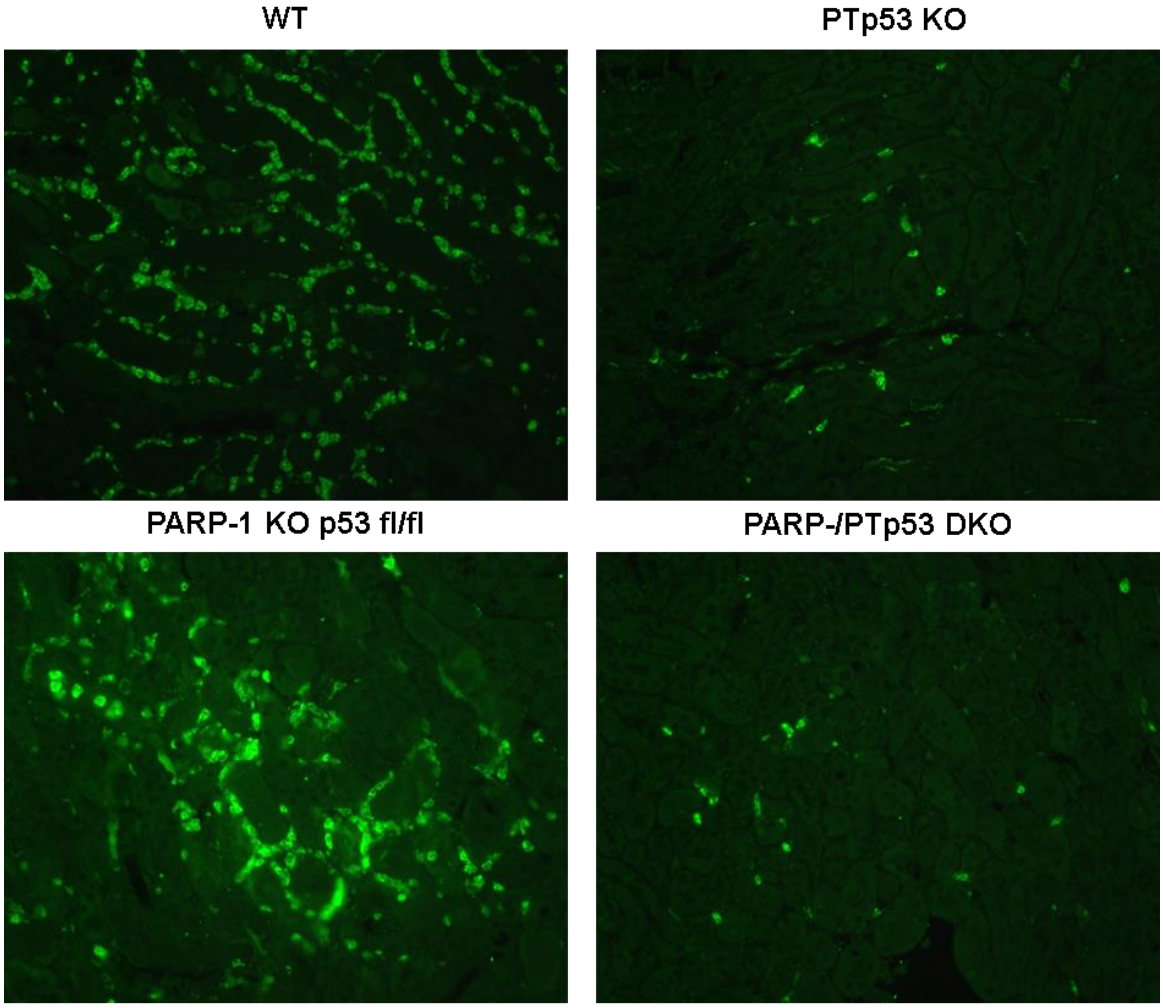
WT
PTp53 KO
PARP-1 KO p53 fl/fl
PARP-/PTp53 DKO

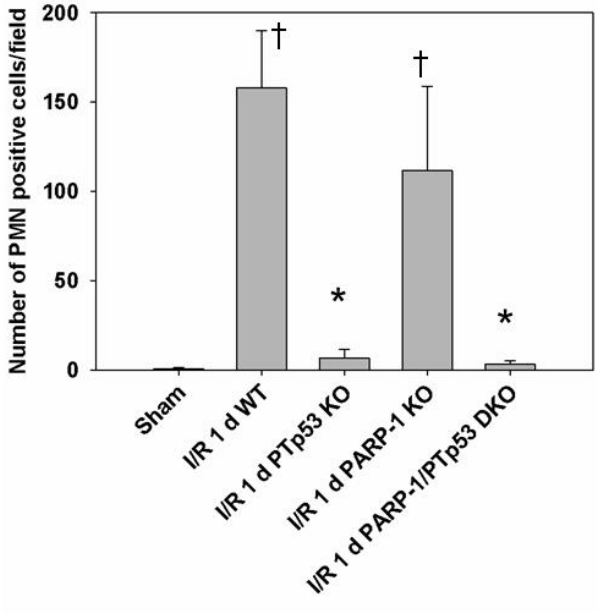
Number of PMN positive cells/field
200
150
100
50
0
†
†
*
*
Sham
I/R 1 d WT
I/R 1 d PTp53 KO
I/R 1 d PARP-1 KO
I/R 1 d PARP-1/PTp53 DKO

Figure 29: TUNEL staining for apoptotic cells in single and double knockout mice. Apoptotic cells were assessed by In Situ Cell death detection assay in WT, PARP-1 KO, PTp53 KO, and PARP-1/PTp53 DKO mice at 1 d after IRI. Number of TUNEL positive cells was measured in 10 randomly chosen high magnification (200×) fields per kidney. * $P < 0.05$ compared with WT-IRI and PARP-1 KO-IRI; † $P < 0.05$ compared with Sham by Tukey's multiple comparison test; $n = 5$.

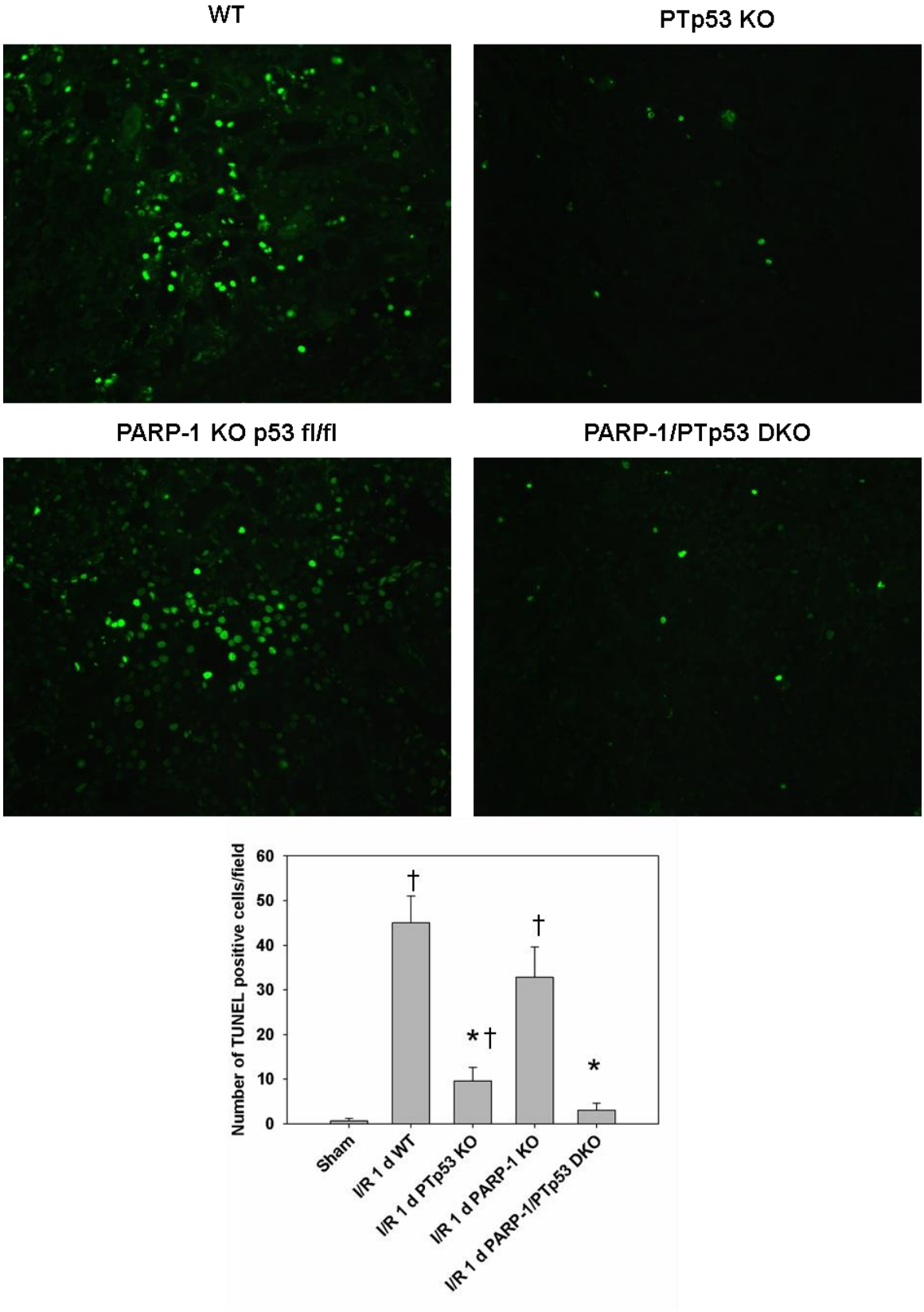
WT
PTp53 KO
PARP-1 KO p53 fl/fl
PARP-1/PTp53 DKO
Number of TUNEL positive cells/field
60
50
40
30
20
10
0
†
*†
†
*
Sham
I/R 1 d WT
I/R 1 d PTp53 KO
I/R 1 d PARP-1 KO
I/R 1 d PARP-1/PTp53 DKO

Figure 30: The expression of p53 and SLC7A11 after IRI in PARP-1 and p53 knockout mice.

Western blot showing the expression levels of p53, and SLC7A11 in WT, PTp53 KO, PARP-1 KO, and PARP-1/PTp53 DKO mice 1 d after IRI. GAPDH level was used as a loading control.

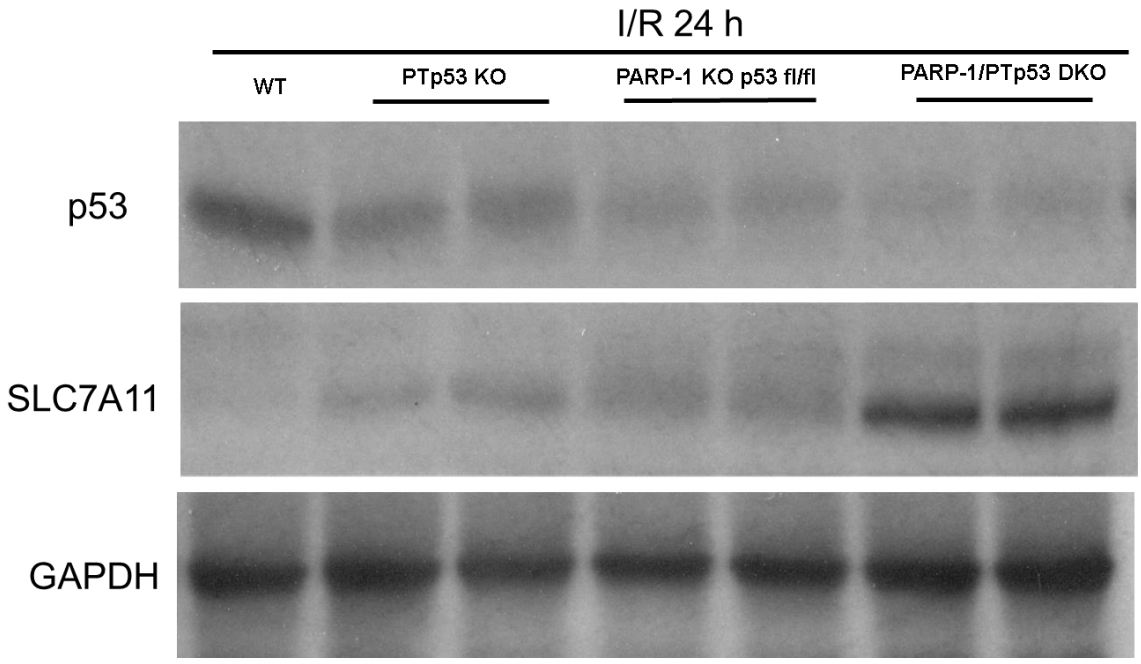
I/R 24 h
WT
PTp53 KO
PARP-1 KO p53 fl/fl
PARP-1/PTp53 DKO
p53
SLC7A11
GAPDH

Figure 31: Kidney function after IRI in PARP-1 KO mice with or without ferrostatin-1.

(A) Plasma creatinine and (B) BUN levels from PARP-1 KO mice with or without of ferroptosis inhibitor ferrostatin-1 treatment (n = 3-4) at 1d after IRI. * $P < 0.05$ compared with PARP-1 KO-IRI; † $P < 0.05$ compared with Sham.

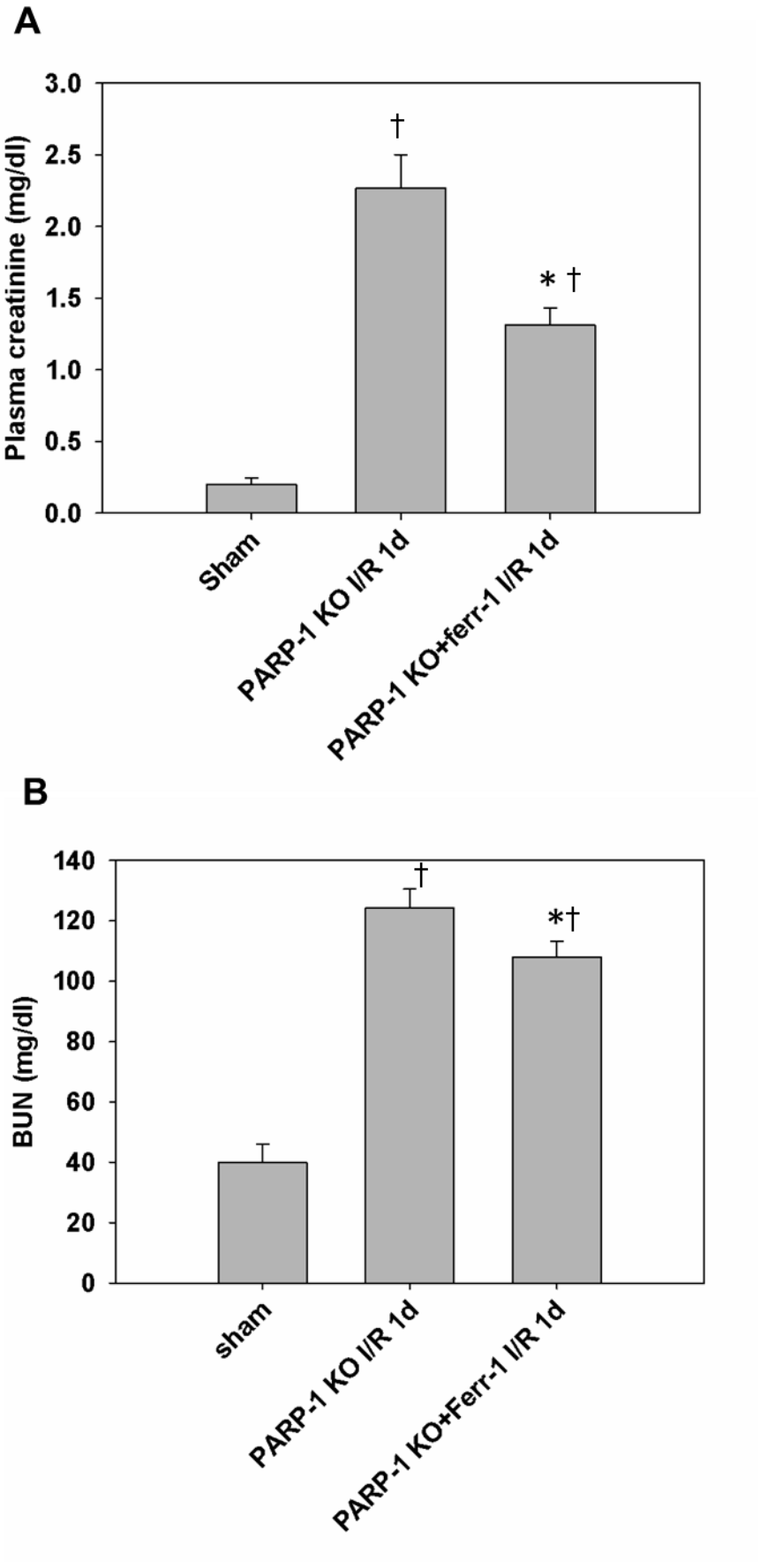
A
Plasma creatinine (mg/dl)
3.0
2.5
2.0
1.5
1.0
0.5
0.0
†
* †
Sham
PARP-1 KO I/R 1d
PARP-1 KO+ferr-1 I/R 1d
B
BUN (mg/dl)
140
120
100
80
60
40
20
0
†
*†
sham
PARP-1 KO I/R 1d
PARP-1 KO+Ferr-1 I/R 1d

Discussion

Ischemic renal injury is strongly associated with proximal tubular cell necrosis and apoptosis (71). It has been shown that interference with many cell death mediators provides protective effects on renal function (76, 87, 88). Proximal tubular cell necrosis directly contributes to the decline in GFR and leads to a sequence of pathophysiological changes in the kidney. During the last few years, certain types of necrotic cell death have been well recognized. Among these pathways, p53 has gained particular attention because of its key role in senescence, apoptosis and even necrosis (166). Indeed, our studies in chapter 1 showed that PTp53 KO significantly improves kidney function and reduces apoptosis after IRI, along with attenuated inflammatory response and later fibrosis. These findings support the concept that p53 is a critical mediator of apoptosis/necrosis after IRI. In this chapter, we showed that double knockout of PARP-1 and PT-specific p53 in the kidney significantly attenuated the decline in kidney function after IRI compared with wild type and single knockout mice. Although PARP-1 single knockout mice had slightly better plasma BUN levels compared with WT, their kidney morphology was not well preserved as PARP-1/PTp53 double knockout mice and p53 single knockout mice. This suggests that PARP-1- or p53-mediated other mechanisms are also involved in the pathogenesis of IRI. Interestingly, animals with both PARP-1/PTp53 genes deleted had less apoptotic cell death and even lower inflammatory infiltration in the kidney. Similar effects were seen in p53 single knockout mice. There data suggest that PARP-1 and p53 have both overlapping and distinctive roles in the pathogenesis of IRI.

Upon DNA damage, p53 is activated and stabilized by reduced activity of MDM2 (99, 166). Various signaling pathways including senescence, cell cycle arrest, apoptosis, autophagy, and necrosis can be activated upon p53 activation (165, 167). Those signals

that activate p53 also can induce the activation of PARP-1. The interaction between p53 and PARP-1 was reported previously by many groups. Our data in chapter 2 also established a regulatory impact of p53 on the expression of PARP-1; however, is the protective effect we have seen in PTp53 KO mice only because the expression of PARP-1 decreases in those mice?

To answer this question, we generated PARP-1/PTp53 DKO mice with mixed background. We have shown that PTp53 KO and PARP-1/PTp53 DKO mice had better kidney function and renal histological scores compared with PARP-1 KO mice. It suggests that p53 have its unique function in mediating IRI injury. PTp53 KO and PARP-1/PTp53 DKO mice had less apoptosis and inflammatory reaction after IRI, suggesting the unique roles of p53 in those pathophysiological processes, which were not apparent in PARP-1 KO mice. PARP-1/PTp53 DKO mice had lowest level of BUN and histological damages compared with PTp53 single knockout mice, indicating deletion of PARP-1 in the kidney added more protection against IRI to PTp53 KO kidney. These data suggest that although p53 regulates the expression of PARP-1, they both have their unique function in the pathogenesis of IRI.

Interestingly, our data also suggested the involvement of a novel type of cell death in IRI: ferroptosis. Ferroptosis is a type of iron-dependent cell death characterized by accumulation of lipid peroxides (37, 104). Morphologically, ferroptosis is characterized by the presence of small mitochondria with condensed membrane densities, and is not associated with chromatin condensation, plasma membrane rupture, swelling of cytoplasmic organelles, or the formation of cytoplasmic vesicles/vacuoles (37). Usually blocking other types of cell death has not direct effect on the process of ferroptosis. Lipid peroxidation and ferroptosis are inhibited physiologically by antioxidant mechanisms including glutathione peroxidase 4 (Gpx4), the only enzyme that reverses the oxidation of membrane lipids. The function of Gpx4 depends on the glutamate/cysteine antiporter

in the plasma membrane known as system Xc^-. SLC7A11 (xCT), together with SLC3A2, encodes the heterodimeric amino acid transport system Xc-, which mediates cysteine-glutamate exchange (47, 147, 176). Decreased cysteine transport results in reduced intracellular glutathione (reduced form) levels and increased production of ROS (48, 182). The activation of p53 suppresses transcription of SLC7A11, leading to reduced cysteine uptake, intracellular glutathione (GSH) and consequent increased ROS levels (79). Thus, in p53 activated cells, the sensitivity to ferroptosis is increased.

We observed a decreased expression of SLC7A11 in wild type mice, but an enhanced expression in PARP-1/PTp53 DKO mice, which have lower levels of p53. Our data suggest that by decreasing the expression of SLC7A11, activated p53 plays a role in mediating ferroptosis. Indeed, when ferroptosis inhibitor ferrostatin-1 was administered to PARP-1 single knockout mice, we observed a better kidney function in those mice. This suggests that ferroptosis after IRI possibly arises through a p53-mediated mechanism. Interestingly, PARP-1/PTp53 DKO mice have the highest level of SLC7A11 expression than both single knockout mice, suggesting that the involvement of PARP-1 in controlling SLC7A11 expression, which has not been reported in any previous studies. The exact mechanism by which SLC7A11 expression is exacerbated in PARP-1/PTp53 DKO mice remains to be defined. Nevertheless, deletion of both PARP-1 and p53 may drastically reduce ferroptosis by the induction of SLC7A11 and may explain why double knockout mice have better kidney function and less necrosis-like cell death compared to the respective single KO mice.

In summary, our data further supported that although p53 regulates PARP-1 expression in the PT, which might play an important role in necrosis after IRI, it can only explain part of the protective effect we saw in PTp53 knockout mice. p53 and PARP-1 both have multiple unique functions other than inducing necrosis. p53-induced

ferroptosis is implicated in the pathogenesis of IRI, and is likely through a PARP-1 independent mechanism.

CHAPTER 4: THE EFFECT OF DOUBLE KNOCKOUT OF PARP-1 /CYPD ON IRI[5]

Introduction

Necrotic cell death, particularly in proximal tubule S3 segment in the outer medulla, is one of the key features of the IRI pathogenesis (16, 17, 162). Tubular cell necrosis after IRI directly contributes to the decline in kidney function and triggers the progression to fibrosis in the kidney (16). A series of necrotic cell death inducers have been involved in this process. Our lab previously reported that two important types of necrotic cell death involved in AKI: PARP-1- and CypD-induced cell death (34, 35, 192). Single knockout of PARP-1 or CypD mice showed reduced necrotic tubules and better outcomes of kidney function. However, whether these two molecules induce necrosis independently or synergistically after IRI is not defined. In order to determine their relative contribution, we present a study using double knockout of PARP-1- and CypD to reveal if there are any intertwines and/or crosstalk between these two molecules in inducing necrosis after IRI.

Activation of PARP-1 is required for DNA repair and in the presence of DNA single- or double-strand breaks (68), PARP-1 transfers the ADP-ribose moiety of NAD^+ to various nuclear proteins. Excessive activation of PARP-1, such as in the setting of IRI, can lead to glycolytic inhibition (35), depletion of NAD^+, and consequent depletion of ATP in the proximal tubule (36). Because of the severe hypoxia in the outer medulla, the limited glycolytic capacity in the proximal tubule cells is further inhibited upon PARP-1

[5] Some of the materials presented in this chapter were previously published: 1. Yuan Ying, Jinu Kim, Sherry N. Westphal, Kelly E. Long, and Babu J. Padanilam. Targeted deletion of p53 in the proximal tubule prevents ischemic renal injury (183). 2. Yuan Ying and Babu J. Padanilam, Regulation of necrotic cell death: p53, PARP1 and Cyclophilin D -overlapping pathways of regulated necrosis? (184)

activation, which makes S3 segment susceptible to necrotic cell death. Indeed, previous reports from our lab and others have demonstrated that PARP-1 inhibition or gene deletion is protective against ischemia-reperfusion (35, 124, 192), diabetes (143), ureteral obstruction (92), and cisplatin nephrotoxicity (91).

A member of the polypeptidyl-prolyl cis-trans isomerase family, CypD is located in the mitochondrial matrix and can interact with mitochondrial inner membrane proteins to induce the opening of the MPTP, which is a crucial step in CypD-induced necrosis (129, 140). As mentioned earlier, excessive activation of PARP-1, like in the setting of IRI, can lead to depletion of NAD+ and consequent ATP depletion. After ATP depletion, a sustained rise in cytosolic free Ca^{2+} was observed (55). It is possible that uptake of excessive Ca^{2+} by mitochondria as well as increased ROS levels in mitochondria during reperfusion triggers the opening of the MPTP, which needs the participation of CypD. This hypothesis connects these two pathways in a reasonable uniform model that has not been investigated before.

Recent studies have greatly expanded our understanding about these two types of cell death. Our laboratory has previously established key roles for both PARP-1 and CypD in necrosis after IRI (34, 192); however, whether these molecules induce necrosis independently of each other or if their signaling pathways integrate to induce necrosis is unclear. Their relative contribution to the pathogenesis of IRI is also poorly understood. In this chapter, we hypothesized that genetic deletion of both PARP-1 and CypD additively protects mice from ischemic renal injury. We showed that double knockout of PARP-1 and CypD in the kidney significantly attenuated kidney dysfunction after IRI and necrotic cell death compared WT and single knockout mice.

Methods (183)

Generating PARP-1/CypD DKO mice. PARP-1 knockout mice (PARP-1 -/-, 129S1/svImJ background) and CypD knockout mice (CypD -/-, B6129 SF2/J background) were obtained from Jackson Laboratories (Bar Harbor, ME). The breeding strategy for double knockout mice is that first we bred those two single knockout mice to generate heterozygotes PARP-1 +/- CypD +/- mice. Then, by breeding those heterozygotes, we generated double knockout mice (PARP-1 -/- CypD -/-), wild type mice (PARP-1 +/+ CypD +/+), and single knockout mice with mixed background. A routine PCR protocol was used for genotyping from tail DNA samples with the following primer pairs: PARP-1, 5'-CCAGCGCAGCTCAGAGAAGCCA-3', 5'-CATGTTCGATGGGAAAGTCCC-3' and 5'-AGGTGAGATGACAGGAGATC-3'; and CypD, 5'-AAACTTCTCAGTCAGCTGTTGCCT CTG -3', 5'- TTCTCACCAGTGCATAGGGCTCTG-3', and 5'- GCTTTGTTATCCCAGCT GGCGC-3'. All animals were born at the expected Mendelian frequency. They were of normal size and did not display any gross physical or behavioral abnormalities. Animal experiments were approved by the Institutional Animal Care and Use Committee of the University of Nebraska Medical Center.

Inducing IRI in mice. IRI was induced in mice as described previously (34, 192). All animals were given free access to food and water. The mice were anesthetized by intraperitoneal administration of a cocktail containing ketamine (200 mg) and xylazine (16 mg) per kilogram of body weight. Ischemic injury was induced by bilateral renal pedicle clamping using microaneurysm clamps (Roboz Surgical Instrument, Gaithersburg, MD). After 30 min of occlusion, the clamps were removed, and kidney reperfusion was verified visually. Sham-operated control animals underwent the same surgical procedure, except for the occlusion of the renal arteries. During the surgery, all animals were placed on a heating pad to maintain body temperature at 37 ℃. Blood

samples were collected from the orbital sinus under isoflurane anesthesia at 0, 6, 24 and 48 h post-IRI for measurement of serum creatinine and blood urea nitrogen (BUN). At the end of each time point (1 d or 16 d), renal tissue was collected, frozen with liquid nitrogen, and stored at -80°C for future experiments.

Measurement of plasma creatinine and BUN. Plasma creatinine and BUN were measured to evaluate renal function using a Quantichrom assay kit (BioAssay Systems, Hayward, CA) according to the manufacturer's protocol.

Morphological studies. Wild type and knockout mice that underwent IRI were sacrificed at 1 or 16 d. The kidneys then were processed at the University of Nebraska Medical Center histology core facility. Briefly, kidneys were fixed in formalin, embedded in paraffin, and cut into 5 μm sections. The tissue sections were then stained with PAS.

Immunofluorescence for neutrophils. Formalin-fixed mouse kidney sections were processed for immunostaining as described previously (192). The slides were sequentially incubated with rabbit anti-mouse neutrophil antibody (Accurate, Westbury, NY) at a 1:100 dilution overnight at 4 ℃, followed by FITC-conjugated goat anti-rabbit IgG (Vector Labs, Burlingame, CA) at a 1:200 dilution for 1 h at room temperature. Neutrophil infiltration was quantified by counting the number of stained cells per field.

Apoptosis detection by TUNEL staining. TUNEL staining of kidney tissue sections was carried out using the In Situ Cell Death Detection kit, Fluorescein (Roche, Mannheim, Germany) according to manufacturer's protocol.

Western blot analysis. Briefly, whole renal tissue extracts (80 μg protein/lane) were separated on 10% SDS-PAGE gels and then transferred to immobilon membranes (Millipore, Bedford, MA). The membranes were incubated with anti-PARP-1 (Cell Signaling, Beverly, MA), and anti-CypD (Santa Cruz, Santa Cruz, CA) antibodies overnight at 4°C. After washing, the membranes were incubated with horseradish peroxidase-conjugated secondary antibodies against the appropriate primary antibodies

(1:5,000, Vector Laboratories, Burlingame, CA), exposed to Western Lighting Plus-ECL (NEL104001EA; PerkinElmer, Waltham, MA), and then developed with X-ray film. The area of each band was analyzed using NIH image software (Image J).

Statistics. All data are expressed as means ± SE. One way ANOVA was used to compare the mean values of all groups, followed by Tukey's Multiple Comparison Test to compare the mean values between two groups. A *P* value < 0.05 was considered statistically significant.

Results

Successful deletion of PARP-1 and CypD in the kidney. First, we analyzed the expression of PARP-1 and CypD before and after injury in whole kidney samples. Indeed, the expression of PARP-1 (Fig. 32) was absent in PARP-1 single knockout mice and PARP-1/CypD double knockout mice. Moreover, the expression of CypD (Fig. 32) was absent in CypD single knockout mice and PARP-1/CypD double knockout mice. Together with genetyping data, it further confirmed successful deletion of PARP-1 and CypD in the kidney.

Double knockout of PARP-1 and CypD reduced deterioration of renal function after IRI. To test whether the absence of PARP-1 and CypD protects kidney function after IRI, the levels of BUN and creatinine after IRI in KO mice and in WT littermates were assessed. BUN levels were significantly increased in WT mice 24 h after IRI compared with WT sham-operated mice. The increase in BUN level was significantly less in PARP-1/CypD DKO mice after IRI compared with WT mice and CypD single knockout mice (Fig. 33). Plasma creatinine levels were also increased in WT mice 24 h after IRI compared with sham-operated mice. Similar to the BUN levels, the increase of plasma creatinine was less in PARP-1/CypD DKO compared with WT 24 h after IRI (Fig. 33). No significant difference in renal function occurred among sham-operated WT and KO mice. Although not statistically significant, the levels of BUN or plasma creatinine in PARP-1 or CypD single knockout mice were trending down compared with WT mice after IRI. These data suggest that double knockout of the PARP-1 and CypD gene in the kidney further protects renal function from ischemic injury.

Double knockout of PARP-1 and CypD decreased renal histological damage and necrosis after IRI. As expected, widespread necrosis, brush border blebbing, sloughed cells, and cast formation were observed in the proximal straight tubule of kidneys from

WT mice after 24 h IRI, whereas these features were much less apparent in kidneys from PARP-1/CypD DKO mice. The histological changes after IRI were quantified by counting and scoring the percentage of tubules that displayed tubular necrosis, cast formation, and tubular dilation (Fig. 34). The cumulative score of histological damage in the outer medulla at 1 day was significantly lower in PARP-1/CypD DKO kidneys compared with WT kidneys post-IRI. Although the histological damage score of PARP-1 and CypD single knockout mice was not significantly lower than WT, the number of necrotic tubules was significantly reduced compared with WT after IRI, while PARP-1/CypD DKO mice had the lowest level of necrotic tubules. These data demonstrated that gene ablation of PARP-1/CypD reduced tubular damage and cellular necrosis.

Renal inflammation was reduced after IRI in single KO and PARP-1/CypD DKO mice. The infiltration of leukocytes in the outer medulla of WT and KO mice at 24 hours post-IRI was assessed by immunostaining. As shown in representative photographs (Fig 35), WT mice exhibited increased infiltration of neutrophils in the outer medulla, which was attenuated in PARP-1 and/or CypD KO mice. The numbers of positively stained cells were counted in a blinded manner and quantitative data indicate that the accumulation of neutrophils was reduced in the outer medulla of PARP-1 and/or CypD KO mice, while PARP-1/CypD DKO mice has the lowest level of neutrophil infiltration compared to that of WT and single KO mice after IRI (Fig. 35).

Double knockout of PARP-1 and CypD decreased apoptosis after IRI. To determine whether there is a change of apoptotic levels in the outer medulla of WT mice compared with KO mice, TUNEL assay was performed to assess apoptotic tubular cells. The outer medulla of wild type mice exhibited increased numbers of TUNEL-positive cells compared with that of PARP-1/CypD DKO mice but not PARP-1 KO or CypD KO mice (Fig. 36). These data suggest that double deletion of PARP-1/CypD in the kidney

decreases apoptotic cell death after IRI, while PARP-1 KO or CypD KO mice do not have these effects.

Figure 32: The expression of PARP-1 and CypD before and after IRI.

Western blots showing the expression levels of PARP-1 and CypD in WT, PARP-1 KO, and PARP-1/CypD DKO mice after IRI.

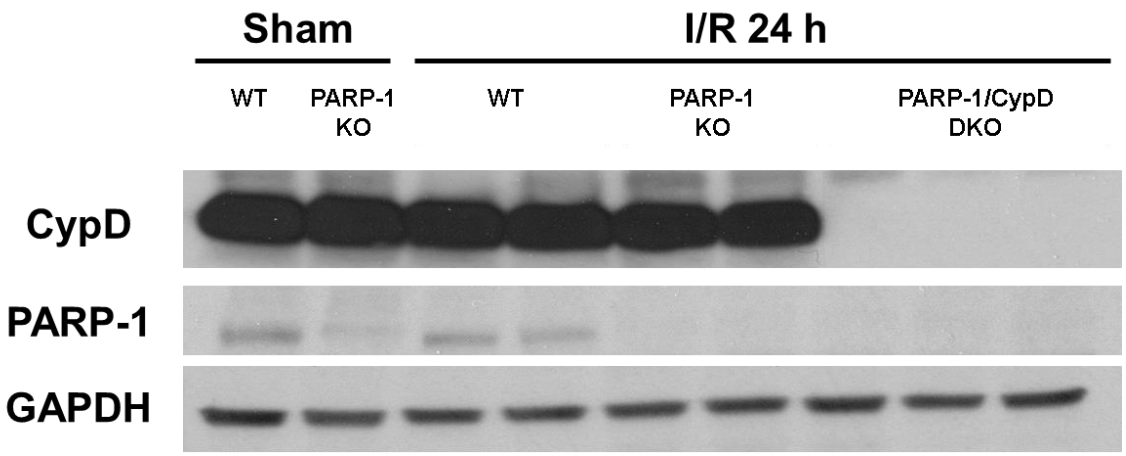
Sham
I/R 24 h
WT
PARP-1 KO
WT
PARP-1 KO
PARP-1/CypD DKO
CypD
PARP-1
GAPDH

Figure 33: Kidney function in PARP-1 and CypD single and double knockout mice after IRI.

(A) Plasma creatinine and (B) BUN levels from WT, PARP-1 KO, CypD KO, and PARP-1/CypD DKO mice (n = 4-6) at 1d after IRI. * $P < 0.05$ compared with WT-IRI; # $P < 0.05$ compared with CypD KO-IRI; † $P < 0.05$ compared with Sham (same genotype) by Tukey's multiple comparison test.

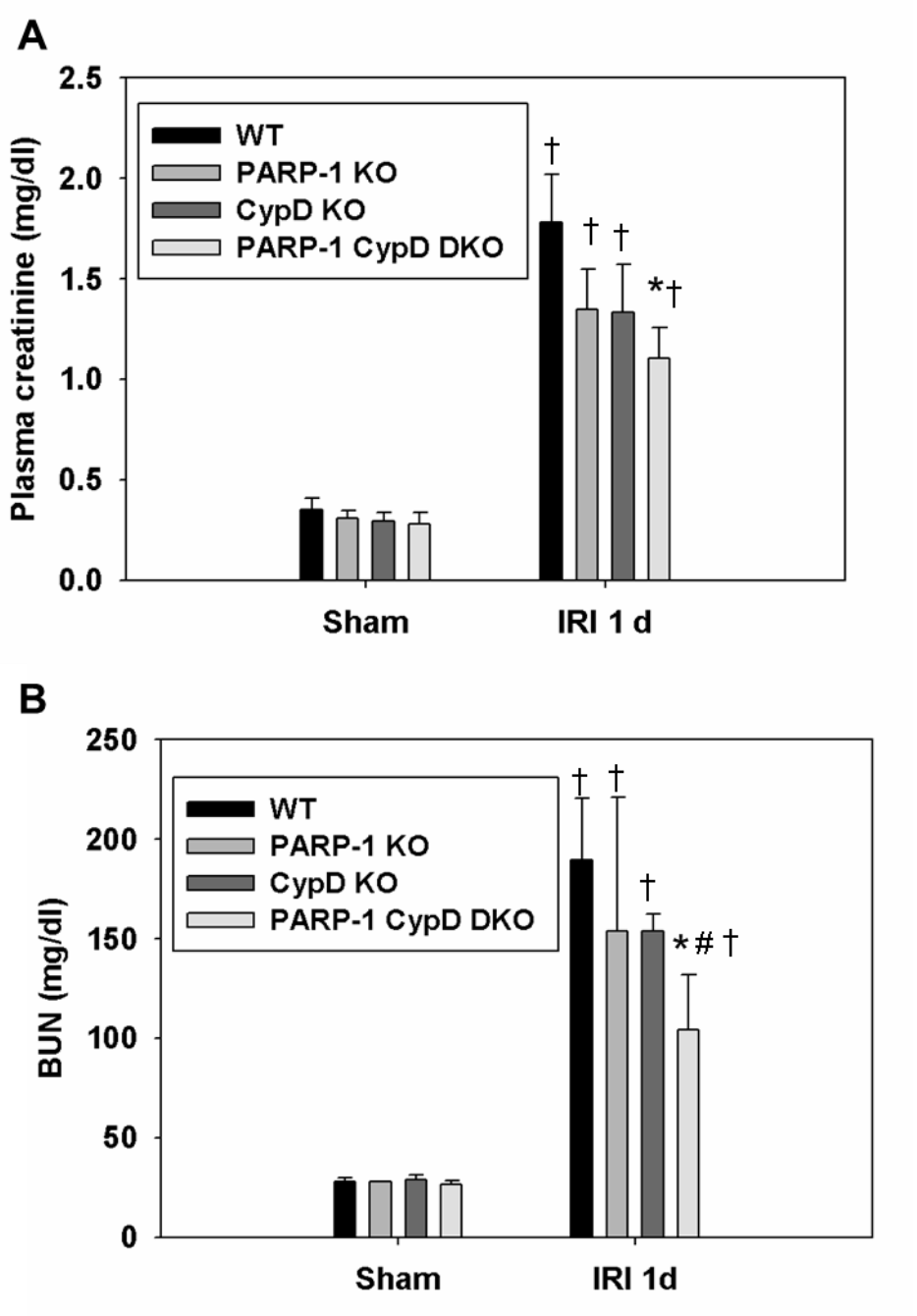
A
Plasma creatinine (mg/dl)
2.5
2.0
1.5
1.0
0.5
0.0
WT
PARP-1 KO
CypD KO
PARP-1 CypD DKO
†
† †
*†
Sham
IRI 1 d
B
BUN (mg/dl)
250
200
150
100
50
0
WT
PARP-1 KO
CypD KO
PARP-1 CypD DKO
† †
†
*# †
Sham
IRI 1d

Figure 34: Kidney histological damage in PARP-1 and CypD single and double knockout mice after IRI.

(A). Histological damage in the outer medulla assessed in PAS-stained kidney sections was scored by counting the percentage of tubules that displayed tubular necrosis, cast formation, and tubular dilation as follows: 0 = normal; 1 = < 10%; 2 = 10–25%; 3 = 26–50%; 4 = 51–75%; and 5 = > 75%. Ten fields (200× magnification) per kidney were used for counting. (B).The number of necrotic tubules in the outer medulla per field was counted. * $P < 0.05$ compared with WT-IRI; # $P < 0.05$ compared with WT-IRI, PARP-1 KO-IRI and CypD KO-IRI; † $P < 0.05$ compared with Sham by Tukey's multiple comparison test; $n = 6$.

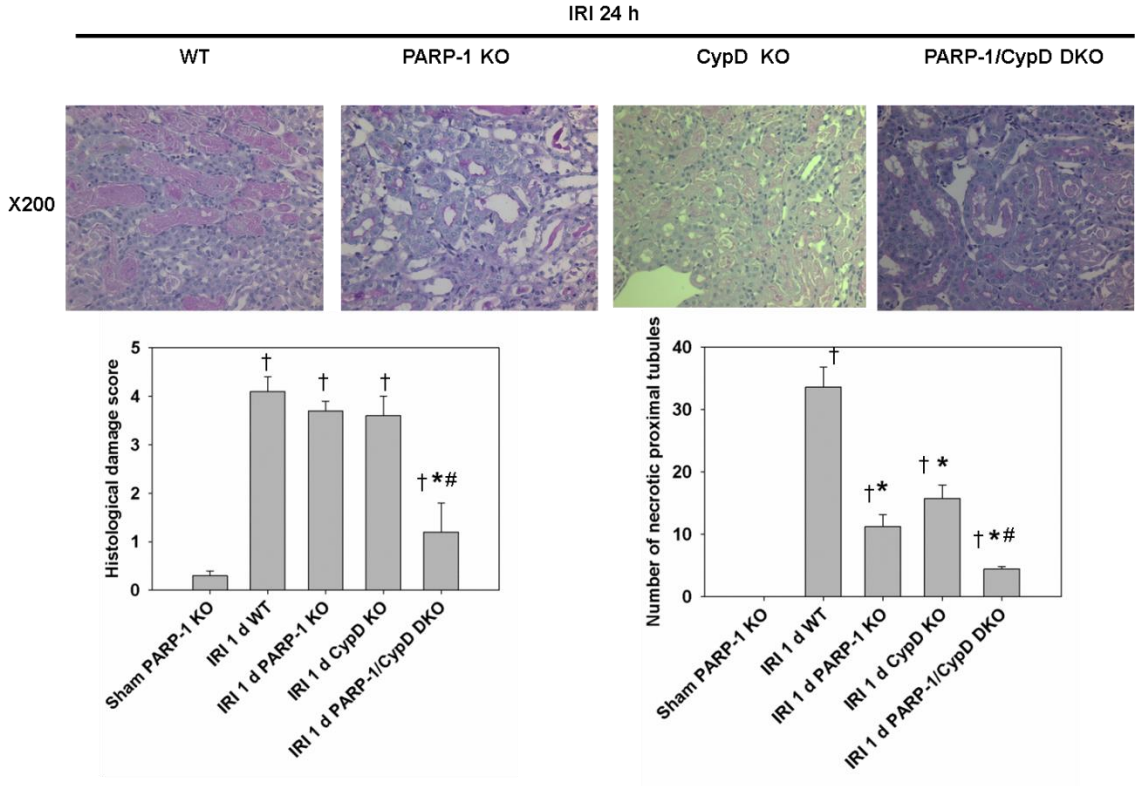
IRI 24 h
WT
PARP-1 KO
CypD KO
PARP-1/CypD DKO
X200
Histological damage score
0
1
2
3
4
5
†
†
†
†*#
Sham PARP-1 KO
IRI 1 d WT
IRI 1 d PARP-1 KO
IRI 1 d CypD KO
IRI 1 d PARP-1/CypD DKO
Number of necrotic proximal tubules
0
10
20
30
40
†
†*
†*
†*#
Sham PARP-1 KO
IRI 1 d WT
IRI 1 d PARP-1 KO
IRI 1 d CypD KO
IRI 1 d PARP-1/CypD DKO

Figure 35: Neutrophil infiltration in the kidney after IRI.

Typical neutrophil accumulation in the outer medulla of WT PARP-1 KO, CypD KO, and PARP-1/CypD DKO mice at 1 day post IRI. Number of neutrophils was measured in 10 randomly chosen high magnification (200×) fields per kidney. * $P < 0.05$ compared with WT-IRI; # $P < 0.05$ compared with both PARP-1 KO-IRI and CypD KO-IRI; † $P < 0.05$ compared with Sham by Tukey's multiple comparison test; $n = 4$.

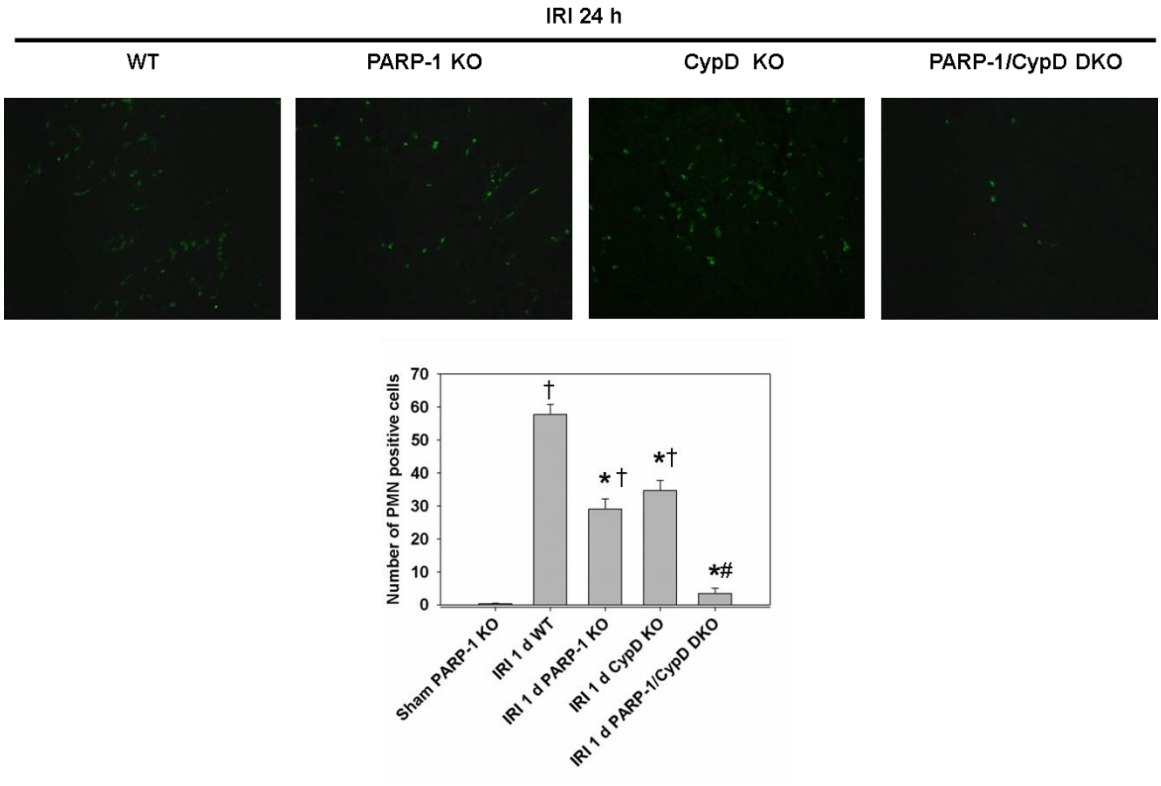
IRI 24 h
WT
PARP-1 KO
CypD KO
PARP-1/CypD DKO
Number of PMN positive cells
70
60
50
40
30
20
10
0
†
*†
*†
*#
Sham PARP-1 KO
IRI 1 d WT
IRI 1 d PARP-1 KO
IRI 1 d CypD KO
IRI 1 d PARP-1/CypD DKO

Figure 36: TUNEL staining for apoptotic cells in PARP-1 and CypD single and double knockout mice after IRI.

Apoptotic cells were assessed by In Situ Cell death detection assay in WT, PARP-1 KO, CypD KO, and PARP-1/CypD DKO mice at 1 day after IRI. Number of TUNEL positive cells was measured in 10 randomly chosen high magnification (200×) fields per kidney. * $P < 0.05$ compared with WT-IRI, PARP-1 KO-IRI and CypD KO-IRI; † $P < 0.05$ compared with Sham by Tukey's multiple comparison test; $n = 4$.

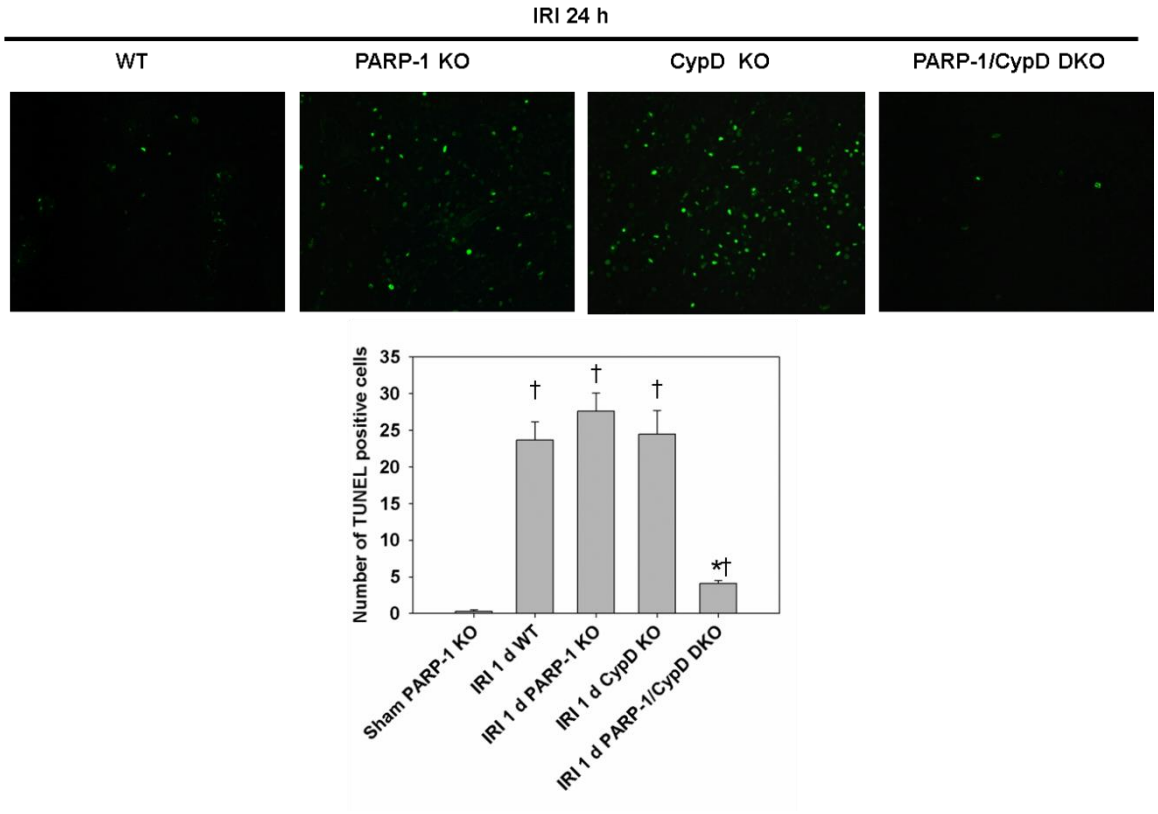
IRI 24 h
WT
PARP-1 KO
CypD KO
PARP-1/CypD DKO
Number of TUNEL positive cells
35
30
25
20
15
10
5
0
†
†
†
*†
Sham PARP-1 KO
IRI 1 d WT
IRI 1 d PARP-1 KO
IRI 1 d CypD KO
IRI 1 d PARP-1/CypD DKO

Discussion

In this study, we showed that double knockout of PARP-1 and CypD in the kidney significantly attenuated the declination of kidney function after IRI compared with wildtype and corresponding single knockout mice. Although PARP-1 and CypD single knockout mice had reduced necrotic tubules in the outer medulla, their kidney function was not well preserved as double knockout mice. It suggests that PARP-1- or CypD-induced necrosis is also involved in the pathogenesis of IRI and they are likely independent pathways. Interestingly, animals with both genes deleted had less apoptotic cell death and even lower inflammatory infiltration in the kidney, which supports the notion that double knockout of PARP-1 and CypD additively protects kidney from IRI.

PARP-1, the most studied member, is an important nuclear enzyme that regulates protein functions by poly(ADP-ribosyl)ation and gene expression as a transcription cofactor (72). Excessive activation of PARP-1, such as in the setting of IRI, can inhibit glycolytic activity in the proximal tubule (35). PARP-1-induced cell death is mediated by its ability to deplete intracellular NAD+ and interfere with energy production. In addition, PARP-1 as a transcriptional regulator exerts its influence on the expression of inflammatory genes including NFκB (36, 69, 91), cytokines (25, 112)(57, 59)(61, 112), ICAM-1 (61, 187), and TLR4 (187). This explains that PARP-1 knockout mice still have robust inflammatory reaction even when the necrotic cell death is reduced. Inflammatory reaction with increased production of cytokines can further cause ROS production and increased secondary apoptotic cell death in PARP-1 knockout mice. The different consequences of PARP-1 activation in tubular cells and interstitial cells might be the key to understand their function as a whole in the kidney. Tissue specific knockout of PARP-1 (for example: in the proximal tubule) will help us to better understand the role of PARP-1 in tubular necrosis and inflammation after IRI.

Previous reports showed that CypD is located in the mitochondrial matrix and can interact with mitochondrial inner membrane proteins to induce the opening of the MPTP. Although numerous molecular constituents of the MPTP have been suggested to be required for pore formation, only CypD has been proved by gene ablation studies (8, 9, 93). ANT in the IMM and VDAC in the OMM were considered as the candidates for the MPTP. However, genetic deletion studies showed that the ANT and voltage-dependent anion channels are dispensable for pore formation (9, 93).

As mentioned previously, excessive activation of PARP-1, like in the setting of IRI, can lead to depletion of NAD+ and consequent ATP depletion (35). After ATP depletion, a sustained rise in cytosolic free Ca^{2+} occurs. Uptake of Ca^{2+} by mitochondria as well as increased ROS levels in mitochondria during reperfusion triggers the opening of the MPTP, which requires a functional CypD. In our model, however, the number of necrotic tubules is significantly lower in PARP-1/CypD double knockout mice rather than single knockout mice, indicating that PARP-1 and CypD probably employ different pathways that do not necessarily converge into the opening of MPTP. Further in vitro experiments are needed to clarify these hypotheses and tease out other players of necrotic cell death in IRI.

In summary, double knockout of PARP-1 and CypD in the mice provides stronger protective effects against IRI than WT mice. Double knockout mice also have less inflammatory infiltration and apoptotic cell death compared with single knockout mice. Thus, double knockout of PARP-1 and CypD in the kidney additively or synergistically protects the kidney from IRI. Although the connections between these pathways were not revealed by our study, our data suggest that these two types of necrotic cell death are possible through two independent pathways.

DISCUSSION[6]

Acute kidney injury

AKI is a clinical syndrome with a rapid decline in GFR over a period of hours to days, leading to retention of metabolic waste and disruption of fluid, electrolytes and acid-base balance (16, 17). A leading cause of AKI is IRI, which results from compromised perfusion to renal tissue. AKI has multiple contributing factors including low blood pressure, cisplatin nephrotoxicity, radiocontrast agent-induced injury, sepsis and various antibiotics used in the clinics. Given the numerous causes of AKI, it occurs in approximately 30% of all patients admitted into intensive care units and is associated with very high mortality rates (50-80%) (110, 141, 151). It also develops in approximately one-third of patients who undergo cardiac surgery (94, 137, 186). Further, for patients who undergo kidney transplants, post-transplant acute tubular necrosis, another cause of AKI, often results in delayed graft functioning and is one of the strongest predictors for the recurrence of end-stage kidney disease (135). Even when patients regain normal, or near normal, kidney function after acute episodes, they still carry significant risks for long-term loss of renal function and development of chronic kidney disease (119). Currently, no effective treatment targeting the pathogenesis of this syndrome is available for AKI patients. Thus, given the increasing frequency of AKI, its related morbidity and mortality and the increasing financial burden, effective treatment options are critically needed.

---

[6] Some of the materials presented in this chapter were previously published: 1. Yuan Ying, Jinu Kim, Sherry N. Westphal, Kelly E. Long, and Babu J. Padanilam. Targeted deletion of p53 in the proximal tubule prevents ischemic renal injury (183). 2. Yuan Ying and Babu J. Padanilam, Regulation of necrotic cell death: p53, PARP1 and Cyclophilin D -overlapping pathways of regulated necrosis? (184)

There are three types of AKI: prerenal, intrarenal, and postrenal AKI. Intrarenal AKI or commonly ATN with the involvement of the renal parenchymal is usually irreversible even with sufficient perfusion (195). It represents a severe form of AKI with selected tubular damage. Although all segments of the nephron may be injured under a severe ischemic insult, the proximal tubules, particularly the S3 segment of the proximal tubule in the outer stripe of outer medulla is usually the most commonly involved segment because of limited glycolytic capacity, high energy requirement, and persistent hypoxia in this area (162). Necrotic cell death in the S3 segment of proximal tubule directly contributes to the declination of GFR. Tubular damage/cell death increases tubular fluid back leak through loose connections between damaged epithelial cells. Absorption dysfunction of the proximal tubule increases tubular fluid solutes in the downstream segment of the nephron, which activates tubuloglomerular feedback as more solute is delivered to the macula densa (16). Necrotic tubules can interact with tubular lumen proteins to form casts in the downstream segments and obstruct the tubular flow and increase back pressure in the glomerulus. All of these factors inevitably lead to a reduced GFR.

Animal models use ischemic reperfusion injury usually result in this type of injury. Some of the pathophysiological processes in ischemic renal injury have also been proved to be true in other types of AKI, although every type of AKI has its unique characteristics. Necrotic and apoptotic cell death are implicated in multiple AKI models (115) and significantly contribute to its pathogenesis. Better understanding of the mechanisms by which different modes of cell death occurs is critical for developing specific therapies targeting specific cell death pathways. The study presented here identified some key players in necrotic cell death such as p53, PARP-1 and CypD and their contribution to the pathogenesis of IRI. Our results suggest that targeting those

molecules in the early stage of IRI might provide therapeutic benefit, improve kidney function, and even reduce long term fibrosis.

The role of p53 in ischemic renal injury

The pathophysiologic abnormalities of IRI are characterized by changes in renal hemodynamics, tubular injury and cell death, and tissue inflammation (16, 106). Ischemia/reperfusion to the kidney parenchyma leads to direct damage to epithelial cells including disruption of cellular energy metabolism, production of ROS, and DNA damage, which cause the activation of nuclear repair enzyme PARP-1 and transcription factor p53. Further, activation of these molecules can initiate pathways that induce necrosis through opening of the MPTP, apoptotic tubular cell death through MOMP, and inflammatory signaling (43, 91). For this reason, the role of p53 and PARP-1 in IRI and other kidney injury models has been heavily investigated.

Several studies have previously investigated the role of p53 in IRI. Kelly *et al*. (88) first showed that p53 expression is increased in the renal medulla after IRI, and pharmacological inhibition of p53 using pifithrin-α can reduce renal injury in rats. Molitoris *et al*. showed that systemic administration of p53-targeted siRNA in mice attenuates ischemic and cisplatin-induced AKI (126). In a recent report, Yang et al. administered pifithrin-α in a single dose 3 and 14 days after unilateral IRI in mice and showed that it relieved epithelial cell cycle arrest and inhibited fibrogenesis (180). However, two recent reports showed that p53 inhibition is detrimental to renal function in IRI. Dagher *et al*. administered Pifithrin-α daily, starting at the time of bilateral IRI in rats and continuing for 7 days, which ultimately increased renal fibrosis (32). To add to the puzzle, Sutton *et al*. showed that global p53 deficiency or pharmacological inhibition of p53 exacerbates the injury by increasing and prolonging leukocyte infiltration into the renal parenchyma (152). These differing results suggest that the role of p53 in the

pathophysiology of IRI is much more complicated and still incompletely understood (183).

For this reason, in chapter 1 we hypothesized that specific knockout of p53 in the proximal tubule reduces kidney injury and necrotic cell death in the S3 segment. We used knockout mice with p53 gene specifically deleted in the PT. This strategy not only specifically targets the proximal tubule, the major injury site of IRI (162), but also avoids the inhibition of normal function of p53 in other cells within the kidney. The activation of p53 may be crucial for the normal response of inflammatory cells recruited after IRI, in which the absence of p53 may prolong inflammatory responses and increase renal injury (152). Our data demonstrate that specific deletion of p53 gene in the proximal tubule significantly improves kidney function, preserves renal histology and reduces necrosis and apoptosis after IRI, along with attenuated inflammatory response and late-term fibrosis. In addition, our data from global knockout rats did not show significant difference in the kidney function and renal histological damage. Although we cannot exclude the possibility that species and model difference are accountable for the distinct response, these data probably indicate opposite effects of p53 activation in different cell types on the pathogenesis of IRI. In summary, these findings support the concept that p53 in the PT is a critical mediator of IRI and its inhibition or its downstream signaling pathways prevents IRI and are suitable therapeutic targets (183). Below we comprehensively discussed all the major p53-mediated mechanisms that are suggested by the data from this study and previous studies.

The mechanism of p53-mediated apoptosis

The role for p53 in apoptosis is well established. p53 can upregulate the expression of several proapoptotic genes including Bax, Fas/Apo-1, Siva, PUMA, and Noxa under stress situations (100). Recently, Dong's group using two Bax-deficient mouse models,

found that only conditional Bax deletion specifically from proximal tubules could ameliorate IRI. Systemic deletion of Bax enhanced neutrophil infiltration without significant effect on kidney injury (169). Our data in chapter 1 indicate that expression of Bax, Bid and Siva are induced in ischemic kidneys but attenuated in p53 KO mice. The significance of Bid and Siva expression in IRI was previously reported. In a previous report, Dong's group demonstrated that Bid deficiency attenuated tubular disruption, tubular cell apoptosis, and caspase-3 activation during 48 h of reperfusion (172). Previous studies from our lab reported that the expression of the pro-apoptotic p53 target Siva, and its cognate receptor CD27, is highly upregulated and co-expressed in the ischemic rat and mouse renal tissues (146), indicating that Siva plays a critical role in apoptosis following IRI. It is likely that synergic functions of these pro-apoptotic molecules may lead to the execution of apoptosis after IRI (183).

The mechanisms of p53-mediated necrosis

p53, MPTP and mitochondrial dynamics

The MPTP-dependent necrosis is a common type of cell death in ischemia-reperfusion injury because of the associated mitochondrial Ca^{2+} overload and ROS production (58). ROS and Ca^{2+} are two of the major inducers of MPTP-mediated necrosis via activation of CypD. Accordingly, genetic deletion of CypD in mice led to significant protection against renal IRI as demonstrated by increased renal function and morphological protection (34). CypD deficient mice have less tubular necrosis as compared with wild type mice after the IRI (34) and these data have been subsequently bolstered by others (133).

It was shown that in mitochondria isolated from Bax/Bak double knockout mice, oxidative stress triggers the p53 translocation to the mitochondria and induces the

formation of a CypD-p53 complex that promotes MPTP opening and necrosis (160). Recently, Vaseva et al. (160) showed that p53 may also be implicated in necrotic cell death through its interaction with CypD in the inner membrane of mitochondria, and subsequent opening of MPTP. These results were supported by independent studies demonstrating p53-CypD interaction in MPTP-dependent necrosis in different cell models, including neuronal (190), pancreatic (23), and osteoblast cells (191). The translocation of p53 to the mitochondria is shown to be dependent on dynamin-related protein 1 (Drp1), a mitochondrial fission protein. Drp1 mediates the mono-ubiquitination of p53 by MDM2 to facilitate its translocation to induce necrosis in the setting of oxidative stress (60). Inhibition of Drp1 by the Drp1 peptide inhibitor P110 prevented p53 association with the mitochondria and reduced brain infarction in rats subjected to brain ischemia/reperfusion injury (60).

Indeed, our data showed significantly reduced tubular cell necrosis in the outer medulla of p53 KO mice kidneys compared to WT after IRI (chapter 1, Fig. 5). The role of CypD in necrotic cell death after IRI is established previously by our lab and other groups (34, 113). Two key factors involved in CypD activation are redox stress and calcium mishandling. Our data indicate that p53 deletion can decrease oxidative stress, which could be a potential mechanism by which p53 inhibits necrosis in renal PT cells. Can p53 translocate to mitochondrial matrix and interact with CypD to open the MPTP after IRI? Our attempts to locate p53 to the mitochondria in various in vitro and in vivo models failed, suggesting that this may not be a prominent mechanism by which p53 induces necrosis in renal PTC (see chapter 2, figure 22). In our in vitro model, we tried to overexpress GFP-p53 in the cell and localize it after injury. To our surprise, GFP-p53 was mainly located in the nucleus rather than the cytoplasm of mitochondria. These data suggest that the mitochondrial translocation of p53 after ROS injury is not the main mechanism of p53-induced necrosis. Although the p53 mitochondrial translocation

provides a novel mechanism by which CypD is activated by p53 to trigger MPTP, a few questions regarding the universal nature of this interaction in MPTP remain to be answered. For example, the formation of MPTP in mitochondria lacking p53 and the absence of p53 involvement in calcium-induced MPTP opening are intriguing (86). Our data cannot exclude the possibility that GFP-p53 has changed the molecular behavior of its original form, although the localization signaling is not at the same end of p53 protein. Further studies using cell fractions that can better distinguish cellular organelles are needed to clarify those questions. It will be also important to know the effects of double knockout of p53 and CypD on the kidney after IRI.

The interaction of a multichaperone complex comprising heat shock protein 60 (Hsp60), Hsp90, and TNFR-associated protein-1, to CypD (82) to regulate MPTP has been previously establishedin tumor cells (54). A recent report by Lam et. al. demonstrates that a newly identified partner of Hsp90, the hematopoietic-substrate-1 associated protein x-1 (HAX-1) is involved in the regulation of CypD in the heart. HAX-1 binds to CypD and interferes with its binding to Hsp-90, rendering CypD ubiquitination and degradation, resulting in protection against MPTP opening and cell death (105). The connection between CypD and the chaperone protein has never been investigated in IRI model. Our data did not show any changes in the expression level of CypD after IRI (see chapter 4). It suggests that the expression of CypD is not a major regulatory mechanism to modulate the function of CypD upon IRI.

p53 and MOMP

The MOMP is required for the execution of necrotic cell death as it forms part of the MPTP. Although Bax and Bak were considered as proapoptotic molecules, emerging evidence clearly demonstrate that Bax and Bak are integral components of the MOMP of the MPTP. p53 can control the MOMP by (1) regulating the expression and function of

Bax and Bid at the transcriptional level (99); (2) direct interaction with pro-apoptotic Bax/Bak and anti-apoptotic Bcl2 to modulate the pore activity (28) and (3) suppressing Bcl2 expression via activation of microRNAs (21). However, the role of p53 in regulating Bcl2 family members to elicit necrosis remains undefined.

Bax/Bak in their non-oligomerized form induced a low level of permeability of the outer mitochondrial membrane, that is distinct from its mode of releasing cyt c in apoptosis, and permits necrosis through the MPTP (84). However, the role of p53 in regulating Bax/Bak is context-dependent. For example, muscle-specific deletion of Bax, but not p53, significantly reduced skeletal muscle necrosis and dystrophic pathology in a mouse model of muscular dystrophy (57). On the other hand, our data demonstrated significant decrease in necrosis in PTp53 KO ischemic kidneys possibly through diminished expression of PARP-1 and Bax (183).

Our findings that expression of Bax are induced in ischemic kidneys but attenuated in PTp53 KO mice could suggest the involvement of p53 and Bax in both apoptosis and necrosis, since the mitochondrial swelling and rupture are reduced in the absence of Bax/Bak. Although we did not directly test this hypothesis, recent studies from another group reported that double knockout of Bax/Bak gene reduced a non-apoptotic cell death in the kidney after IRI (169). This suggests that the p53-Bax/Bak pathway might be indeed involved in necrotic cell death after IRI.

p53 and ferroptosis

As discussed earlier, ferroptosis is a type of iron-dependent cell death characterized by accumulation of lipid peroxides (108). Ferroptosis is characterized by the presence of small mitochondria with condensed membrane densities. Usual morphological features of necrosis such as chromatin condensation, plasma membrane rupture, swelling of cytoplasmic organelles, or the formation of cytoplasmic vesicles/vacuoles, were not

observed in ferroptosis (37). Lipid peroxidation and ferroptosis are inhibited physiologically by antioxidant mechanisms including Gpx4, an enzyme, whose function depends on the glu/cys antiporter in the plasma membrane known as system Xc^-. SLC7A11, together with SLC3A2, mediates cystine-glutamate exchange (47, 79, 176). Decreased cystine transport results in reduced intracellular glutathione (reduced form) levels and increased production of ROS (37). A recent report shows that p53 activation suppresses transcription of SLC7A11, leading to reduced cystine uptake, intracellular GSH and consequent increased ROS levels. Thus, the sensitivity to ROS-induced ferroptosis is increased in cells with activated p53. The effect of p53 on ferroptosis was independent of the ability of p53 to induce cell cycle arrest or apoptosis as a p53 mutant ($p53^{KR}$) lacking these functions retained the capacity to induce ferroptosis (79). Further, erastin-induced ferroptosis was not prevented by inhibitors of autophagy, apoptosis or necroptosis suggesting that regulation of cystine uptake by p53 to promote ferroptosis is a distinct mechanism (79). However, it should be noted that this study did not exclude the possibility that CypD could be a downstream responder after p53 activation, even though MPTP driven necrosis and ferroptosis are reported to be distinct mechanisms (37, 118).

Our data suggest that by decreasing the expression of SLC7A11, activated p53 plays a role in mediating ferroptosis. Indeed, when ferroptosis inhibitor ferrostatin-1 was administered into PARP-1 single knockout mice, we observed a better kidney function in those mice. It suggests the ferroptosis after IRI is conducted through a p53-mediated mechanism. Interestingly, PARP-1/PTp53 double knockout mice have the highest level of SLC7A11 expression than the respective single knockout mice, suggesting that the involvement of PARP-1 in controlling SLC7A11 expression, which has not been reported in any previous studies. The effect of both PARP-1 and p53 on the ferroptosis pathway can partially explain why double knockout mice have better kidney function and less

necrosis-like cell death. Future in vivo and in vitro studies using PARP-1/PTp53 DKO or PTp53 single knockout mice and cells with ferrostatin-1 inhibitor might clarify the exact role of PARP-1 and p53 in ferroptosis.

p53 and inflammation in IRI

Inflammatory cells such as neutrophils, monocytes/macrophages, and T cells are major players in the pathophysiology of renal IRI in animal models and in human AKI (6, 7, 89, 148), Blocking the inflammatory reaction in the kidney is shown to prevent renal function deterioration and histological damage. A recent study from Sutton et al. (152) utilized bone marrow transplantation to produce chimeric mice lacking p53 in leukocytes and demonstrated that p53 deletion prevents leukocyte apoptosis and increases their potential for cytokine secretion and thus worsens the pathophysiology of IRI. This study also demonstrated that systemic deletion of p53 can worsen the injury. Our studies using mice lacking p53 in PT showed that it can profoundly decrease the infiltration of leukocytes and thus protect the kidneys from IRI, while p53 global knockout rats had significant increased inflammatory reaction similar to wild type rats. The apparent paradox in these data from the two studies could be due to the variations in the experimental protocol, the differences between the animal models, and the differing effects of inhibition of p53 in specific cell types within the kidney (183).

p53 and fibrosis after IRI

p53 is well known for its role in cell cycle regulation. The role of cell-cycle arrest and tubular apoptosis on the fibrogenic response of kidney tissue has recently been established in different injury models of CKD (180). The cell cycle arrest at G1/G0 or G2/M phase after injury switches tubular cells into a profibrotic phenotype with an increased expression and release of TGF-β, thereby promoting fibrosis (180). The effect

of pharmacological inhibition of p53 using pifithrin-α in fibrosis development after IRI was previously examined by two groups (32, 180), but with opposing results as detailed above. Although the exact cause of these differing results is not clear, the different species and the timing of p53 inhibition in the two experiments may have contributed. Our data indicate that G2/M cell-cycle arrest occurs after IRI in WT mice but not in PTp53 KO mice, as demonstrated by reduced phospho-histone-3 staining, and may contribute to the attenuation of fibrosis. PT-specific deletion of p53 downregulated p21 expression suggesting that it may titrate the level of p21 which allows the cells to progress through G2 and into M phase. On the other hand, our data demonstrate that PTp53 deletion can prevent inflammation and both necrotic and apoptotic cell death. Although it is unclear if the severity of the injury after an ischemic episode directly affects the progression of chronic kidney disease, it is likely that the attenuated inflammation and injury in the PTp53 KO mice may contribute to the decreased fibrosis. Further studies are needed to answer this question (183).

PARP-1-mediated necrosis in AKI

Our lab previously reported that pharmacological inhibition or gene ablation of PARP-1 protects rats and mice kidneys from ischemic injury (124, 192). These data have shown that in ischemic kidneys, PARP-1 expression and activity significantly increased specifically in the S_3 segments of the proximal tubule. PARP-1 inhibition protects from IRI by improving renal function and tissue morphology, attenuated ATP depletion, leukocyte infiltration and activation of inflammatory molecules. An interesting observation from these studies is that PARP-1 inhibition blocked necrosis but had no effect on apoptosis. These results suggest that necrosis and inflammation are primary mediators of ischemic renal injury (124, 192). Similarly, data from our lab showed that PARP-1 deficiency reduced cisplatin-induced kidney dysfunction, oxidative stress, and

tubular necrosis, but not apoptosis (91). Moreover, neutrophil infiltration, activation of nuclear factor-κB, c-Jun N-terminal kinases, p38 mitogen-activated protein kinase, and upregulation of pro-inflammatory genes were all abrogated by PARP-1 deficiency. It demonstrated evidence for a PARP-1/TLR 4/p38/TNF-α axis following cisplatin injury, suggesting that PARP-1 activation is a primary signal and its inhibition/loss protects against cisplatin-induced nephrotoxicity (91). Collectively, these data suggest that targeting PARP-1 may offer a potential therapeutic strategy for both cisplatin and IRI-mediated AKI by preventing necrosis and inflammation.

Although the energy catastrophe theory and parthanatos have been suggested to explain the mechanism of PARP-1-induced cell death, previous studies demonstrated that PARP-1 plays a critical role in energy depletion after AKI. In the ischemic kidneys, lack of oxygen leaves the glycolytic metabolism as the main pathway for ATP production in proximal straight tubules, thick ascending limbs and collecting ducts located in the severely hypoxic outer medullary region. However, glycolytic capacity in PST is selectively inhibited under ischemic conditions accounting for the incurred selective damage (17, 125, 130, 178). It was suggested that the differences in glucose utilization are not due to a difference in the distribution of glycolytic enzyme activities but due to a differential regulation of hemodynamic factors (138, 139). Studies from our lab, however, indicate that PARP-1 inhibits glycolysis specifically in the proximal tubule S_3 segments by poly(ADP-ribosyl)ation of GAPDH. Decreased activity of GAPDH makes proximal tubular cells vulnerable to necrotic cell death when subjected to ischemic injury. These data indicate that poly(ADP-ribosyl)ation of GAPDH and the subsequent inhibition of anaerobic respiration exacerbate ATP depletion and induce necrosis selectively in the proximal tubule cells after IRI.

Cross talk between defined necrotic pathways

The distinctive and overlapping roles of PARP-1 and p53 in IRI

Cellular stress such as DNA damage, oncogene activation or hypoxia can activate and stabilize p53 (99, 166). The direct consequences of p53 activation depend largely on the initial stress, the level of p53 expression and activation and the cellular milieu, in which different factors that modulate various signaling pathways, to elicit apoptosis, autophagy, cell cycle arrest or necrosis (165, 167). PARP-1 is also activated by various agents capable of inducing DNA breaks, including reactive oxygen and nitrogen species, ionizing radiation and alkylating agents (68). As discussed earlier, PARP-1 activation could lead to necrotic cell death by different mechanisms, although the initial response to DNA damage by both p53 and PARP-1 is to repair the damaged DNA and thus maintain genomic integrity (73, 80).

The interaction between p53 and PARP-1 was reported previously in several studies. In aging cells undergoing telomere shortening, PARP-1 binding was shown to be critical for p53 activation and function (161). A reciprocal regulation of PARP-1 by p53 was described by Montero et al. (127) in ROS-induced cell death. Genetic deletion of p53 conferred increased resistance to ROS and PARP-mediated necrotic cell death in various cell types (127). PARP activity at baseline and after ROS stimulation was reduced in the absence of p53. The mechanism by which p53 regulates PARP-1 activation and necrosis, in the setting of ROS-induced DNA damage, remains to be defined. Interestingly, inhibition of PARP-1-mediated necrosis led to p53-mediated caspase activation and apoptosis. p53 can also induce necrotic cell death in response to ROS-induced DNA damage, through the activation of the lysosomal cysteine protease cathepsin Q (156). Our data in chapter 1 and 2 also established a regulatory effect of p53 on the expression of PARP-1.

In chapter 1, we showed that PTp53-KO mice had significantly reduced levels of plasma creatinine and BUN after IRI, and improved renal morphology compared to WT mice (183). Quantitative studies indicated that necrosis is significantly reduced in the PTs after IRI. Although the mechanism by which p53 deletion results in decreased necrosis is not defined, our results demonstrated that the expression level of PARP is attenuated in PTp53 KO compared to wild type mice ischemic kidneys. In chapter 2, we went further to look at the regulatory effect of p53 on the expression of PARP-1 in vitro. Indeed, in our injury model, hypoxia-reoxygenation increased PARP-1 expression in WT primary cell culture, but it was attenuated in p53 KO cells. When we overexpressed GFP-p53 in LLC-PK cells, it increased PARP-1 expression. These data suggest that PARP-1 expression is regulated by p53 in ischemic kidneys and tubular cells.

Our novel finding that p53 inhibition can downregulate PARP-1 expression in kidney suggests that this could be an alternate mechanism by which p53 regulates necrosis after IRI. Activation of PARP-1 is required for DNA repair, but excessive activation leads to necrotic cell death by depletion of intracellular ATP (61, 62). Data from our lab previously reported that pharmacological and genetic inhibition of PARP-1 can prevent kidney dysfunction, oxidative stress, inflammation and tubular necrosis, but not apoptosis after ischemia/reperfusion (35, 124), and cisplatin nephrotoxicity (91).

Although the activation of p53 up-regulates PARP-1 expression after IRI, both molecules have their own unique roles in the pathogenesis of IRI. In chapter 3, we explored the response of double knockout of PARP-1 and PTp53 in the kidney to IRI. PTp53 knockout kidney had less neutrophils infiltration and reduced TUNEL positive cells compared with PARP-1 single knockout mice, indicating a unique role of p53 in apoptosis and inflammation. PTp53 knockout mice also had better kidney function performance and histological score. On the other hand, PARP-1/PTp53 DKO mice showed even better kidney function and histological score, suggesting deletion of PARP-

1 in the kidney added more protective effect than knockout of PTp53 alone. These unique and overlapping roles of PARP-1 and p53 can explain why PARP-1/PTp53 DKO mice have the best renal protective effects. Targeting those molecules might achieve better effects when considering blocking necrotic pathways.

Is MPTP required for PARP-1-induced necrosis?

It was not clear if PARP-1 medicated necrosis and CypD-mediated MPTP are two independent pathways. Xu et al. (177) proposed that PARP-1 activation is mediated through the pro-necrotic kinase RIP1-JNK1 axis, which induced necrosis through MPTP. Data from Alano et al. also suggested that PARP-1-mediated NAD^+ depletion could lead to MPTP opening and necrosis. However, Dodoni et al. demonstrated that the alkylating agent could directly induce MPTP independent of PARP-1 suggesting that the MPTP pore may in fact be upstream of PARP-1 activation and NAD^+ depletion (38). Further, inhibition of PARP-1 failed to block TNFα-induced necrosis and inhibition of RIP1 or RIP3 could not prevent PARP-1-induced necrosis (149). In addition, the protective effects of RIP1 and PARP-1 are additive in oxidative-stress induced necrosis suggesting that they represent separate necrotic pathways (149). It is also noteworthy that although a role for MPTP in PARP-1-induced AIF translocation is suggested by two reports (2, 29), a recent study suggest that PARP-1 and MPTP can induce necrosis independent of each other (40).

In chapter 4, we showed that double knockout of PARP-1 and CypD in the kidney significantly attenuated the declination of kidney function after IRI compared with wild type mice. Although PARP-1 and CypD single knockout mice had reduced necrotic tubules in the outer medulla, their kidney function was not well preserved as double knockout mice. This suggests that PARP-1- or CypD-induced necrosis is also involved in the pathogenesis of IRI and they are likely independent pathways. Interestingly, animals

with both genes deleted had less apoptotic cell death and even lower inflammatory infiltration in the kidney, which supports the notion that double knockout of PARP-1 and CypD additively protects kidney from IRI. Collectively, these data suggest that PARP-1 and CypD-mediated necrotic pathways may be independent of each other. Since we cannot totally exclude other possible mechanisms that make double mice more resistant to IRI, future studies using PARP-1/CypD PT-specific knockout mice may be useful to exclude other factors from the system.

To our knowledge, this is the first study that looked at the renal protective effects of PARP-1/PTp53 and PARP-1/CypD double knockout mice in IRI. Previous studies using single gene ablation of these genes achieved moderate renal protective effects. In this study, however, we showed that double knockout of PARP-1/PTp53 or PARP-1/CypD has significantly better protective effects than their individual single knockout mice. It suggests that the pathogenesis of AKI is a far more complicated process with the participation of multiple cell death pathways. Since double knockout mice still have kidney injury after IRI, it raises an interesting question: Will blocking more necrotic cell death pathways will further protect the kidney from IRI? Future studies using triple knockout mice might be able to answer this question. In addition, tubular specific knockout mice might provide more information about the specific role of PARP-1 and CypD in the proximal tubular cells, and delineate the downstream mechanisms of necrosis after IRI.

Conclusion

Acute kidney injury is a common clinical syndrome with no effective treatment, indicating an incompletely understood pathophysiology. Our data established the importance of p53-induced necrotic cell death in this syndrome. Other molecules including PARP-1, Bax/Bid, and CypD participate in necrotic cell death insinuate that integration of their signaling pathways may be required to elicit necrotic cell death in IRI. Although the hierarchy of their activation, physical interactions and crosstalk between these molecules and how these molecules interact and integrate their functions to elicit necrosis in distinct AKI settings remain largely undefined, our data from double knockout mice suggest that PARP-1- and CypD-induced necrosis are likely independent pathways while p53- and PARP-1- induced necrosis might overlap to some extent. Targeting necrotic cell inducers such as p53, PARP-1, and CypD might be useful therapeutic methods in treating this disorder. In particular, our data demonstrate that p53 has profound effects on tubular cell necrosis, ferroptosis, and apoptosis after IRI. Although targeting proximal tubular cell death by modulating p53 or its downstream signaling pathways may provide an efficient therapeutic strategy for IRI, combination therapies that target multiple modalities of cell death may be required to completely prevent necrosis and maintain renal function (see figure 37).

Figure 37: Molecular mechanism of necrotic cell death in ischemic renal injury.

In the ischemic renal injury model, necrosis in proximal tubular cells is a common type of cell death. Initial injury results in DNA damage and rapid activation of p53 and PARP-1. p53 induces the expression of Bax, which will facilitate the MOMP for necrosis. Activated PARP-1 will rapidly deplete intracellular NAD+ and ATP, and simultaneously inhibit GAPDH, which reduces glycolytic capacity in proximal tubules. p53 induced TIGAR expression inhibits the rate limiting PFK and the glycolytic pathway. The severe ATP depletion from glycolytic inhibition and PARP-1 activation shuts down ion homeostasis resulting in Ca^{2+} influx and uptake into mitochondria. PARP-1 as a transcriptional cofactor induces several cytokines and promotes infiltration of inflammatory cells to the injured renal parenchyma, all leading to increased ROS production. ROS and Ca^{2+}, the most prominent mediators of permeability transition, increase the probability of MPTP opening via activation of CypD and the ATP synthasome complex. Osmotic influx of water and solutes into the mitochondrial matrix leads to mitochondrial swelling and rupture of outermembrane, to elicit mitochondrial dysfunction and necrosis. Although recent evidence suggests that p53 can mediate ferroptosis by regulating the expression of SLC7A11, this pathway has not been tested in ischemic renal injury model. The contribution of necroptosis in proximal tubule cell death has recently been challenged and the mechanism by which RIP1K blockade prevents renal injury remains to be elucidated. Although, recent evidences suggest p53 translocation to mitochondrial matrix and activation of CypD, such a role for p53 is not established in kidney injury (184).

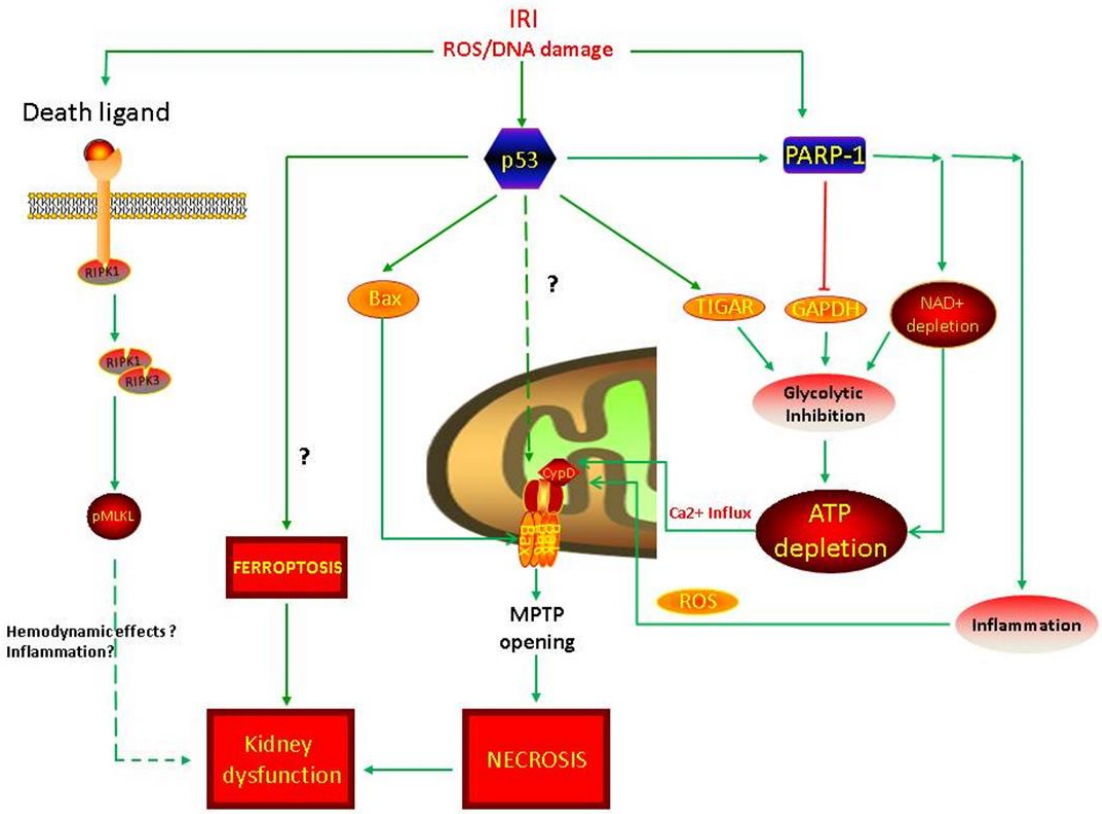
IRI
ROS/DNA damage
Death ligand
RIPK1
RIPK1
RIPK3
pMLKL
Hemodynamic effects ?
Inflammation?
p53
PARP-1
Bax
?
TIGAR
GAPDH
NAD+ depletion
Glycolytic Inhibition
?
CypD
Ca2+ Influx
ATP depletion
ROS
Inflammation
FERROPTOSIS
MPTP opening
Kidney dysfunction
NECROSIS

BIBLIOGRAPHY

1. **Alam MR, Baetz D and Ovize M.** Cyclophilin D and myocardial ischemia-reperfusion injury: a fresh perspective. *J Mol Cell Cardiol* 78: 80-89, 2015.

2. **Alano CC, Ying W and Swanson RA.** Poly(ADP-ribose) polymerase-1-mediated cell death in astrocytes requires NAD+ depletion and mitochondrial permeability transition. *J Biol Chem* 279: 18895-18902, 2004.

3. **Alavian KN, Beutner G, Lazrove E, Sacchetti S, Park HA, Licznerski P, Li H, Nabili P, Hockensmith K, Graham M, Porter GA,Jr and Jonas EA.** An uncoupling channel within the c-subunit ring of the F1FO ATP synthase is the mitochondrial permeability transition pore. *Proc Natl Acad Sci U S A* 111: 10580-10585, 2014.

4. **Ame JC, Spenlehauer C and de Murcia G.** The PARP superfamily. *Bioessays* 26: 882-893, 2004.

5. **Andrabi SA, Umanah GK, Chang C, Stevens DA, Karuppagounder SS, Gagne JP, Poirier GG, Dawson VL and Dawson TM.** Poly(ADP-ribose) polymerase-dependent energy depletion occurs through inhibition of glycolysis. *Proc Natl Acad Sci U S A* 111: 10209-10214, 2014.

6. **Awad AS, Rouse M, Huang L, Vergis AL, Reutershan J, Cathro HP, Linden J and Okusa MD.** Compartmentalization of neutrophils in the kidney and lung following acute ischemic kidney injury. *Kidney Int* 75: 689-698, 2009.

7. **Awad AS, Ye H, Huang L, Li L, Foss FW,Jr, Macdonald TL, Lynch KR and Okusa MD.** Selective sphingosine 1-phosphate 1 receptor activation reduces ischemia-reperfusion injury in mouse kidney. *Am J Physiol Renal Physiol* 290: F1516-24, 2006.

8. **Baines CP, Kaiser RA, Purcell NH, Blair NS, Osinska H, Hambleton MA, Brunskill EW, Sayen MR, Gottlieb RA, Dorn GW, Robbins J and Molkentin JD.** Loss of cyclophilin D reveals a critical role for mitochondrial permeability transition in cell death. *Nature* 434: 658-662, 2005.

9. **Baines CP, Kaiser RA, Sheiko T, Craigen WJ and Molkentin JD.** Voltage-dependent anion channels are dispensable for mitochondrial-dependent cell death. *Nat Cell Biol* 9: 550-555, 2007.

10. **Basso E, Fante L, Fowlkes J, Petronilli V, Forte MA and Bernardi P.** Properties of the permeability transition pore in mitochondria devoid of Cyclophilin D. *J Biol Chem* 280: 18558-18561, 2005.

11. **Bensaad K, Tsuruta A, Selak MA, Vidal MN, Nakano K, Bartrons R, Gottlieb E and Vousden KH.** TIGAR, a p53-inducible regulator of glycolysis and apoptosis. *Cell* 126: 107-120, 2006.

12. **Bernardi P, Di Lisa F, Fogolari F and Lippe G.** From ATP to PTP and Back: A Dual Function for the Mitochondrial ATP Synthase. *Circ Res* 116: 1850-1862, 2015.

13. **Bernardi P and Petronilli V.** The permeability transition pore as a mitochondrial calcium release channel: a critical appraisal. *J Bioenerg Biomembr* 28: 131-138, 1996.

14. **Blantz RC, Deng A, Miracle CM and Thomson SC.** Regulation of kidney function and metabolism: a question of supply and demand. *Trans Am Clin Climatol Assoc* 118: 23-43, 2007.

15. **Bonora M, Bononi A, De Marchi E, Giorgi C, Lebiedzinska M, Marchi S, Patergnani S, Rimessi A, Suski JM, Wojtala A, Wieckowski MR, Kroemer G, Galluzzi L and Pinton P.** Role of the c subunit of the FO ATP synthase in mitochondrial permeability transition. *Cell Cycle* 12: 674-683, 2013.

16. **Bonventre JV and Weinberg JM.** Recent advances in the pathophysiology of ischemic acute renal failure. *J Am Soc Nephrol* 14: 2199-2210, 2003.

17. **Bonventre JV and Yang L.** Cellular pathophysiology of ischemic acute kidney injury. *J Clin Invest* 121: 4210-4221, 2011.

18. **Brezis M and Rosen S.** Hypoxia of the renal medulla--its implications for disease. *N Engl J Med* 332: 647-655, 1995.

19. **Brugarolas J, Chandrasekaran C, Gordon JI, Beach D, Jacks T and Hannon GJ.** Radiation-induced cell cycle arrest compromised by p21 deficiency. *Nature* 377: 552-557, 1995.

20. **Cai Z, Jitkaew S, Zhao J, Chiang HC, Choksi S, Liu J, Ward Y, Wu LG and Liu ZG.** Plasma membrane translocation of trimerized MLKL protein is required for TNF-induced necroptosis. *Nat Cell Biol* 16: 55-65, 2014.

21. **Chakraborty S, Mazumdar M, Mukherjee S, Bhattacharjee P, Adhikary A, Manna A, Chakraborty S, Khan P, Sen A and Das T.** Restoration of p53/miR-34a regulatory

axis decreases survival advantage and ensures Bax-dependent apoptosis of non-small cell lung carcinoma cells. *FEBS Lett* 588: 549-559, 2014.

22. **Chawla LS, Eggers PW, Star RA and Kimmel PL.** Acute kidney injury and chronic kidney disease as interconnected syndromes. *N Engl J Med* 371: 58-66, 2014.

23. **Chen B, Xu M, Zhang H, Wang JX, Zheng P, Gong L, Wu GJ and Dai T.** Cisplatin-induced non-apoptotic death of pancreatic cancer cells requires mitochondrial cyclophilin-D-p53 signaling. *Biochem Biophys Res Commun* 437: 526-531, 2013.

24. **Chen X, Li W, Ren J, Huang D, He WT, Song Y, Yang C, Li W, Zheng X, Chen P and Han J.** Translocation of mixed lineage kinase domain-like protein to plasma membrane leads to necrotic cell death. *Cell Res* 24: 105-121, 2014.

25. **Chiarugi A and Moskowitz MA.** Poly(ADP-ribose) polymerase-1 activity promotes NF-kappaB-driven transcription and microglial activation: implication for neurodegenerative disorders. *J Neurochem* 85: 306-317, 2003.

26. **Chien CT, Chang TC, Tsai CY, Shyue SK and Lai MK.** Adenovirus-mediated bcl-2 gene transfer inhibits renal ischemia/reperfusion induced tubular oxidative stress and apoptosis. *Am J Transplant* 5: 1194-1203, 2005.

27. **Chipuk JE and Green DR.** Dissecting p53-dependent apoptosis. *Cell Death Differ* 13: 994-1002, 2006.

28. **Chipuk JE, Kuwana T, Bouchier-Hayes L, Droin NM, Newmeyer DD, Schuler M and Green DR.** Direct activation of Bax by p53 mediates mitochondrial membrane permeabilization and apoptosis. *Science* 303: 1010-1014, 2004.

29. **Chiu LY, Ho FM, Shiah SG, Chang Y and Lin WW.** Oxidative stress initiates DNA damager MNNG-induced poly(ADP-ribose)polymerase-1-dependent parthanatos cell death. *Biochem Pharmacol* 81: 459-470, 2011.

30. **Conger JD.** Vascular abnormalities in the maintenance of acute renal failure. *Circ Shock* 11: 235-244, 1983.

31. **Dagher PC.** Apoptosis in ischemic renal injury: roles of GTP depletion and p53. *Kidney Int* 66: 506-509, 2004.

32. **Dagher PC, Mai EM, Hato T, Lee SY, Anderson MD, Karozos SC, Mang HE, Knipe NL, Plotkin Z and Sutton TA.** The p53 inhibitor pifithrin-alpha can stimulate fibrosis in a rat model of ischemic acute kidney injury. *Am J Physiol Renal Physiol* 302: F284-91, 2012.

33. **Daugas E, Nochy D, Ravagnan L, Loeffler M, Susin SA, Zamzami N and Kroemer G.** Apoptosis-inducing factor (AIF): a ubiquitous mitochondrial oxidoreductase involved in apoptosis. *FEBS Lett* 476: 118-123, 2000.

34. **Devalaraja-Narashimha K, Diener AM and Padanilam BJ.** Cyclophilin D gene ablation protects mice from ischemic renal injury. *Am J Physiol Renal Physiol* 297: F749-59, 2009.

35. **Devalaraja-Narashimha K and Padanilam BJ.** PARP-1 inhibits glycolysis in ischemic kidneys. *J Am Soc Nephrol* 20: 95-103, 2009.

36. **Devalaraja-Narashimha K, Singaravelu K and Padanilam BJ.** Poly(ADP-ribose) polymerase-mediated cell injury in acute renal failure. *Pharmacol Res* 52: 44-59, 2005.

37. **Dixon SJ, Lemberg KM, Lamprecht MR, Skouta R, Zaitsev EM, Gleason CE, Patel DN, Bauer AJ, Cantley AM, Yang WS, Morrison B,3rd and Stockwell BR.** Ferroptosis: an iron-dependent form of nonapoptotic cell death. *Cell* 149: 1060-1072, 2012.

38. **Dodoni G, Canton M, Petronilli V, Bernardi P and Di Lisa F.** Induction of the mitochondrial permeability transition by the DNA alkylating agent N-methyl-N'-nitro-N-nitrosoguanidine. Sorting cause and consequence of mitochondrial dysfunction. *Biochim Biophys Acta* 1658: 58-63, 2004.

39. **Dondelinger Y, Declercq W, Montessuit S, Roelandt R, Goncalves A, Bruggeman I, Hulpiau P, Weber K, Sehon CA, Marquis RW, Bertin J, Gough PJ, Savvides S, Martinou JC, Bertrand MJ and Vandenabeele P.** MLKL compromises plasma membrane integrity by binding to phosphatidylinositol phosphates. *Cell Rep* 7: 971-981, 2014.

40. **Douglas DL and Baines CP.** PARP1-mediated necrosis is dependent on parallel JNK and Ca(2)(+)/calpain pathways. *J Cell Sci* 127: 4134-4145, 2014.

41. **el-Deiry WS.** P21/p53, Cellular Growth Control and Genomic Integrity. *Curr Top Microbiol Immunol* 227: 121-137, 1998.

42. **el-Deiry WS, Tokino T, Velculescu VE, Levy DB, Parsons R, Trent JM, Lin D, Mercer WE, Kinzler KW and Vogelstein B.** WAF1, a potential mediator of p53 tumor suppression. *Cell* 75: 817-825, 1993.

43. **Elrod JW and Molkentin JD.** Physiologic functions of cyclophilin D and the mitochondrial permeability transition pore. *Circ J* 77: 1111-1122, 2013.

44. **Erdelyi K, Bai P, Kovacs I, Szabo E, Mocsar G, Kakuk A, Szabo C, Gergely P and Virag L.** Dual role of poly(ADP-ribose) glycohydrolase in the regulation of cell death in oxidatively stressed A549 cells. *FASEB J* 23: 3553-3563, 2009.

45. **Fatokun AA, Dawson VL and Dawson TM.** Parthanatos: mitochondrial-linked mechanisms and therapeutic opportunities. *Br J Pharmacol* 171: 2000-2016, 2014.

46. **Feldkamp T, Park JS, Pasupulati R, Amora D, Roeser NF, Venkatachalam MA and Weinberg JM.** Regulation of the mitochondrial permeability transition in kidney proximal tubules and its alteration during hypoxia-reoxygenation. *Am J Physiol Renal Physiol* 297: F1632-46, 2009.

47. **Friedmann Angeli JP, Schneider M, Proneth B, Tyurina YY, Tyurin VA, Hammond VJ, Herbach N, Aichler M, Walch A, Eggenhofer E, Basavarajappa D, Radmark O, Kobayashi S, Seibt T, Beck H, Neff F, Esposito I, Wanke R, Forster H, Yefremova O, Heinrichmeyer M, Bornkamm GW, Geissler EK, Thomas SB, Stockwell BR, O'Donnell VB, Kagan VE, Schick JA and Conrad M.** Inactivation of the ferroptosis regulator Gpx4 triggers acute renal failure in mice. *Nat Cell Biol* 16: 1180-1191, 2014.

48. **Galluzzi L, Bravo-San Pedro JM and Kroemer G.** Ferroptosis in p53-dependent oncosuppression and organismal homeostasis. *Cell Death Differ* 22: 1237-1238, 2015.

49. **Galluzzi L, Bravo-San Pedro JM, Vitale I, Aaronson SA, Abrams JM, Adam D, Alnemri ES, Altucci L, Andrews D, Annicchiarico-Petruzzelli M, Baehrecke EH, Bazan NG, Bertrand MJ, Bianchi K, Blagosklonny MV, Blomgren K, Borner C, Bredesen DE, Brenner C, Campanella M, Candi E, Cecconi F, Chan FK, Chandel NS, Cheng EH, Chipuk JE, Cidlowski JA, Ciechanover A, Dawson TM, Dawson VL,**

De Laurenzi V, De Maria R, Debatin KM, Di Daniele N, Dixit VM, Dynlacht BD, El-Deiry WS, Fimia GM, Flavell RA, Fulda S, Garrido C, Gougeon ML, Green DR, Gronemeyer H, Hajnoczky G, Hardwick JM, Hengartner MO, Ichijo H, Joseph B, Jost PJ, Kaufmann T, Kepp O, Klionsky DJ, Knight RA, Kumar S, Lemasters JJ, Levine B, Linkermann A, Lipton SA, Lockshin RA, Lopez-Otin C, Lugli E, Madeo F, Malorni W, Marine JC, Martin SJ, Martinou JC, Medema JP, Meier P, Melino S, Mizushima N, Moll U, Munoz-Pinedo C, Nunez G, Oberst A, Panaretakis T, Penninger JM, Peter ME, Piacentini M, Pinton P, Prehn JH, Puthalakath H, Rabinovich GA, Ravichandran KS, Rizzuto R, Rodrigues CM, Rubinsztein DC, Rudel T, Shi Y, Simon HU, Stockwell BR, Szabadkai G, Tait SW, Tang HL, Tavernarakis N, Tsujimoto Y, Vanden Berghe T, Vandenabeele P, Villunger A, Wagner EF, Walczak H, White E, Wood WG, Yuan J, Zakeri Z, Zhivotovsky B, Melino G and Kroemer G. Essential versus accessory aspects of cell death: recommendations of the NCCD 2015. *Cell Death Differ* 22: 58-73, 2015.

50. **Galluzzi L, Kepp O, Krautwald S, Kroemer G and Linkermann A.** Molecular mechanisms of regulated necrosis. *Semin Cell Dev Biol* 35: 24-32, 2014.

51. **Galluzzi L, Pietrocola F, Bravo-San Pedro JM, Amaravadi RK, Baehrecke EH, Cecconi F, Codogno P, Debnath J, Gewirtz DA, Karantza V, Kimmelman A, Kumar S, Levine B, Maiuri MC, Martin SJ, Penninger J, Piacentini M, Rubinsztein DC, Simon HU, Simonsen A, Thorburn AM, Velasco G, Ryan KM and Kroemer G.** Autophagy in malignant transformation and cancer progression. *EMBO J* 34: 856-880, 2015.

52. **Galluzzi L, Pietrocola F, Levine B and Kroemer G.** Metabolic control of autophagy. *Cell* 159: 1263-1276, 2014.

53. **Galluzzi L, Vitale I, Abrams JM, Alnemri ES, Baehrecke EH, Blagosklonny MV, Dawson TM, Dawson VL, El-Deiry WS, Fulda S, Gottlieb E, Green DR, Hengartner MO, Kepp O, Knight RA, Kumar S, Lipton SA, Lu X, Madeo F, Malorni W, Mehlen P, Nunez G, Peter ME, Piacentini M, Rubinsztein DC, Shi Y, Simon HU, Vandenabeele P, White E, Yuan J, Zhivotovsky B, Melino G and Kroemer G.** Molecular definitions of cell death subroutines: recommendations of the Nomenclature Committee on Cell Death 2012. *Cell Death Differ* 19: 107-120, 2012.

54. **Ghosh JC, Siegelin MD, Dohi T and Altieri DC.** Heat shock protein 60 regulation of the mitochondrial permeability transition pore in tumor cells. *Cancer Res* 70: 8988-8993, 2010.

55. **Giorgio V, Bisetto E, Soriano ME, Dabbeni-Sala F, Basso E, Petronilli V, Forte MA, Bernardi P and Lippe G.** Cyclophilin D modulates mitochondrial F0F1-ATP synthase by interacting with the lateral stalk of the complex. *J Biol Chem* 284: 33982-33988, 2009.

56. **Giorgio V, von Stockum S, Antoniel M, Fabbro A, Fogolari F, Forte M, Glick GD, Petronilli V, Zoratti M, Szabo I, Lippe G and Bernardi P.** Dimers of mitochondrial ATP synthase form the permeability transition pore. *Proc Natl Acad Sci U S A* 110: 5887-5892, 2013.

57. **Goonasekera SA, Davis J, Kwong JQ, Accornero F, Wei-LaPierre L, Sargent MA, Dirksen RT and Molkentin JD.** Enhanced Ca(2)(+) influx from STIM1-Orai1 induces muscle pathology in mouse models of muscular dystrophy. *Hum Mol Genet* 23: 3706-3715, 2014.

58. **Gottlieb RA.** Cell death pathways in acute ischemia/reperfusion injury. *J Cardiovasc Pharmacol Ther* 16: 233-238, 2011.

59. **Green DR and Chipuk JE.** p53 and metabolism: Inside the TIGAR. *Cell* 126: 30-32, 2006.

60. **Guo X, Sesaki H and Qi X.** Drp1 stabilizes p53 on the mitochondria to trigger necrosis under oxidative stress conditions in vitro and in vivo. *Biochem J* 461: 137-146, 2014.

61. **Ha HC, Hester LD and Snyder SH.** Poly(ADP-ribose) polymerase-1 dependence of stress-induced transcription factors and associated gene expression in glia. *Proc Natl Acad Sci U S A* 99: 3270-3275, 2002.

62. **Ha HC and Snyder SH.** Poly(ADP-ribose) polymerase is a mediator of necrotic cell death by ATP depletion. *Proc Natl Acad Sci U S A* 96: 13978-13982, 1999.

63. **Halestrap AP.** The mitochondrial permeability transition: its molecular mechanism and role in reperfusion injury. *Biochem Soc Symp* 66: 181-203, 1999.

64. **Halestrap AP and Richardson AP.** The mitochondrial permeability transition: a current perspective on its identity and role in ischaemia/reperfusion injury. *J Mol Cell Cardiol* 78: 129-141, 2015.

65. **Hammond EM and Giaccia AJ.** The role of p53 in hypoxia-induced apoptosis. *Biochem Biophys Res Commun* 331: 718-725, 2005.

66. **Hara-Chikuma M and Verkman AS.** Aquaporin-1 facilitates epithelial cell migration in kidney proximal tubule. *J Am Soc Nephrol* 17: 39-45, 2006.

67. **Harberts E, Fishelevich R, Liu J, Atamas SP and Gaspari AA.** MyD88 mediates the decision to die by apoptosis or necroptosis after UV irradiation. *Innate Immun* 20: 529-539, 2014.

68. **Hassa PO and Hottiger MO.** The diverse biological roles of mammalian PARPS, a small but powerful family of poly-ADP-ribose polymerases. *Front Biosci* 13: 3046-3082, 2008.

69. **Hassa PO and Hottiger MO.** The functional role of poly(ADP-ribose)polymerase 1 as novel coactivator of NF-kappaB in inflammatory disorders. *Cell Mol Life Sci* 59: 1534-1553, 2002.

70. **Hausenloy D, Kunst G, Boston-Griffiths E, Kolvekar S, Chaubey S, John L, Desai J and Yellon D.** The effect of cyclosporin-A on peri-operative myocardial injury in adult patients undergoing coronary artery bypass graft surgery: a randomised controlled clinical trial. *Heart* 100: 544-549, 2014.

71. **Havasi A and Borkan SC.** Apoptosis and acute kidney injury. *Kidney Int* 80: 29-40, 2011.

72. **Hegedus C and Virag L.** Inputs and outputs of poly(ADP-ribosyl)ation: Relevance to oxidative stress. *Redox Biol* 2C: 978-982, 2014.

73. **Herceg Z and Wang ZQ.** Functions of poly(ADP-ribose) polymerase (PARP) in DNA repair, genomic integrity and cell death. *Mutat Res* 477: 97-110, 2001.

74. **Holler N, Zaru R, Micheau O, Thome M, Attinger A, Valitutti S, Bodmer JL, Schneider P, Seed B and Tschopp J.** Fas triggers an alternative, caspase-8-

independent cell death pathway using the kinase RIP as effector molecule. *Nat Immunol* 1: 489-495, 2000.

75. **Hong LZ, Zhao XY and Zhang HL.** P53-Mediated Neuronal Cell Death in Ischemic Brain Injury. *Neurosci Bull* 26: 232-240, 2010.

76. **Howard C, Tao S, Yang HC, Fogo AB, Woodgett JR, Harris RC and Rao R.** Specific deletion of glycogen synthase kinase-3beta in the renal proximal tubule protects against acute nephrotoxic injury in mice. *Kidney Int* 82: 1000-1009, 2012.

77. **Humphreys BD.** Kidney injury, stem cells and regeneration. *Curr Opin Nephrol Hypertens* 23: 25-31, 2014.

78. **Humphreys BD and DiRocco DP.** Lineage-tracing methods and the kidney. *Kidney Int* 86: 481-488, 2014.

79. **Jiang L, Kon N, Li T, Wang SJ, Su T, Hibshoosh H, Baer R and Gu W.** Ferroptosis as a p53-mediated activity during tumour suppression. *Nature* 520: 57-62, 2015.

80. **Junttila MR and Evan GI.** p53--a Jack of all trades but master of none. *Nat Rev Cancer* 9: 821-829, 2009.

81. **Kaiser WJ, Sridharan H, Huang C, Mandal P, Upton JW, Gough PJ, Sehon CA, Marquis RW, Bertin J and Mocarski ES.** Toll-like receptor 3-mediated necrosis via TRIF, RIP3, and MLKL. *J Biol Chem* 288: 31268-31279, 2013.

82. **Kang BH, Plescia J, Dohi T, Rosa J, Doxsey SJ and Altieri DC.** Regulation of tumor cell mitochondrial homeostasis by an organelle-specific Hsp90 chaperone network. *Cell* 131: 257-270, 2007.

83. **Karch J, Kanisicak O, Brody MJ, Sargent MA, Michael DM and Molkentin JD.** Necroptosis Interfaces with MOMP and the MPTP in Mediating Cell Death. *PLoS One* 10: e0130520, 2015.

84. **Karch J, Kwong JQ, Burr AR, Sargent MA, Elrod JW, Peixoto PM, Martinez-Caballero S, Osinska H, Cheng EH, Robbins J, Kinnally KW and Molkentin JD.** Bax and Bak function as the outer membrane component of the mitochondrial permeability pore in regulating necrotic cell death in mice. *Elife* 2: e00772, 2013.

85. **Karch J and Molkentin JD.** Regulated necrotic cell death: the passive aggressive side of Bax and Bak. *Circ Res* 116: 1800-1809, 2015.

86. **Karch J and Molkentin JD.** Is p53 the long-sought molecular trigger for cyclophilin D-regulated mitochondrial permeability transition pore formation and necrosis? *Circ Res* 111: 1258-1260, 2012.

87. **Kelly KJ, Plotkin Z and Dagher PC.** Guanosine supplementation reduces apoptosis and protects renal function in the setting of ischemic injury. *J Clin Invest* 108: 1291-1298, 2001.

88. **Kelly KJ, Plotkin Z, Vulgamott SL and Dagher PC.** P53 mediates the apoptotic response to GTP depletion after renal ischemia-reperfusion: protective role of a p53 inhibitor. *J Am Soc Nephrol* 14: 128-138, 2003.

89. **Kelly KJ, Williams WW,Jr, Colvin RB, Meehan SM, Springer TA, Gutierrez-Ramos JC and Bonventre JV.** Intercellular adhesion molecule-1-deficient mice are protected against ischemic renal injury. *J Clin Invest* 97: 1056-1063, 1996.

90. **Kim J, Devalaraja-Narashimha K and Padanilam BJ.** TIGAR regulates glycolysis in ischemic kidney proximal tubules. *Am J Physiol Renal Physiol* 308: F298-308, 2015.

91. **Kim J, Long KE, Tang K and Padanilam BJ.** Poly(ADP-ribose) polymerase 1 activation is required for cisplatin nephrotoxicity. *Kidney Int* 82: 193-203, 2012.

92. **Kim J and Padanilam BJ.** Loss of poly(ADP-ribose) polymerase 1 attenuates renal fibrosis and inflammation during unilateral ureteral obstruction. *Am J Physiol Renal Physiol* 301: F450-9, 2011.

93. **Kokoszka JE, Waymire KG, Levy SE, Sligh JE, Cai J, Jones DP, MacGregor GR and Wallace DC.** The ADP/ATP translocator is not essential for the mitochondrial permeability transition pore. *Nature* 427: 461-465, 2004.

94. **Koreny M, Karth GD, Geppert A, Neunteufl T, Priglinger U, Heinz G and Siostrzonek P.** Prognosis of patients who develop acute renal failure during the first 24 hours of cardiogenic shock after myocardial infarction. *Am J Med* 112: 115-119, 2002.

95. **Kraus WL and Lis JT.** PARP goes transcription. *Cell* 113: 677-683, 2003.

96. **Krishnakumar R, Gamble MJ, Frizzell KM, Berrocal JG, Kininis M and Kraus WL.** Reciprocal binding of PARP-1 and histone H1 at promoters specifies transcriptional outcomes. *Science* 319: 819-821, 2008.

97. **Kroemer G, Galluzzi L, Vandenabeele P, Abrams J, Alnemri ES, Baehrecke EH, Blagosklonny MV, El-Deiry WS, Golstein P, Green DR, Hengartner M, Knight RA, Kumar S, Lipton SA, Malorni W, Nunez G, Peter ME, Tschopp J, Yuan J, Piacentini M, Zhivotovsky B, Melino G and Nomenclature Committee on Cell Death 2009.** Classification of cell death: recommendations of the Nomenclature Committee on Cell Death 2009. *Cell Death Differ* 16: 3-11, 2009.

98. **Kroemer G and Reed JC.** Mitochondrial control of cell death. *Nat Med* 6: 513-519, 2000.

99. **Kruiswijk F, Labuschagne CF and Vousden KH.** P53 in Survival, Death and Metabolic Health: a Lifeguard with a Licence to Kill. *Nat Rev Mol Cell Biol* 16: 393-405, 2015.

100. **Kruse JP and Gu W.** Modes of p53 regulation. *Cell* 137: 609-622, 2009.

101. **Kuang J, Ashorn CL, Gonzalez-Kuyvenhoven M and Penkala JE.** cdc25 is one of the MPM-2 antigens involved in the activation of maturation-promoting factor. *Mol Biol Cell* 5: 135-145, 1994.

102. **Kumari SR, Mendoza-Alvarez H and Alvarez-Gonzalez R.** Functional interactions of p53 with poly(ADP-ribose) polymerase (PARP) during apoptosis following DNA damage: covalent poly(ADP-ribosyl)ation of p53 by exogenous PARP and noncovalent binding of p53 to the M(r) 85,000 proteolytic fragment. *Cancer Res* 58: 5075-5078, 1998.

103. **Kusaba T, Lalli M, Kramann R, Kobayashi A and Humphreys BD.** Differentiated kidney epithelial cells repair injured proximal tubule. *Proc Natl Acad Sci U S A* 111: 1527-1532, 2014.

104. **Lachaier E, Louandre C, Ezzoukhry Z, Godin C, Maziere JC, Chauffert B and Galmiche A.** Ferroptosis, a new form of cell death relevant to the medical treatment of cancer. *Med Sci (Paris)* 30: 779-783, 2014.

105. **Lam CK, Zhao W, Liu GS, Cai WF, Gardner G, Adly G and Kranias EG.** HAX-1 regulates cyclophilin-D levels and mitochondria permeability transition pore in the heart. *Proc Natl Acad Sci U S A* 112: E6466-75, 2015.

106. **Lameire N, Van Biesen W and Vanholder R.** Acute renal failure. *Lancet* 365: 417-430, 2005.

107. **Lee Y, Kang HC, Lee BD, Lee YI, Kim YP and Shin JH.** Poly (ADP-ribose) in the pathogenesis of Parkinson's disease. *BMB Rep* 47: 424-432, 2014.

108. **Li J, McQuade T, Siemer AB, Napetschnig J, Moriwaki K, Hsiao YS, Damko E, Moquin D, Walz T, McDermott A, Chan FK and Wu H.** The RIP1/RIP3 necrosome forms a functional amyloid signaling complex required for programmed necrosis. *Cell* 150: 339-350, 2012.

109. **Li YZ, Lu DY, Tan WQ, Wang JX and Li PF.** p53 initiates apoptosis by transcriptionally targeting the antiapoptotic protein ARC. *Mol Cell Biol* 28: 564-574, 2008.

110. **Liano F and Pascual J.** Outcomes in acute renal failure. *Semin Nephrol* 18: 541-550, 1998.

111. **Liano F and Pascual J.** Epidemiology of acute renal failure: a prospective, multicenter, community-based study. Madrid Acute Renal Failure Study Group. *Kidney Int* 50: 811-818, 1996.

112. **Liaudet L, Pacher P, Mabley JG, Virag L, Soriano FG, Hasko G and Szabo C.** Activation of poly(ADP-Ribose) polymerase-1 is a central mechanism of lipopolysaccharide-induced acute lung inflammation. *Am J Respir Crit Care Med* 165: 372-377, 2002.

113. **Linkermann A, Brasen JH, Darding M, Jin MK, Sanz AB, Heller JO, De Zen F, Weinlich R, Ortiz A, Walczak H, Weinberg JM, Green DR, Kunzendorf U and Krautwald S.** Two independent pathways of regulated necrosis mediate ischemia-reperfusion injury. *Proc Natl Acad Sci U S A* 110: 12024-12029, 2013.

114. **Linkermann A, Brasen JH, Himmerkus N, Liu S, Huber TB, Kunzendorf U and Krautwald S.** Rip1 (receptor-interacting protein kinase 1) mediates necroptosis and contributes to renal ischemia/reperfusion injury. *Kidney Int* 81: 751-761, 2012.

115. **Linkermann A, Chen G, Dong G, Kunzendorf U, Krautwald S and Dong Z.** Regulated cell death in AKI. *J Am Soc Nephrol* 25: 2689-2701, 2014.

116. **Linkermann A and Green DR.** Necroptosis. *N Engl J Med* 370: 455-465, 2014.

117. **Linkermann A, Heller JO, Prokai A, Weinberg JM, De Zen F, Himmerkus N, Szabo AJ, Brasen JH, Kunzendorf U and Krautwald S.** The RIP1-kinase inhibitor necrostatin-1 prevents osmotic nephrosis and contrast-induced AKI in mice. *J Am Soc Nephrol* 24: 1545-1557, 2013.

118. **Linkermann A, Skouta R, Himmerkus N, Mulay SR, Dewitz C, De Zen F, Prokai A, Zuchtriegel G, Krombach F, Welz PS, Weinlich R, Vanden Berghe T, Vandenabeele P, Pasparakis M, Bleich M, Weinberg JM, Reichel CA, Brasen JH, Kunzendorf U, Anders HJ, Stockwell BR, Green DR and Krautwald S.** Synchronized

renal tubular cell death involves ferroptosis. *Proc Natl Acad Sci U S A* 111: 16836-16841, 2014.

119. **Lo LJ, Go AS, Chertow GM, McCulloch CE, Fan D, Ordonez JD and Hsu CY.** Dialysis-requiring acute renal failure increases the risk of progressive chronic kidney disease. *Kidney Int* 76: 893-899, 2009.

120. **Luongo TS, Lambert JP, Yuan A, Zhang X, Gross P, Song J, Shanmughapriya S, Gao E, Jain M, Houser SR, Koch WJ, Cheung JY, Madesh M and Elrod JW.** The Mitochondrial Calcium Uniporter Matches Energetic Supply with Cardiac Workload during Stress and Modulates Permeability Transition. *Cell Rep* 12: 23-34, 2015.

121. **Malanga M, Pleschke JM, Kleczkowska HE and Althaus FR.** Poly(ADP-ribose) binds to specific domains of p53 and alters its DNA binding functions. *J Biol Chem* 273: 11839-11843, 1998.

122. **Mandir AS, Simbulan-Rosenthal CM, Poitras MF, Lumpkin JR, Dawson VL, Smulson ME and Dawson TM.** A novel in vivo post-translational modification of p53 by PARP-1 in MPTP-induced parkinsonism. *J Neurochem* 83: 186-192, 2002.

123. **Marshall KD and Baines CP.** Necroptosis: is there a role for mitochondria? *Front Physiol* 5: 323, 2014.

124. **Martin DR, Lewington AJ, Hammerman MR and Padanilam BJ.** Inhibition of poly(ADP-ribose) polymerase attenuates ischemic renal injury in rats. *Am J Physiol Regul Integr Comp Physiol* 279: R1834-40, 2000.

125. **Mason J, Torhorst J and Welsch J.** Role of the medullary perfusion defect in the pathogenesis of ischemic renal failure. *Kidney Int* 26: 283-293, 1984.

126. **Molitoris BA, Dagher PC, Sandoval RM, Campos SB, Ashush H, Fridman E, Brafman A, Faerman A, Atkinson SJ, Thompson JD, Kalinski H, Skaliter R, Erlich S and Feinstein E.** siRNA targeted to p53 attenuates ischemic and cisplatin-induced acute kidney injury. *J Am Soc Nephrol* 20: 1754-1764, 2009.

127. **Montero J, Dutta C, van Bodegom D, Weinstock D and Letai A.** p53 regulates a non-apoptotic death induced by ROS. *Cell Death Differ* 20: 1465-1474, 2013.

128. **Murphy JM, Lucet IS, Hildebrand JM, Tanzer MC, Young SN, Sharma P, Lessene G, Alexander WS, Babon JJ, Silke J and Czabotar PE.** Insights into the evolution of divergent nucleotide-binding mechanisms among pseudokinases revealed by crystal structures of human and mouse MLKL. *Biochem J* 457: 369-377, 2014.

129. **Nakagawa T, Shimizu S, Watanabe T, Yamaguchi O, Otsu K, Yamagata H, Inohara H, Kubo T and Tsujimoto Y.** Cyclophilin D-dependent mitochondrial permeability transition regulates some necrotic but not apoptotic cell death. *Nature* 434: 652-658, 2005.

130. **Olof P, Hellberg A, Kallskog O and Wolgast M.** Red cell trapping and postischemic renal blood flow. Differences between the cortex, outer and inner medulla. *Kidney Int* 40: 625-631, 1991.

131. **Ouyang Z, Zhu S, Jin J, Li J, Qiu Y, Huang M and Huang Z.** Necroptosis contributes to the cyclosporin A-induced cytotoxicity in NRK-52E cells. *Pharmazie* 67: 725-732, 2012.

132. **Padanilam BJ.** Cell death induced by acute renal injury: a perspective on the contributions of apoptosis and necrosis. *Am J Physiol Renal Physiol* 284: F608-27, 2003.

133. **Park JS, Pasupulati R, Feldkamp T, Roeser NF and Weinberg JM.** Cyclophilin D and the mitochondrial permeability transition in kidney proximal tubules after hypoxic and ischemic injury. *Am J Physiol Renal Physiol* 301: F134-50, 2011.

134. **Pasparakis M and Vandenabeele P.** Necroptosis and its role in inflammation. *Nature* 517: 311-320, 2015.

135. **Perico N, Cattaneo D, Sayegh MH and Remuzzi G.** Delayed graft function in kidney transplantation. *Lancet* 364: 1814-1827, 2004.

136. **Polosukhina D, Singaravelu K and Padanilam BJ.** Activation of protein kinase C isozymes protects LLCPK1 cells from H2O2 induced necrotic cell death. *Am J Nephrol* 23: 380-389, 2003.

137. **Rosner MH and Okusa MD.** Acute kidney injury associated with cardiac surgery. *Clin J Am Soc Nephrol* 1: 19-32, 2006.

138. **Ruegg CE and Mandel LJ.** Bulk isolation of renal PCT and PST. I. Glucose-dependent metabolic differences. *Am J Physiol* 259: F164-75, 1990.

139. **Ruegg CE and Mandel LJ.** Bulk isolation of renal PCT and PST. II. Differential responses to anoxia or hypoxia. *Am J Physiol* 259: F176-85, 1990.

140. **Schinzel AC, Takeuchi O, Huang Z, Fisher JK, Zhou Z, Rubens J, Hetz C, Danial NN, Moskowitz MA and Korsmeyer SJ.** Cyclophilin D is a component of mitochondrial permeability transition and mediates neuronal cell death after focal cerebral ischemia. *Proc Natl Acad Sci U S A* 102: 12005-12010, 2005.

141. **Schrier RW, Wang W, Poole B and Mitra A.** Acute renal failure: definitions, diagnosis, pathogenesis, and therapy. *J Clin Invest* 114: 5-14, 2004.

142. **Scrittori L, Hans F, Angelov D, Charra M, Prigent C and Dimitrov S.** pEg2 aurora-A kinase, histone H3 phosphorylation, and chromosome assembly in Xenopus egg extract. *J Biol Chem* 276: 30002-30010, 2001.

143. **Shevalye H, Stavniichuk R, Xu W, Zhang J, Lupachyk S, Maksimchyk Y, Drel VR, Floyd EZ, Slusher B and Obrosova IG.** Poly(ADP-ribose) polymerase (PARP) inhibition counteracts multiple manifestations of kidney disease in long-term streptozotocin-diabetic rat model. *Biochem Pharmacol* 79: 1007-1014, 2010.

144. **Sica V, Galluzzi L, Bravo-San Pedro JM, Izzo V, Maiuri MC and Kroemer G.** Organelle-Specific Initiation of Autophagy. *Mol Cell* 59: 522-539, 2015.

145. **Simbulan-Rosenthal CM, Rosenthal DS, Luo R and Smulson ME.** Poly(ADP-ribosyl)ation of p53 during apoptosis in human osteosarcoma cells. *Cancer Res* 59: 2190-2194, 1999.

146. **Singaravelu K and Padanilam BJ.** p53 target Siva regulates apoptosis in ischemic kidneys. *Am J Physiol Renal Physiol* 300: F1130-41, 2011.

147. **Skouta R, Dixon SJ, Wang J, Dunn DE, Orman M, Shimada K, Rosenberg PA, Lo DC, Weinberg JM, Linkermann A and Stockwell BR.** Ferrostatins inhibit oxidative lipid damage and cell death in diverse disease models. *J Am Chem Soc* 136: 4551-4556, 2014.

148. **Solez K, Morel-Maroger L and Sraer JD.** The morphology of "acute tubular necrosis" in man: analysis of 57 renal biopsies and a comparison with the glycerol model. *Medicine (Baltimore)* 58: 362-376, 1979.

149. **Sosna J, Voigt S, Mathieu S, Lange A, Thon L, Davarnia P, Herdegen T, Linkermann A, Rittger A, Chan FK, Kabelitz D, Schutze S and Adam D.** TNF-induced necroptosis and PARP-1-mediated necrosis represent distinct routes to programmed necrotic cell death. *Cell Mol Life Sci* 71: 331-348, 2014.

150. **Spivey JR, Bronk SF and Gores GJ.** Glycochenodeoxycholate-induced lethal hepatocellular injury in rat hepatocytes. Role of ATP depletion and cytosolic free calcium. *J Clin Invest* 92: 17-24, 1993.

151. **Star RA.** Treatment of acute renal failure. *Kidney Int* 54: 1817-1831, 1998.

152. **Sutton TA, Hato T, Mai E, Yoshimoto M, Kuehl S, Anderson M, Mang H, Plotkin Z, Chan RJ and Dagher PC.** P53 is Renoprotective After Ischemic Kidney Injury by Reducing Inflammation. *J Am Soc Nephrol* 24: 113-124, 2013.

153. **Suzuki HI, Yamagata K, Sugimoto K, Iwamoto T, Kato S and Miyazono K.** Modulation of microRNA processing by p53. *Nature* 460: 529-533, 2009.

154. **Thapa RJ, Basagoudanavar SH, Nogusa S, Irrinki K, Mallilankaraman K, Slifker MJ, Beg AA, Madesh M and Balachandran S.** NF-kappaB protects cells from gamma interferon-induced RIP1-dependent necroptosis. *Mol Cell Biol* 31: 2934-2946, 2011.

155. **Tristao VR, Goncalves PF, Dalboni MA, Batista MC, Durao Mde S,Jr and Monte JC.** Nec-1 protects against nonapoptotic cell death in cisplatin-induced kidney injury. *Ren Fail* 34: 373-377, 2012.

156. **Tu HC, Ren D, Wang GX, Chen DY, Westergard TD, Kim H, Sasagawa S, Hsieh JJ and Cheng EH.** The p53-cathepsin axis cooperates with ROS to activate programmed necrotic death upon DNA damage. *Proc Natl Acad Sci U S A* 106: 1093-1098, 2009.

157. **Upton JW, Kaiser WJ and Mocarski ES.** DAI/ZBP1/DLM-1 complexes with RIP3 to mediate virus-induced programmed necrosis that is targeted by murine cytomegalovirus vIRA. *Cell Host Microbe* 11: 290-297, 2012.

158. **Valenzuela MT, Guerrero R, Nunez MI, Ruiz De Almodovar JM, Sarker M, de Murcia G and Oliver FJ.** PARP-1 modifies the effectiveness of p53-mediated DNA damage response. *Oncogene* 21: 1108-1116, 2002.

159. **Vanden Berghe T, Linkermann A, Jouan-Lanhouet S, Walczak H and Vandenabeele P.** Regulated necrosis: the expanding network of non-apoptotic cell death pathways. *Nat Rev Mol Cell Biol* 15: 135-147, 2014.

160. **Vaseva AV, Marchenko ND, Ji K, Tsirka SE, Holzmann S and Moll UM.** P53 Opens the Mitochondrial Permeability Transition Pore to Trigger Necrosis. *Cell* 149: 1536-1548, 2012.

161. **Vaziri H, West MD, Allsopp RC, Davison TS, Wu YS, Arrowsmith CH, Poirier GG and Benchimol S.** ATM-dependent telomere loss in aging human diploid fibroblasts

and DNA damage lead to the post-translational activation of p53 protein involving poly(ADP-ribose) polymerase. *EMBO J* 16: 6018-6033, 1997.

162. **Venkatachalam MA, Bernard DB, Donohoe JF and Levinsky NG.** Ischemic damage and repair in the rat proximal tubule: differences among the S1, S2, and S3 segments. *Kidney Int* 14: 31-49, 1978.

163. **Venkatachalam MA, Griffin KA, Lan R, Geng H, Saikumar P and Bidani AK.** Acute kidney injury: a springboard for progression in chronic kidney disease. *Am J Physiol Renal Physiol* 298: F1078-94, 2010.

164. **Vercammen D, Beyaert R, Denecker G, Goossens V, Van Loo G, Declercq W, Grooten J, Fiers W and Vandenabeele P.** Inhibition of caspases increases the sensitivity of L929 cells to necrosis mediated by tumor necrosis factor. *J Exp Med* 187: 1477-1485, 1998.

165. **Vogelstein B, Lane D and Levine AJ.** Surfing the p53 network. *Nature* 408: 307-310, 2000.

166. **Vousden KH and Lane DP.** P53 in Health and Disease. *Nat Rev Mol Cell Biol* 8: 275-283, 2007.

167. **Vousden KH and Lu X.** Live or let die: the cell's response to p53. *Nat Rev Cancer* 2: 594-604, 2002.

168. **Wang H, Sun L, Su L, Rizo J, Liu L, Wang LF, Wang FS and Wang X.** Mixed lineage kinase domain-like protein MLKL causes necrotic membrane disruption upon phosphorylation by RIP3. *Mol Cell* 54: 133-146, 2014.

169. **Wei Q, Dong G, Chen JK, Ramesh G and Dong Z.** Bax and Bak have critical roles in ischemic acute kidney injury in global and proximal tubule-specific knockout mouse models. *Kidney Int* 84: 138-148, 2013.

170. **Wei Q, Dong G, Yang T, Megyesi J, Price PM and Dong Z.** Activation and involvement of p53 in cisplatin-induced nephrotoxicity. *Am J Physiol Renal Physiol* 293: F1282-91, 2007.

171. **Wei Q and Dong Z.** Mouse model of ischemic acute kidney injury: technical notes and tricks. *Am J Physiol Renal Physiol* 303: F1487-94, 2012.

172. **Wei Q, Yin XM, Wang MH and Dong Z.** Bid deficiency ameliorates ischemic renal failure and delays animal death in C57BL/6 mice. *Am J Physiol Renal Physiol* 290: F35-42, 2006.

173. **Westendorf JM, Rao PN and Gerace L.** Cloning of cDNAs for M-phase phosphoproteins recognized by the MPM2 monoclonal antibody and determination of the phosphorylated epitope. *Proc Natl Acad Sci U S A* 91: 714-718, 1994.

174. **Whelan RS, Konstantinidis K, Wei AC, Chen Y, Reyna DE, Jha S, Yang Y, Calvert JW, Lindsten T, Thompson CB, Crow MT, Gavathiotis E, Dorn GW,2nd, O'Rourke B and Kitsis RN.** Bax regulates primary necrosis through mitochondrial dynamics. *Proc Natl Acad Sci U S A* 109: 6566-6571, 2012.

175. **Wieler S, Gagne JP, Vaziri H, Poirier GG and Benchimol S.** Poly(ADP-ribose) polymerase-1 is a positive regulator of the p53-mediated G1 arrest response following ionizing radiation. *J Biol Chem* 278: 18914-18921, 2003.

176. **Xie Y, Hou W, Song X, Yu Y, Huang J, Sun X, Kang R and Tang D.** Ferroptosis: process and function. *Cell Death Differ* 23: 369-379, 2016.

177. **Xu Y, Huang S, Liu ZG and Han J.** Poly(ADP-ribose) polymerase-1 signaling to mitochondria in necrotic cell death requires RIP1/TRAF2-mediated JNK1 activation. *J Biol Chem* 281: 8788-8795, 2006.

178. **Yagil Y, Miyamoto M and Jamison RL.** Inner medullary blood flow in postischemic acute renal failure in the rat. *Am J Physiol* 256: F456-61, 1989.

179. **Yamamoto K, Wilson DR and Baumal R.** Outer medullary circulatory defect in ischemic acute renal failure. *Am J Pathol* 116: 253-261, 1984.

180. **Yang L, Besschetnova TY, Brooks CR, Shah JV and Bonventre JV.** Epithelial cell cycle arrest in G2/M mediates kidney fibrosis after injury. *Nat Med* 16: 535-43, 1p following 143, 2010.

181. **Yang L, Humphreys BD and Bonventre JV.** Pathophysiology of acute kidney injury to chronic kidney disease: maladaptive repair. *Contrib Nephrol* 174: 149-155, 2011.

182. **Yang WS and Stockwell BR.** Ferroptosis: Death by Lipid Peroxidation. *Trends Cell Biol* 26: 165-176, 2016.

183. **Ying Y, Kim J, Westphal SN, Long KE and Padanilam BJ.** Targeted deletion of p53 in the proximal tubule prevents ischemic renal injury. *J Am Soc Nephrol* 25: 2707-2716, 2014.

184. **Ying Y and Padanilam BJ.** Regulation of necrotic cell death: p53, PARP1 and cyclophilin D-overlapping pathways of regulated necrosis? *Cell Mol Life Sci* 2016.

185. **Youle RJ and Strasser A.** The BCL-2 protein family: opposing activities that mediate cell death. *Nat Rev Mol Cell Biol* 9: 47-59, 2008.

186. **Zanardo G, Michielon P, Paccagnella A, Rosi P, Calo M, Salandin V, Da Ros A, Michieletto F and Simini G.** Acute renal failure in the patient undergoing cardiac operation. Prevalence, mortality rate, and main risk factors. *J Thorac Cardiovasc Surg* 107: 1489-1495, 1994.

187. **Zerfaoui M, Errami Y, Naura AS, Suzuki Y, Kim H, Ju J, Liu T, Hans CP, Kim JG, Abd Elmageed ZY, Koochekpour S, Catling A and Boulares AH.** Poly(ADP-ribose) polymerase-1 is a determining factor in Crm1-mediated nuclear export and retention of p65 NF-kappa B upon TLR4 stimulation. *J Immunol* 185: 1894-1902, 2010.

188. **Zhang D, Liu Y, Wei Q, Huo Y, Liu K, Liu F and Dong Z.** Tubular p53 regulates multiple genes to mediate AKI. *J Am Soc Nephrol* 25: 2278-2289, 2014.

189. **Zhang L, Jiang F, Chen Y, Luo J, Liu S, Zhang B, Ye Z, Wang W, Liang X and Shi W.** Necrostatin-1 attenuates ischemia injury induced cell death in rat tubular cell line NRK-52E through decreased Drp1 expression. *Int J Mol Sci* 14: 24742-24754, 2013.

190. **Zhao LP, Ji C, Lu PH, Li C, Xu B and Gao H.** Oxygen glucose deprivation (OGD)/re-oxygenation-induced in vitro neuronal cell death involves mitochondrial cyclophilin-D/P53 signaling axis. *Neurochem Res* 38: 705-713, 2013.

191. **Zhen YF, Wang GD, Zhu LQ, Tan SP, Zhang FY, Zhou XZ and Wang XD.** P53 dependent mitochondrial permeability transition pore opening is required for dexamethasone-induced death of osteoblasts. *J Cell Physiol* 229: 1475-1483, 2014.

192. **Zheng J, Devalaraja-Narashimha K, Singaravelu K and Padanilam BJ.** Poly(ADP-ribose) polymerase-1 gene ablation protects mice from ischemic renal injury. *Am J Physiol Renal Physiol* 288: F387-98, 2005.

193. **Zheng X, Zhang X, Sun H, Feng B, Li M, Chen G, Vladau C, Chen D, Suzuki M, Min L, Liu W, Zhong R, Garcia B, Jevnikar A and Min WP.** Protection of renal ischemia injury using combination gene silencing of complement 3 and caspase 3 genes. *Transplantation* 82: 1781-1786, 2006.

194. **Zhou L, Fu P, Huang XR, Liu F, Lai KN and Lan HY.** Activation of p53 promotes renal injury in acute aristolochic acid nephropathy. *J Am Soc Nephrol* 21: 31-41, 2010.

195. **Zuk A and Bonventre JV.** Acute Kidney Injury. *Annu Rev Med* 67: 293-307, 2016.